On the Linear Stability and Causality of Relativistic Regularized Hydrodynamics

DASEN YE, Department of Physics, Faculty of Science
McGill University, Montreal

A thesis submitted to McGill University in partial fulfillment of the requirements of the degree of

Master of Science (M.Sc.) Physics (Thesis)

Supervisor: Prof. Dr. Sangyong Jeon

July 12, 2023

Abstract

In this dissertation, we first introduced the concept of regularized 13-moment (R13) hydrodynamics initially developed by Struchtrup and Torrilhon in the non-relativistic scenario. By adopting a similar methodology in the relativistic case, we derived the second and third-order R14 hydrodynamics. For both theories, a series of linear stability and causality analysis was carried out with the assumption of massless particles without particle number conservation. This is realized by decomposing the linearized evolution equations into longitudinal and transverse components and then analyzing each of them independently. As a result, the second-order theory is shown to be linearly stable and causal. The third-order theory, on the other hand, is forbiddingly analytically complex but is also shown to be linearly stable and causal using numerical approaches.

Key Words: relativistic viscous hydrodynamics, linear stability, linear causality, second-order relativistic hydrodynamics, third-order relativistic hydrodynamics, regularized hydrodynamics

Abrégé

Dans cette dissertation, nous avons introduit le concept d'hydrodynamique de 13 moments régularisés (R13) développé initialement par Struchtrup et Torrilhon dans le scénario non-relativiste. En adoptant une méthodologie similaire dans le cas relativiste, nous avons obtenu l'hydrodynamique R14 de deuxième ordre et de troisième ordre. Pour toutes les deux théories, une série d'analyses de stabilité et causalité linéaires a été effectuée sur les solutions des équations hydrodynamiques correspondents en supposant que les particules sont sans masse et que le nombre des particules ne se conserve pas. Cela est réalisé en décomposant les équations d'évolution linéarisées en composantes longitudinales et transversales, puis en les analysant indépendamment. Comme un résultat, la théorie de deuxième ordre s'avère linéairement stable et causale. La théorie de troisième ordre, par contre, est extrêmement compliquée analytiquement, mais s'avère également linéairement stable et causale en utilisant des approches numériques.

Acknowledgements

This dissertation is the result of two years of hard work and would not have been possible without the support of many individuals. Specifically, I would like to express my gratitude to the following people:

Firstly, I would like to thank my supervisor, Prof. Sangyong Jeon, who has been supporting me for the past two years and introduced me to the field of relativistic viscous hydrodynamics and high-energy nuclear physics in general. I have learned a great deal under his guidance, and I am deeply appreciative of that. Thank you very much!

Secondly, I would like to extend my gratitude to all the McGill Nuclear Theory group members. I have received help from many of them during the past two years, and I am incredibly grateful for their support. Thank you so much!

Lastly, I want to thank my family and friends, who have continuously encouraged and supported me throughout the years. Without their support, I would not be the person I am today. Thank you very much!

Contribution of Authors

Dasen Ye contributed to the writing of all chapters in this dissertation, while Sangyong Jeon contributed to the revision and verification of the dissertation.

五载春秋赛白驹，牛犊初心存往昔。
长夜漫漫似无尽，岚霭重重阻前行。
报国豪志犹未灭，暗淡朦胧一点明。
旭日东出终有时，晨风轻抚万物清。

——叶达森《癸卯年四月二日深夜有感》

Table of Contents

List of Figures

Chapter 1

Introduction

Quantum Chromodynamics (QCD) is the study of the fundamental processes involving *quarks* and *gluons*. Quarks have two degrees of freedom that are especially interesting, *flavor* and *color charge*. Flavor composes of up, down, strange, charm, top, and bottom. On the other hand, color charge is the analog of electric charge in QCD, and it has three degrees of freedom: red, green, and blue. It is worth noting that singly color-charged hadron does not exist. In other words, all naturally occurring particles are color-neutral [7], a phenomenon known as "*color confinement*". In a manner similar to photons in *Quantum Electrodynamics* (QED), the force carrier responsible for exchanging the energy and momentum of quarks is referred to as a gluon. But unlike photon which is electrically neutral, gluon actually carries color charges. This makes the interactions between gluons possible, making the QCD calculations much more complicated than those in QED. In terms of Feynman diagrams, this complexity appears as extra gluon-gluon interaction vertices in addition to the quark-gluon interaction vertex [7].

Another interesting aspect of QCD is its *coupling constant*, which indicates the corresponding interaction strength. Although commonly referred to as "constant", it is actually not (that's why it is sometimes also referred to as the "*running coupling constant*") and its value depends on the length scale, or equivalently, the energy scale of the system of interacting particles. At a low energy scale, this value is relatively large. But at a high

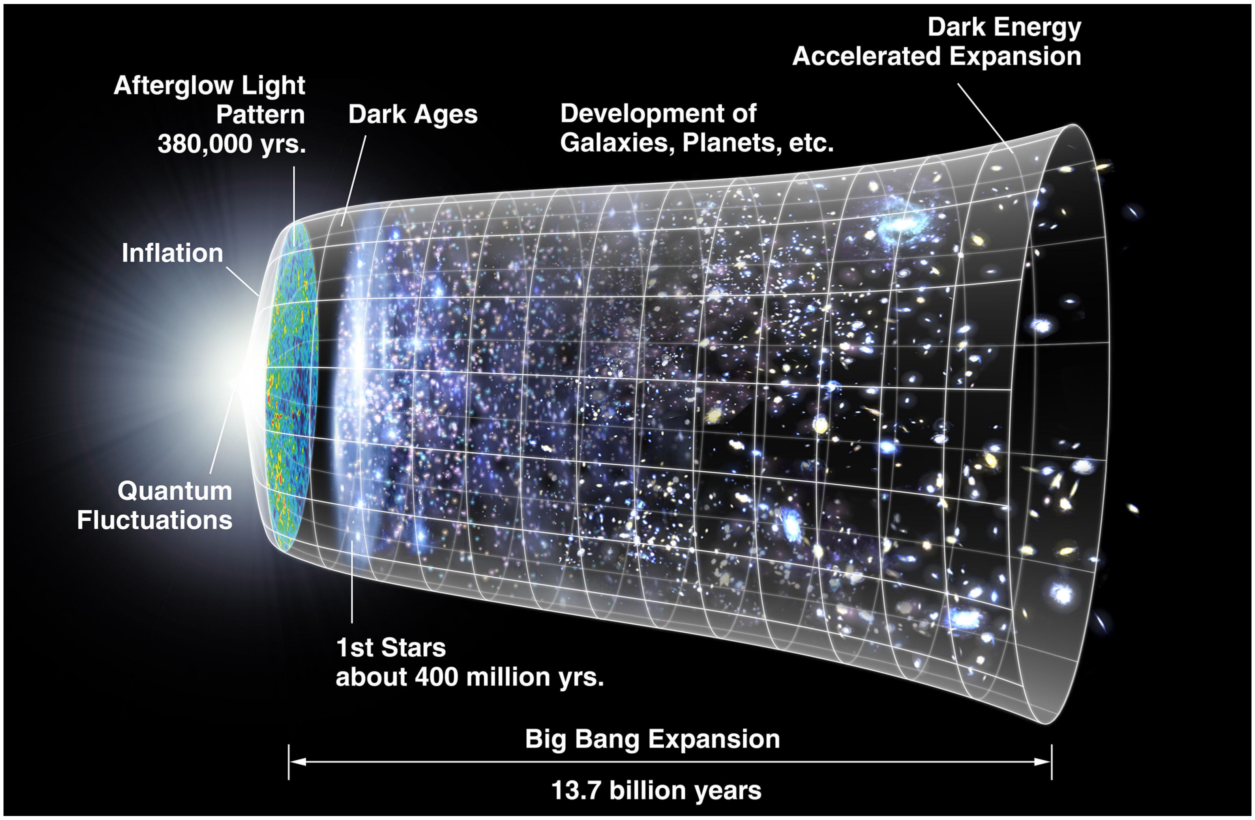

Figure 1.1: The Big Bang and expansion of the universe [1]. This figure shows different stages of the universe's evolution, starting from the Big Bang to the present.

energy scale (short distance), the value becomes small. This phenomenon is referred to as *asymptotic freedom* [8–10], which suggests that at extremely high energy scales, quarks and gluons interact very weakly. Now, let's imagine that there is a perfect and empty container with just vacuum inside. As the energy and temperature increase (energy and temperature are correlated through Boltzmann constant, $E \sim k_B T$), hadrons start to be pair-produced. At $k_B T \approx 200$ MeV, the number density of hadrons becomes so large that they start to overlap each other. Along with the increment of elementary particle's kinetic energy, this leads to the deconfinement of quarks and gluons which are now free to move across the interior of hadrons [11], causing the appearance of a new phase of matter called *quark-gluon plasma* (QGP), which, according to the theory of asymptotic freedom, should be weakly-interacting at high energy scale.

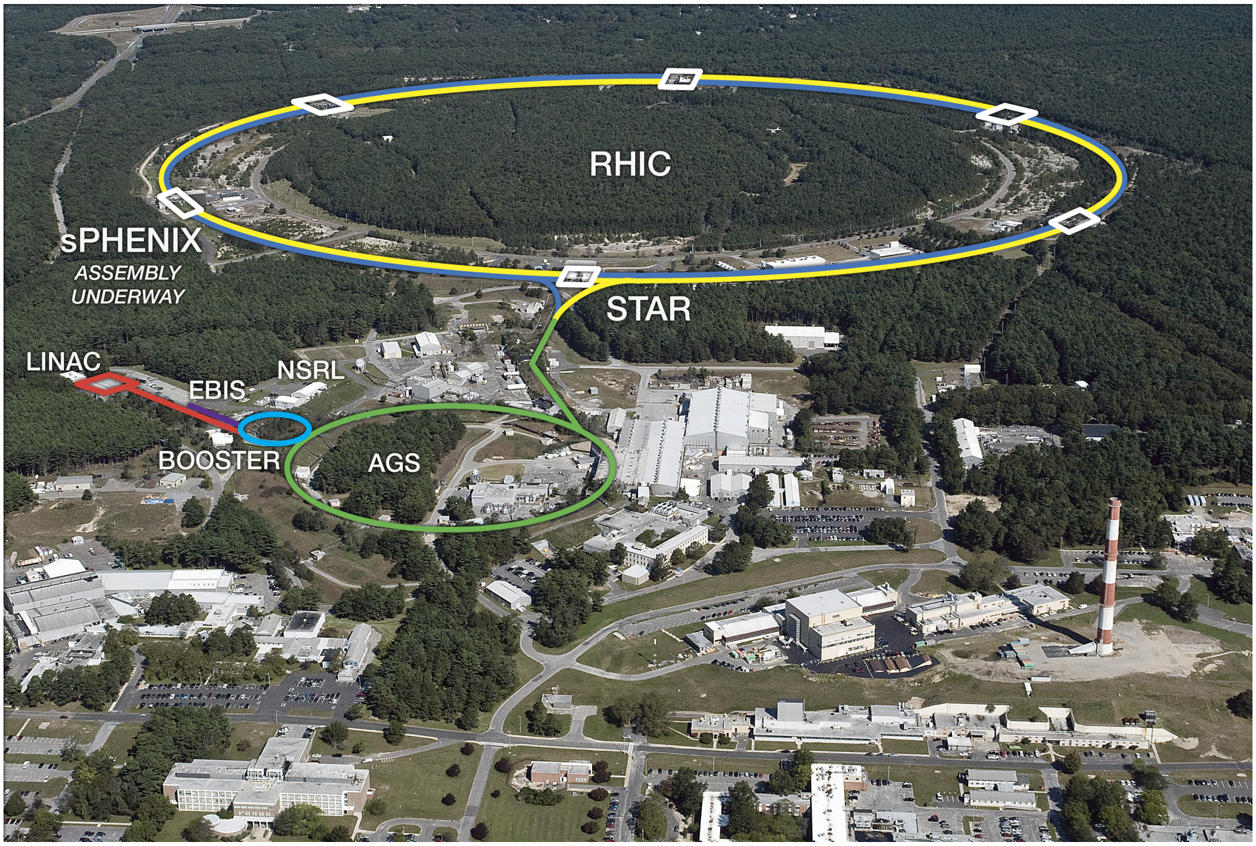

Figure 1.2: This aerial photograph shows the RHIC facility's layout, highlighting the locations of major detectors and the accelerator complex. This picture is taken from Ref. [2].

The theory explaining the origin of our universe is the *Big Bang theory*, which proposes that our universe expanded from a singularity with almost infinite energy density and temperature [12, 13] about 13.7 billion years ago (see Fig.1.1 [1]). The temperature of the universe stayed above 150 MeV (about 2×10^{12} K) during the first 10 microseconds after the Big Bang [12, 14], and such a condition is sufficient to create QGP. Therefore, it is believed that QGP exists for a small amount of time after the universe's birth.

Experimentally, it can also be created via heavy-ion collisions conducted in powerful colliders such as the Relativistic Heavy Ion Collider (RHIC) in Brookhaven National Laboratory located in Long Island, USA, and the Large Hadron Collider (LHC) at European Organization for Nuclear Research (CERN), located in Geneva, Switzerland. Specifically, four detectors are dedicated to studying QGP at RHIC, which are STAR (stands for "The

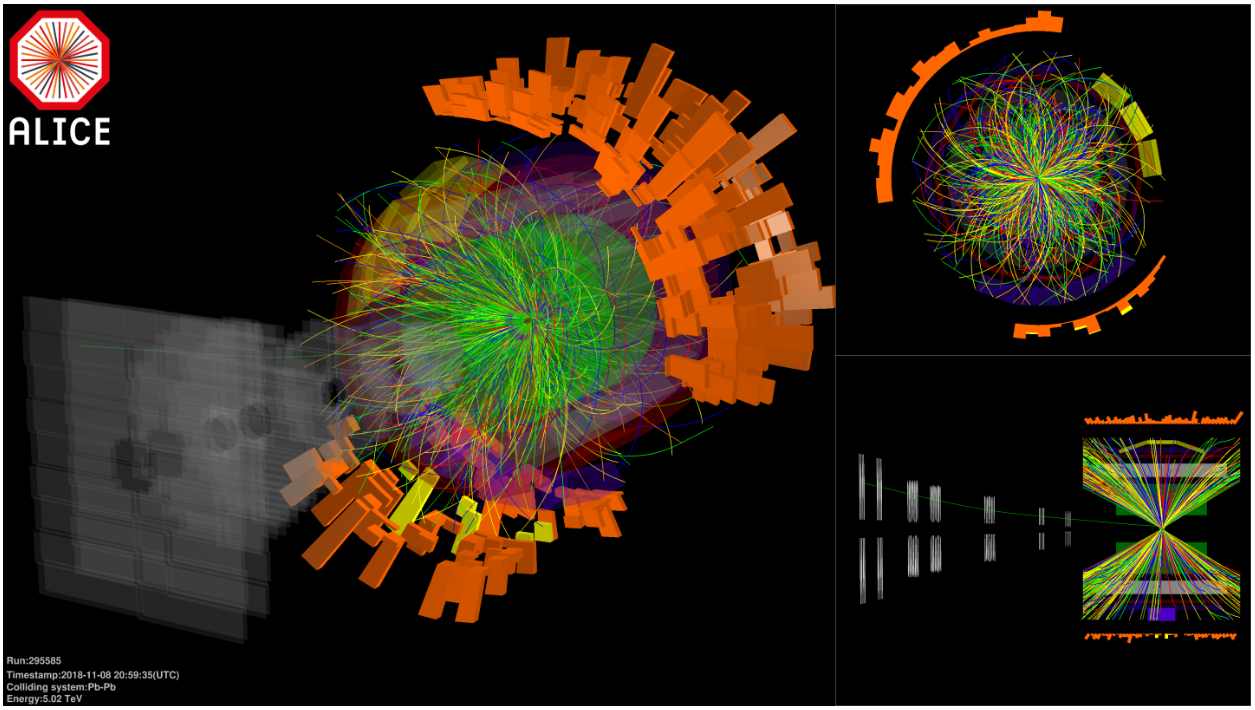

Figure 1.3: The first lead-lead collisions of 2018 send showers of particles through the ALICE detector [3].

Solenoidal Tracker at RHIC") [15], sPHENIX (an upgrade of the PHENIX detector, which is now decommissioned. PHENIX stands for "the Pioneering High Energy Nuclear Interaction eXperiment") [16, 17], PHOBOS and BRAHMS [18]. Fig.1.2 shows the locations of the two major detectors, STAR and sPHENIX, along with the accelerator complex. including the two mentioned above. As a powerful collider, RHIC can collide all ion beam species from protons to uranium, with the primary use of gold ions [19, 20]. On the other hand, the detector dedicated to the QGP study at LHC is called ALICE (A Large Ion Collider Experiment) [21], Fig.1.3 shows the trajectories of showers of particles detected by ALICE during the first lead-lead collisions in 2018 [3]. However, unlike RHIC which specializes in heavy-ion collision experiments, LHC only collides heavy ions one month per year [20].

Contrary to the study of heavy-ion collisions, which probes the *hot and dense* system of QCD, there exists a natural laboratory in the cosmos that enables us to study the *cold and dense* QCD: neutron stars and their mergers. Stars that have a similar mass ($\sim 1M_{\odot}$)

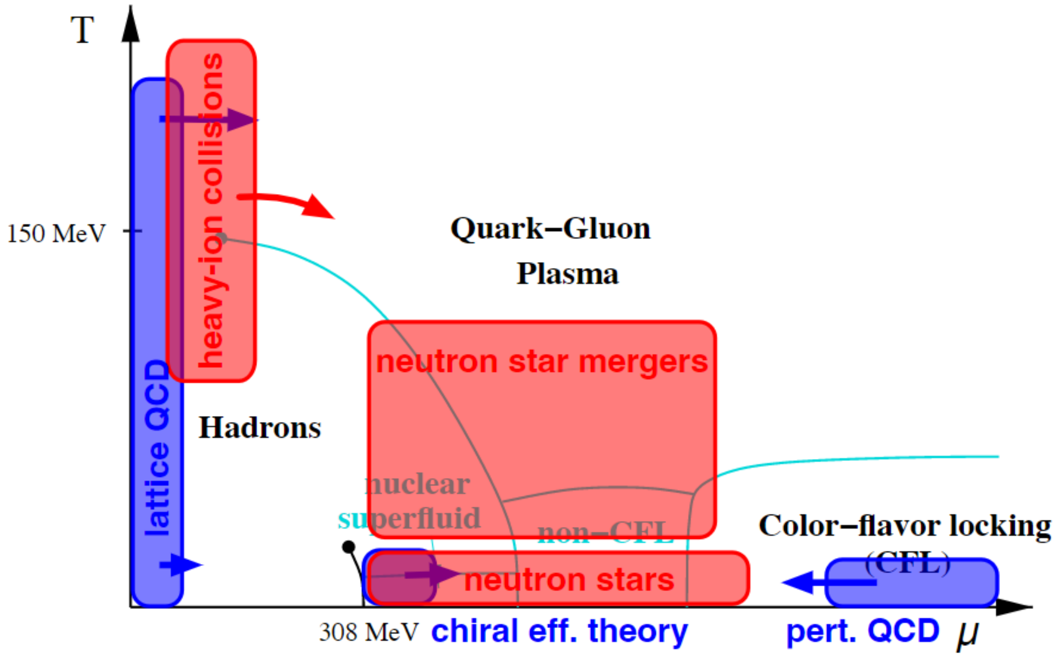

Figure 1.4: QCD Phase Diagram: Experimental Input [4]. This figure shows the phase diagram of QCD matter along with the common theories (in blue) and experimental/observational subjects (in red), with the temperature being the vertical axis and the baryon chemical potential being the horizontal axis.

to the Sun become *white dwarfs* at the end of their life. Unlike ordinary stars, in which the gravitational collapse is offset by thermal pressure produced via nuclear fusion, the degeneracy pressure due to the Pauli exclusion principle of electrons is responsible for fighting against the gravity inside a white dwarf. However, there is a limit on the mass above which the degeneracy pressure becomes inferior to gravity, known as the *Chandrasekhar limit*, which is equal to $1.44M_{\odot}$ [22]. For stars with a mass greater than this limit, their remnants become so dense that the protons and electrons are "squished" together to form neutrons, and the remnants which are now mostly made of neutrons, are called *neutron stars*. Neutron stars are extremely dense, according to the NICER mission of NASA, a typical neutron star with $1.4M_{\odot}$ mass has a radius of about 13 km [23]. Furthermore, the typical temperature for a neutron star is on the order of 100 eV ($\sim 10^6$ K) [24]. This seems like a very high temperature, but it is in fact negligible when compared to the typical energy scale of 1 GeV in QCD, that's why neutron stars are "cold" in the context of QCD [25]. However, the temperature can reach tens of MeV during the birth of a neutron star in a supernova and to ~ 100 MeV in a merger event [26]. It is worth mentioning that QGP also exists in the interior of neutron stars due to the extremely high density even though the system is "cold", unlike the case of heavy-ion collisions in which the temperature is high rather than the density. Fig.1.4 shows a typical QCD phase diagram along with the positions of different research methods and theories on this diagram. In this dissertation, we will focus on the hot and dense system in the context of heavy-ion collision and will not discuss the cold and dense part in detail.

Due to the weakly-interacting property of QGP predicted by the theory, it was expected that the system created by highly energetic heavy-ion collisions should behave like a gas and expand isotropically before the first RHIC experiment in 2000 [27]. However, the first results from RHIC actually showed that the system exhibits azimuthal anisotropy in the form of elliptic flow [28], and QGP turned out to be *the* most strongly-interacting system ever observed. Furthermore, the data was shown to be in good agreement with the description of ideal hydrodynamics [29–31]. Hydrodynamics is chosen because it is challenging to obtain an analytic or numerical solution to a microscopic many-body QCD problem such as this using first-principles calculations. What is accessible is the coarse-grained collective motion of the fluid-like system once the local thermal equilibrium is achieved [32]. Therefore, it is natural to use hydrodynamics, especially ideal hydrodynamics in which the fluid is always assumed to be in local thermal equilibrium, as the theoretical tool for modeling the evolution of QGP. The success of the ideal hydrodynamics further implies that the system is an almost-ideal fluid with small shear viscosity over entropy density ratio η/s, where η is the shear viscosity and s is the entropy density ratio.

However, a study in 2005 imposed a lower bound of $1/4\pi$ on the value of η/s in a strongly-coupled system using AdS/CFT calculations [33], which raised the question "How perfect is the QGP?". The acquisition of the answer relies on using a stronger tool than ideal hydrodynamics, the latter is only applicable to systems near local thermal equilibrium [30]. The lower bound $\eta/s \geq 1/4\pi$ suggests that there are some non-negligible off-equilibrium viscous effects that must be considered [34]. Therefore, a robust relativistic viscous hydrodynamics theory is needed to better describe the properties of an evolving QGP.

The most intuitive and straightforward way of obtaining a relativistic viscous hydrodynamics theory is to extend the non-relativistic Navier-Stokes theory to a relativistic one, and this was done independently by Eckart [35] and by Landau and Lifshitz [36]. These theories are also commonly referred to as the "first-order theory", which only includes terms up to first order in gradients. Historically, such theories were commonly obtained by using a technique called *Chapman-Enskog expansion* [37], in which the phase density function is expanded in powers of Knudsen number. Here, the phase density function $f(x, p)$ gives the number of particles in an infinitesimal momentum-position space $dpdx$, at position x and with momentum p. As for the Knudsen number, it is defined as the ratio of the particle's mean free path to the representative length scale of the problem. In particular, hydrodynamics is a theory with small Knudsen numbers. However, the first-order theory is unstable and acausal when slightly perturbed around thermal equilibrium in linear regime [38–41], and it has been shown that this instability is in fact caused by the acausality of the theory [41–43]. For this reason, the first-order theory is abandoned as being the standard theory of relativistic viscous hydrodynamics.

The first linearly stable and causal relativistic viscous hydrodynamics theory was developed by Israel and Stewart [44–46] using the 14-moment approximation, initially adopted by Grad [47] as the 5- and 9-moment approximation in the non-relativistic case. In his paper, Grad has considered, for the first time, the transient effects of dissipative current using the method of moments. In this method, the Boltzmann equation is replaced by a set of partial differential equations expressed in terms of the moments of the phase density function. To make this set of equations closed, a truncation process is necessary, and this is done by approximating the phase distribution function with a series expansion in terms of the Hermite polynomials around the equilibrium distribution, where the coefficients are determined in terms of moments. Unlike the first-order theories, the Israel-Stewart theory contains terms that are up to second-order in gradients, thus it is also commonly referred to as the "second-order theory". However, it has been shown that even the Israel-Stewart theory is not always linearly stable and causal, their transport coefficients must satisfy a set of constraints in order to be so [41–43, 48, 49].

Although the second-order theory possesses many advantages that the first-order theory does not and is now considered as the standard theory of relativistic viscous hydrodynamics, there are still issues with it. When deriving hydrodynamics from the Boltzmann equation, the Israel-Stewart theory, the Chapman-Enskog expansion, and the method of moments all give slightly different combinations of terms. The second-order theory is in fact, not unique. There are two main sources of difference, the first one is the representation of the non-equilibrium terms in the expansion of the phase density function in terms of the 14 moments. The second one is the procedure adopted to truncate the expansion in order to make the equations closed. In this dissertation, we will explore a method that allows us to systematically derive a unique relativistic viscous hydrodynamics to *any order* starting from the evolution equations of the energy-momentum moments, followed by a linear stability and causality analysis for the case of the second-order and third-order theories. This is accomplished by generalizing the non-relativistic 13-moment regularized hydrodynamics (R13) developed by Struchtrup and Torrilhon [50–53], to the relativistic second-order regularized 14-moment hydrodynamics (R14). In short, The Regularization method combines both the method of moments and Chapman-Enskog expansion, by applying a Chapman-Enskog-like expansion to the energy-momentum moments *except for* the moments that are considered as the hydrodynamic variables, instead of the phase density function. A more detailed elaboration on this method will be presented in the following chapters.

The second-order theory has been proven to be quite successful in describing the evolution of QGP, but it still has a few limitations. Under the assumption of Bjorken scaling solution [54], and for large viscosity or small initial time, the Israel-Stewart theory displays unphysical effects such as negative effective enthalpy [55] and longitudinal pressure [56]. A straightforward and natural way to improve the theory is to consider the effects of high-order correction. Therefore, in recent years, the *third-order* theory has started to catch people's attention. These high-order terms significantly improved the agreement with a large value of η/s obtained with kinetic transport calculation [57, 58], and a few third-order theories of relativistic viscous hydrodynamics have already been developed [58–60]. In this work, we will also derive a third-order theory using the regularization technique, followed by a linear stability and causality analysis. By implementing this approach, we will obtain a more precise theory by taking into account the higher-order correction effects.

This dissertation is organized as the following: in Chapter 2 we will begin by introducing some background knowledge in kinetic theory and deriving the conservation laws of energy, momentum, and particle number. We will then proceed to derive the evolution equation for a general rank-n energy-momentum moment of the small perturbation δf in the phase density function so that the hydrodynamic equations for the specific moments that we are interested in can be easily obtained in the subsequent chapters. In Chapter 3, we will derive the second-order R14 hydrodynamics using the regularization method, followed by the linear stability and causality analysis on such theory. In particular, the R14 equations will be first linearized and then decomposed into longitudinal and transverse parts so that each component can be analyzed independently. We will show that the second-order R14 theory is linearly stable and causal regardless of the choice of transport coefficients, with the assumption of massless particles without particle number conservation. In Chapter 4, we will commence by obtaining the third-order R14 theory, and then carry out a linear stability and causality analysis on this theory, following the same procedure outlined in Chapter 3. We will demonstrate that this theory is extremely analytically complex but still linearly stable and causal, proven by numerical approaches. Finally, we will conclude this dissertation in Chapter 5.

Throughout the dissertation, we will utilize natural units $c = \hbar = k_B = 1$, and adopt the mostly-positive Minkowski metric $g_{\mu\nu} = diag(-1, 1, 1, 1)$.

Chapter 2

General Moment Equation and Conservation Laws

2.1 Kinetic Theory and Conservation Laws

To begin the derivation of the general hydrodynamic equation, we shall start with the relativistic Boltzmann equation, which describes the dynamical behavior of relativistic particles. For simplicity, we assume single particle species:

$$p^\mu \partial_\mu f(x,p) = C[f] \tag{2.1}$$

where f is the phase space density function, and $C[f]$ is the collision term which takes into account the changes in f due to the collisions of particles. Again for simplicity, we only consider elastic scatterings. Using Boltzmann statistics, the collision term becomes:

$$\begin{aligned} p^\mu \partial_\mu f(x,p) = \frac{1}{2} \int \frac{d^3p_1}{(2\pi)^3 p_1^0} \int \frac{d^3k}{(2\pi)^3 k^0} \int \frac{d^3k_1}{(2\pi)^3 k_1^0} |M|^2_{pp_1 \leftrightarrow kk_1} (2\pi)^4 \delta(p + p_1 - k - k_1) \\ \times \left[f(x,k) f(x,k_1) - f(x,p) f(x,p_1) \right] \end{aligned} \tag{2.2}$$

where $p^0 = \sqrt{\mathbf{p}^2 + m^2}$ is the on-shell energy of the particle. In the remainder of this dissertation, we will not consider quantum statistical effects such as Bose enhancement or Pauli blocking for simplicity. One can include these effects by changing the right-hand side of Eq. (2.2) appropriately [61]. However, doing so will not affect the derivations below too much. The *energy-momentum tensor* (or *stress-energy tensor*) is given by:

$$T^{\mu\nu} = \int \frac{d^3p}{(2\pi)^3 p^0} p^\mu p^\nu f(x,p) \tag{2.3}$$

Taking the space-time derivative we get:

$$\begin{aligned}
\partial_\mu T^{\mu\nu} &= \int \frac{d^3p}{(2\pi)^3 p^0} p^\mu p^\nu \partial_\mu f(x,p) \\
&= \frac{1}{2} \int \frac{d^3p}{(2\pi)^3 p^0} \int \frac{d^3p_1}{(2\pi)^3 p_1^0} \int \frac{d^3k}{(2\pi)^3 k^0} \int \frac{d^3k_1}{(2\pi)^3 k_1^0} |M|^2_{pp_1\leftrightarrow kk_1} (2\pi)^4 \delta(p+p_1-k-k_1) \\
&\times p^\nu [f(x,k)f(x,k_1) - f(x,p)f(x,p_1)] \\
&= \frac{1}{8} \int \frac{d^3p}{(2\pi)^3 p^0} \int \frac{d^3p_1}{(2\pi)^3 p_1^0} \int \frac{d^3k}{(2\pi)^3 k^0} \int \frac{d^3k_1}{(2\pi)^3 k_1^0} |M|^2_{pp_1\leftrightarrow kk_1} (2\pi)^4 \delta(p+p_1-k-k_1) \\
&\times (p^\nu + p_1^\nu - k^\nu - k_1^\nu)[f(x,k)f(x,k_1) - f(x,p)f(x,p_1)] \\
&= 0
\end{aligned} \tag{2.4}$$

Note that in the third step, we have used the fact that the above expression is symmetric under the exchange of p and p_1 and anti-symmetric under the exchange of (p, p_1) and (k, k_1). Also observe that the time component ($\nu = 0$) and the spacial components ($\nu = 1, 2, 3$) of the above equation correspond to the conservation of energy and momentum, respectively. In a similar manner, we can define the *particle number current* as:

$$J^\mu = \int \frac{d^3p}{(2\pi)^3 p^0} p^\mu f(x,p) \tag{2.5}$$

Taking the space-time derivative, we get:

$$\begin{aligned}
\partial_\mu J^\mu &= \int \frac{d^3p}{(2\pi)^3 p^0} p^\mu \partial_\mu f(x,p) \\
&= \frac{1}{2}\int \frac{d^3p}{(2\pi)^3 p^0}\int \frac{d^3p_1}{(2\pi)^3 p_1^0}\int \frac{d^3k}{(2\pi)^3 k^0}\int \frac{d^3k_1}{(2\pi)^3 k_1^0} |M|^2_{pp_1\leftrightarrow kk_1}(2\pi)^4\delta(p+p_1-k-k_1) \\
&\quad \times [f(x,k)f(x,k_1) - f(x,p)f(x,p_1)] \\
&= 0
\end{aligned} \tag{2.6}$$

where we used the fact that the right-hand side is anti-symmetric under the exchange of (p, p_1) and (k, k_1). Therefore, the particle number is conserved as expected since we consider elastic collisions only.

We further define the fluid-flow velocity $u^\mu = \gamma(1, \mathbf{V})$ as being parallel to the energy density flow, where γ is the Lorentz factor, $\mathbf{V}$ is the fluid-flow 3-velocity, and ϵ is the energy density:

$$T^{\mu\nu}u_\nu = -\epsilon u^\mu \tag{2.7}$$

Similarly, we can define the particle number density ν as:

$$J^\mu u_\mu = -\nu \tag{2.8}$$

Note that in the above definitions, we used the mostly positive Minkowski metric, and all quantities depend on space-time coordinates x. The flow velocity u^μ is normalized to $u^\mu u_\mu = -1$. Now, the phase space density function can be considered as a small fluctuation based on a local equilibrium part:

$$f(x,p) = f_0(x,p) + \delta f(x,p) \tag{2.9}$$

where the local equilibrium part f_0 is:

$$f_0(x,p) = e^{\beta(x) u_\mu p^\mu + \alpha(x)} \tag{2.10}$$

Here, $\beta = 1/T$ is the inverse of temperature, and $\alpha = \beta\mu$ is the local chemical potential over temperature. The corresponding energy-momentum tensor and particle number current at local equilibrium are naturally defined as:

$$T_0^{\mu\nu} = \int \frac{d^3p}{(2\pi)^3 p^0} p^\mu p^\nu f_0(x,p) \tag{2.11}$$

$$J_0^\mu = \int \frac{d^3p}{(2\pi)^3 p^0} p^\mu f_0(x,p) \tag{2.12}$$

Observe that in $T_0^{\mu\nu}$, the only two quantities that are available for us to form a rank-2 tensor are $u^\mu u^\nu$ and $g^{\mu\nu}$. Therefore, $T_0^{\mu\nu}$ must be a linear combination of the two:

$$T_0^{\mu\nu} = A u^\mu u^\nu + B \Delta^{\mu\nu} \tag{2.13}$$

where we define the local 3-metric $\Delta^{\mu\nu}$ to be:

$$\Delta^{\mu\nu} = g^{\mu\nu} + u^\mu u^\nu \tag{2.14}$$

which satisfies:

$$\begin{aligned} \Delta^{\mu\nu} u_\nu &= g^{\mu\nu} u_\nu + u^\mu u^\nu u_\nu \\ &= u^\mu - u^\mu \\ &= 0 \end{aligned} \tag{2.15}$$

Note that for static fluids the time components of $\Delta^{\mu\nu}$ vanish and $\Delta^{\mu\nu}$ becomes purely spacial since $g^{\mu\nu} = diag(-1,1,1,1)$ and $u^\mu = (1, \mathbf{0})$ for static fluids. Furthermore, $\Delta^{\mu\nu}$ can also be considered as the projector which projects the components that are orthogonal to u^μ of an arbitrary 4-vector.

Similar to $T_0^{\mu\nu}$, the only vector that is available for us to write J_0^μ is u^μ. Thus,

$$J_0^\mu = Cu^\mu \tag{2.16}$$

We now need to calculate the quantities A, B, and C. To do so, we use the following matching condition (also known as "*Landau condition*"):

$$T^{\mu\nu}u_\nu = T_0^{\mu\nu}u_\nu = -\epsilon u^\mu \tag{2.17}$$

$$J^\mu u_\mu = J_0^\mu u_\mu = -\nu \tag{2.18}$$

It immediately follows that $A = \epsilon$ and $C = \nu$, and they can be written as:

$$\epsilon = T_0^{\mu\nu}u_\mu u_\nu = \int \frac{d^3p}{(2\pi)^3 p^0} W_p^2 e^{-\beta W_p} e^\alpha = \int \frac{d^3p}{(2\pi)^3} p^0 e^{-\beta p^0} e^\alpha \tag{2.19}$$

$$\nu = -J_0^\mu u_\mu = \int \frac{d^3p}{(2\pi)^3 p^0} W_p e^{-\beta W_p} e^\alpha = \int \frac{d^3p}{(2\pi)^3} e^{-\beta p^0} e^\alpha \tag{2.20}$$

where the quantity $W_p = -u_\mu p^\mu$ is Lorentz-invariant and therefore can be evaluated in the fluid cell rest frame, leading to $W_p = p^0 = \sqrt{\mathbf{p}^2 + m^2}$, the energy of a particle in the fluid cell rest frame.

We still need to calculate the coefficient B. This can be done by taking the trace of the energy-momentum tensor at the local equilibrium using the local 3-metric $\Delta^{\mu\nu}$. Once again, the trace is Lorentz-invariant and we can evaluate it in the fluid rest frame:

$$\Delta_{\mu\nu}T_0^{\mu\nu} = 3B \tag{2.21}$$

Recall that $\Delta^{\mu\nu}$ is purely spacial in the fluid rest frame. Therefore, only the spacial entries along the diagonal of $T_0^{\mu\nu}$, which correspond to the thermal pressure, contribute to the trace. The factor of 3 in front of B indicates the contribution to the pressure from each spacial component. Consequently, it follows that $B = P_0$, the thermal pressure at local equilibrium. By going to the fluid cell rest frame, we get:

$$
\begin{aligned}
P_0 &= \frac{1}{3}\Delta_{\mu\nu}T_0^{\mu\nu} \\
&= \frac{1}{3}\int \frac{d^3p}{(2\pi)^3 p^0} p^\mu p^\nu (g_{\mu\nu} + u_\mu u_\nu) e^{-\beta p^0} e^\alpha \\
&= \frac{1}{3}\int \frac{d^3p}{(2\pi)^3 p^0} (p^\mu p_\mu + W_p^2) e^{-\beta p^0} e^\alpha \\
&= \frac{1}{3}\int \frac{d^3p}{(2\pi)^3 p^0} (-m^2 + p^{0\,2}) e^{-\beta p^0} e^\alpha \\
&= \frac{1}{3}\int \frac{d^3p}{(2\pi)^3 p^0} \mathbf{p}^2 e^{-\beta p^0} e^\alpha
\end{aligned}
\tag{2.22}
$$

Note that $P_0 = \frac{1}{3}\epsilon$ if $m = 0$. We can now write the full energy-momentum tensor and particle number current as:

$$
T^{\mu\nu} = T_0^{\mu\nu} + \int \frac{d^3p}{(2\pi)^3 p^0} p^\mu p^\nu \delta f(x,p) \tag{2.23}
$$

$$
J^\mu = J_0^\mu + \int \frac{d^3p}{(2\pi)^3 p^0} p^\mu \delta f(x,p) \tag{2.24}
$$

By the matching conditions Eq. (2.17) and (2.18), we arrive at the following requirements:

$$
\int \frac{d^3p}{(2\pi)^3 p^0} W_p p^\mu \delta f(x,p) = \int \frac{d^3p}{(2\pi)^3 p^0} W_p \delta f(x,p) = 0 \tag{2.25}
$$

Before we start calculating $\delta T^{\mu\nu}$ and δJ^μ, it is convenient to define the projected momentum $p^{\langle\mu\rangle}$:

$$
\begin{aligned}
p^{\langle\mu\rangle} &= \Delta^{\mu\nu} p_\nu \\
&= (g^{\mu\nu} + u^\mu u^\nu) p_\nu \\
&= p^\mu - W_p u^\mu
\end{aligned}
\tag{2.26}
$$

Notice that by applying the projector Δ_μ^ν along with Eq. (2.26) to Eq. (2.25), we get

$$
\int \frac{d^3p}{(2\pi)^3 p^0} W_p p^{\langle\nu\rangle} \delta f(x,p) = 0 \tag{2.27}
$$

which is another useful relationship. Now, with Eq. (2.26) and Eq. (2.27), the small fluctuation in $T^{\mu\nu}$ is given by:

$$\begin{aligned}\delta T^{\mu\nu} &= \int \frac{d^3p}{(2\pi)^3 p^0} p^\mu p^\nu \delta f(x,p) \\ &= \int \frac{d^3p}{(2\pi)^3 p^0} (p^{\langle\mu\rangle} + W_p u^\mu)(p^{\langle\nu\rangle} + W_p u^\nu)\delta f(x,p) \\ &= \int \frac{d^3p}{(2\pi)^3 p^0} p^{\langle\mu\rangle} p^{\langle\nu\rangle} \delta f(x,p)\end{aligned} \tag{2.28}$$

where we have also used the fact that

$$\int \frac{d^3p}{(2\pi)^3 p^0} W_p^2 u^\mu u^\nu \delta f(x,p) = -u^\mu u^\nu u_\alpha \int \frac{d^3p}{(2\pi)^3 p^0} W_p p^\alpha \delta f(x,p) = 0 \tag{2.29}$$

with the help of Eq. (2.25). Then

$$\begin{aligned}\delta T^{\mu\nu} &= \Delta^\mu_\alpha \Delta^\nu_\beta \int \frac{d^3p}{(2\pi)^3 p^0} p^\alpha p^\beta \delta f(x,p) \\ &= \left[\frac{1}{2}(\Delta^\mu_\alpha \Delta^\nu_\beta + \Delta^\nu_\alpha \Delta^\mu_\beta) - \frac{1}{3}\Delta^{\mu\nu}\Delta_{\alpha\beta}\right] \int \frac{d^3p}{(2\pi)^3 p^0} p^\alpha p^\beta \delta f(x,p) \\ &\quad + \frac{1}{3}\Delta^{\mu\nu}\Delta_{\alpha\beta} \int \frac{d^3p}{(2\pi)^3 p^0} p^\alpha p^\beta \delta f(x,p) \\ &= \Delta^{\mu\nu}_{\alpha\beta} \int \frac{d^3p}{(2\pi)^3 p^0} p^\alpha p^\beta \delta f(x,p) + \frac{1}{3}\Delta^{\mu\nu} \int \frac{d^3p}{(2\pi)^3 p^0} p^\alpha p_\alpha \delta f(x,p) \\ &= \int \frac{d^3p}{(2\pi)^3 p^0} p^{\langle\mu} p^{\nu\rangle} \delta f(x,p) - \frac{m^2}{3}\Delta^{\mu\nu} \int \frac{d^3p}{(2\pi)^3 p^0} \delta f(x,p) \\ &= \pi^{\mu\nu} + \Pi\Delta^{\mu\nu}\end{aligned} \tag{2.30}$$

where in the second step, we have used the fact that the expression is symmetric under the exchange of indices α and β. Here, $\pi^{\mu\nu}$ is the *shear-stress tensor*, Π is the *bulk viscous pressure* which is a measure of the resistance of the fluid to be compressed or expanded, and

$$\Delta^{\mu\nu}_{\alpha\beta} = \frac{1}{2}\left(\Delta^\mu_\alpha \Delta^\nu_\beta + \Delta^\mu_\beta \Delta^\nu_\alpha - \frac{2}{3}\Delta^{\mu\nu}\Delta_{\alpha\beta}\right) \tag{2.31}$$

is the rank-2 traceless and symmetric projector. Consequently, $\pi^{\mu\nu}$ is also symmetric and traceless. Similarly, one can show that:

$$\begin{aligned}
\delta J^{\mu} &= \int \frac{d^3p}{(2\pi)^3 p^0} p^{\mu} \delta f(x,p) \\
&= \int \frac{d^3p}{(2\pi)^3 p^0} p^{\langle\mu\rangle} \delta f(x,p) \\
&= q^{\mu}
\end{aligned} \tag{2.32}$$

which turns out to be the *diffusion current*. Therefore, the full energy-momentum tensor and particle number current are given by:

$$T^{\mu\nu} = \epsilon u^{\mu} u^{\nu} + (P_0 + \Pi)\Delta^{\mu\nu} + \pi^{\mu\nu} \tag{2.33}$$

$$J^{\mu} = \nu u^{\mu} + q^{\mu} \tag{2.34}$$

Observe that Π, q^{μ}, and $\pi^{\mu\nu}$ are scalar, vector, and rank-2 energy-momentum moments of δf, respectively. One can easily generalize this concept to higher order by defining the *rank-n energy-momentum moments*:

$$\rho_r^{\mu_1 \cdots \mu_n} = \int \frac{d^3p}{(2\pi)^3 p^0} \delta f W_p^r p^{\langle\mu_1 \cdots} p^{\mu_n\rangle} \tag{2.35}$$

with $\Pi = -\frac{m^2}{3}\rho_0$, $q^{\mu} = \rho_0^{\mu}$ and $\pi^{\mu\nu} = \rho_0^{\mu\nu}$. Here, the integer n is the momentum order, and W_p^r is the energy weight in which the integer r indicates the energy order. The angular bracket represents the transverse (with respect to u^{μ}, as mentioned previously), symmetric, and traceless combination of Lorentz indices. This is obtained by acting the *rank-n projector* (see Eq. (A.1)) which extracts the transverse, symmetric, and traceless part of any rank-n tensor, on n momenta:

$$p^{\langle\mu_1 \cdots \mu_n\rangle} = \Delta^{\mu_1 \cdots \mu_n}_{\nu_1 \cdots \nu_n} p^{\nu_1} \ldots p^{\nu_n} \tag{2.36}$$

2.2 General Moment Equation

As we will see later in this dissertation, the energy and momentum conservation laws (Eq. (2.4)), along with the particle number conservation (Eq. (2.6)) serve as the evolution equations for the energy density ϵ, the fluid flow velocity u^μ, and the particle number density ν, respectively. However, the evolution equations for all the other moments remain unknown at this point. Therefore, it seems natural to derive the hydrodynamic equations for these moments as the next step, the corresponding equations will serve as the evolution equations for these moments. Starting with the general rank-n energy-momentum moments of δf:

$$\rho_r^{\mu_1...\mu_n} = \int \frac{d^3p}{(2\pi)^3 p^0} \delta f W_p^r p^{\langle\mu_1} p^{\mu_2} ... p^{\mu_n\rangle} \tag{2.37}$$

Taking the *comoving derivative* $D = u^\mu \partial_\mu$, which corresponds to the time derivative in the fluid rest-frame, and then projecting onto the transverse space, we get

$$\begin{aligned}
\Delta^{\mu_1...\mu_n}_{\nu_1...\nu_n} D\rho_r^{\nu_1...\nu_n} &= \Delta^{\mu_1...\mu_n}_{\nu_1...\nu_n} \int \frac{d^3p}{(2\pi)^3 p^0} (D\delta f) W_p^r p^{\langle\nu_1} p^{\nu_2} ... p^{\nu_n\rangle} \\
&\quad + \Delta^{\mu_1...\mu_n}_{\nu_1...\nu_n} \int \frac{d^3p}{(2\pi)^3 p^0} \delta f W_p^r D p^{\langle\nu_1} p^{\nu_2} ... p^{\nu_n\rangle} \\
&\quad + \Delta^{\mu_1...\mu_n}_{\nu_1...\nu_n} \int \frac{d^3p}{(2\pi)^3 p^0} \delta f (D W_p^r) p^{\langle\nu_1} p^{\nu_2} ... p^{\nu_n\rangle} \\
&= \Delta^{\mu_1...\mu_n}_{\nu_1...\nu_n} \int \frac{d^3p}{(2\pi)^3 p^0} (D\delta f) W_p^r p^{\langle\nu_1} p^{\nu_2} ... p^{\nu_n\rangle} \\
&\quad - n \int \frac{d^3p}{(2\pi)^3 p^0} \delta f W_p^{r+1} p^{\langle\mu_1} p^{\mu_2} ... a^{\mu_n\rangle} \\
&\quad - r \Delta^{\mu_1...\mu_n}_{\nu_1...\nu_n} a_\sigma \int \frac{d^3p}{(2\pi)^3 p^0} \delta f W_p^{r-1} p^{\langle\sigma\rangle} p^{\langle\nu_1} p^{\nu_2} ... p^{\nu_n\rangle}
\end{aligned} \tag{2.38}$$

where we defined the fluid acceleration by $a^\mu = Du^\mu$, and used the fact that $DW_p = -a_\mu p^\mu = -a_\mu p^{\langle\mu\rangle}$, along with Eq. (A.8). Now, using Eq. (C.21) in [62]:

$$p^{\langle\lambda\rangle} p^{\langle\mu_1} ... p^{\mu_n\rangle} = p^{\langle\lambda} p^{\mu_1} ... p^{\mu_n\rangle} + \frac{n}{2n+1} (W_p^2 - m^2) p^{\langle\mu_1} ... \Delta^{\mu_n\rangle\lambda} \tag{2.39}$$

we can expand the last term on the right-hand side as the following:

$$
\begin{aligned}
\Delta^{\mu_1...\mu_n}_{\nu_1...\nu_n} D\rho_r^{\nu_1...\nu_n} = \Delta^{\mu_1...\mu_n}_{\nu_1...\nu_n} &\int \frac{d^3p}{(2\pi)^3p^0}(D\delta f)W_p^r p^{\langle\nu_1}p^{\nu_2}...p^{\nu_n\rangle} \\
&- n\int \frac{d^3p}{(2\pi)^3p^0}\delta f W_p^{r+1} p^{\langle\mu_1}p^{\mu_2}...a^{\mu_n\rangle} \\
&- ra_\sigma \int \frac{d^3p}{(2\pi)^3p^0}\delta f W_p^{r-1} p^{\langle\sigma}p^{\mu_1}p^{\mu_2}...p^{\mu_n\rangle} \\
&- r\frac{n}{2n+1}a_\sigma \int \frac{d^3p}{(2\pi)^3p^0}\delta f W_p^{r-1}(W_p^2-m^2) p^{\langle\mu_1}p^{\mu_2}...\Delta^{\mu_n\rangle\sigma}
\end{aligned}
\tag{2.40}
$$

To express $D\delta f$ in terms of δf, we can use the following form of the Boltzmann equation

$$
p^\mu\partial_\mu f_0 + W_p D\delta f + p^{\langle\mu\rangle}\nabla_\mu\delta f = C[f] \tag{2.41}
$$

in Eq. (2.40), which gives

$$
\begin{aligned}
\Delta^{\mu_1...\mu_n}_{\nu_1...\nu_n} D\rho_r^{\nu_1...\nu_n} = &-n\int \frac{d^3p}{(2\pi)^3p^0}\delta f W_p^{r+1} p^{\langle\mu_1}p^{\mu_2}...a^{\mu_n\rangle} \\
&- ra_\sigma \int \frac{d^3p}{(2\pi)^3p^0}\delta f W_p^{r-1} p^{\langle\sigma}p^{\mu_1}p^{\mu_2}...p^{\mu_n\rangle} \\
&- r\frac{n}{2n+1} \int \frac{d^3p}{(2\pi)^3p^0}\delta f W_p^{r-1}(W_p^2-m^2) p^{\langle\mu_1}p^{\mu_2}...a^{\mu_n\rangle} \\
&+ \Delta^{\mu_1...\mu_n}_{\nu_1...\nu_n} \int \frac{d^3p}{(2\pi)^3p^0} C[f] W_p^{r-1} p^{\langle\nu_1}p^{\nu_2}...p^{\nu_n\rangle} \\
&- \Delta^{\mu_1...\mu_n}_{\nu_1...\nu_n} \int \frac{d^3p}{(2\pi)^3p^0} (\partial_\lambda f_0) W_p^{r-1} p^\lambda p^{\langle\nu_1}p^{\nu_2}...p^{\nu_n\rangle} \\
&- \Delta^{\mu_1...\mu_n}_{\nu_1...\nu_n} \int \frac{d^3p}{(2\pi)^3p^0} (\nabla_\lambda \delta f) W_p^{r-1} p^{\langle\lambda\rangle} p^{\langle\nu_1}p^{\nu_2}...p^{\nu_n\rangle}
\end{aligned}
\tag{2.42}
$$

Here, we define $\nabla_\mu = \Delta_\mu^\nu\partial_\nu$ as the *projected derivative*, corresponding to the spatial gradient in the fluid rest-frame. Eq. (2.41) can be easily obtained using the Boltzmann equation and by realizing that:

$$
\partial_\mu = g_\mu^\alpha\partial_\alpha = \left(-u_\mu u^\alpha + \Delta_\mu^\alpha\right)\partial_\alpha = -u_\mu D + \nabla_\mu \tag{2.43}
$$

Using the chain rule, we can pull ∇_λ in the last term on the right-hand side of Eq. (2.42) out of the integral:

$$\begin{aligned}
\Delta^{\mu_1\ldots\mu_n}_{\nu_1\ldots\nu_n} D\rho_r^{\nu_1\ldots\nu_n} = &-n\int \frac{d^3p}{(2\pi)^3p^0}\delta f W_p^{r+1} p^{\langle\mu_1}p^{\mu_2}\ldots a^{\mu_n\rangle} \\
&- r a_\sigma \int \frac{d^3p}{(2\pi)^3p^0}\delta f W_p^{r-1} p^{\langle\sigma}p^{\mu_1}p^{\mu_2}\ldots p^{\mu_n\rangle} \\
&- r\frac{n}{2n+1}\int \frac{d^3p}{(2\pi)^3p^0}\delta f W_p^{r-1}(W_p^2-m^2) p^{\langle\mu_1}p^{\mu_2}\ldots a^{\mu_n\rangle} \\
&+ \Delta^{\mu_1\ldots\mu_n}_{\nu_1\ldots\nu_n}\int \frac{d^3p}{(2\pi)^3p^0} C[f] W_p^{r-1} p^{\langle\nu_1}p^{\nu_2}\ldots p^{\nu_n\rangle} \\
&- \Delta^{\mu_1\ldots\mu_n}_{\nu_1\ldots\nu_n}\int \frac{d^3p}{(2\pi)^3p^0} (\partial_\lambda f_0) W_p^{r-1} p^\lambda p^{\langle\nu_1}p^{\nu_2}\ldots p^{\nu_n\rangle} \\
&- \Delta^{\mu_1\ldots\mu_n}_{\nu_1\ldots\nu_n}\nabla_\lambda\int \frac{d^3p}{(2\pi)^3p^0}\delta f W_p^{r-1} p^{\langle\lambda\rangle} p^{\langle\nu_1}p^{\nu_2}\ldots p^{\nu_n\rangle} \\
&+ \Delta^{\mu_1\ldots\mu_n}_{\nu_1\ldots\nu_n}\int \frac{d^3p}{(2\pi)^3p^0}\delta f (\nabla_\lambda W_p^{r-1}) p^{\langle\lambda\rangle} p^{\langle\nu_1}p^{\nu_2}\ldots p^{\nu_n\rangle} \\
&+ \Delta^{\mu_1\ldots\mu_n}_{\nu_1\ldots\nu_n}\int \frac{d^3p}{(2\pi)^3p^0}\delta f W_p^{r-1} (\nabla_\lambda p^{\langle\lambda\rangle}) p^{\langle\nu_1}p^{\nu_2}\ldots p^{\nu_n\rangle} \\
&+ \Delta^{\mu_1\ldots\mu_n}_{\nu_1\ldots\nu_n}\int \frac{d^3p}{(2\pi)^3p^0}\delta f W_p^{r-1} p^{\langle\lambda\rangle} (\nabla_\lambda p^{\langle\nu_1}p^{\nu_2}\ldots p^{\nu_n\rangle})
\end{aligned} \tag{2.44}$$

Now, note that the second-last term on the right-hand side can be simplified as

$$\begin{aligned}
&\Delta^{\mu_1\ldots\mu_n}_{\nu_1\ldots\nu_n}\int \frac{d^3p}{(2\pi)^3p^0}\delta f W_p^{r-1} (\nabla_\lambda p^{\langle\lambda\rangle}) p^{\langle\nu_1}p^{\nu_2}\ldots p^{\nu_n\rangle} \\
&= \Delta^{\mu_1\ldots\mu_n}_{\nu_1\ldots\nu_n}\int \frac{d^3p}{(2\pi)^3p^0}\delta f W_p^{r-1} \nabla_\lambda (p^\lambda - W_p u^\lambda) p^{\langle\nu_1}p^{\nu_2}\ldots p^{\nu_n\rangle} \\
&= -\theta\int \frac{d^3p}{(2\pi)^3p^0}\delta f W_p^{r} p^{\langle\mu_1}p^{\mu_2}\ldots p^{\mu_n\rangle}
\end{aligned} \tag{2.45}$$

since $\nabla_\lambda p^\lambda = 0$ and $u^\lambda\nabla_\lambda W_p = u^\lambda \Delta^\alpha_\lambda \partial_\alpha W_p = 0$. Here, we define $\theta = \partial_\mu u^\mu = \nabla_\mu u^\mu$, which represents the expansion rate of the fluid.

To briefly summarize, so far we have:

$$
\begin{aligned}
\Delta^{\mu_1\ldots\mu_n}_{\nu_1\ldots\nu_n} D\rho_r^{\nu_1\ldots\nu_n} &= -n\int \frac{d^3p}{(2\pi)^3p^0}\delta f W_p^{r+1} p^{\langle\mu_1}p^{\mu_2}\ldots a^{\mu_n\rangle} \\
&- ra_\sigma \int \frac{d^3p}{(2\pi)^3p^0}\delta f W_p^{r-1} p^{\langle\sigma}p^{\mu_1}p^{\mu_2}\ldots p^{\mu_n\rangle} \\
&- r\frac{n}{2n+1}\int \frac{d^3p}{(2\pi)^3p^0}\delta f W_p^{r-1}(W_p^2-m^2) p^{\langle\mu_1}p^{\mu_2}\ldots a^{\mu_n\rangle} \\
&+ \int \frac{d^3p}{(2\pi)^3p^0} C[f] W_p^{r-1} p^{\langle\mu_1}p^{\mu_2}\ldots p^{\mu_n\rangle} \\
&- \int \frac{d^3p}{(2\pi)^3p^0}(\partial_\lambda f_0) W_p^{r-1} p^\lambda p^{\langle\mu_1}p^{\mu_2}\ldots p^{\mu_n\rangle} \\
&- \Delta^{\mu_1\ldots\mu_n}_{\nu_1\ldots\nu_n}\nabla_\lambda \int \frac{d^3p}{(2\pi)^3p^0}\delta f W_p^{r-1} p^{\langle\lambda\rangle} p^{\langle\nu_1}p^{\nu_2}\ldots p^{\nu_n\rangle} \\
&+ \Delta^{\mu_1\ldots\mu_n}_{\nu_1\ldots\nu_n} \int \frac{d^3p}{(2\pi)^3p^0}\delta f W_p^{r-1} p^{\langle\lambda\rangle} (\nabla_\lambda p^{\langle\nu_1}p^{\nu_2}\ldots p^{\nu_n\rangle}) \\
&- \theta \int \frac{d^3p}{(2\pi)^3p^0} W_p^r \delta f p^{\langle\mu_1}p^{\mu_2}\ldots p^{\mu_n\rangle} \\
&+ \int \frac{d^3p}{(2\pi)^3p^0}\delta f (\nabla_\lambda W_p^{r-1}) p^{\langle\lambda\rangle} p^{\langle\mu_1}p^{\mu_2}\ldots p^{\mu_n\rangle}
\end{aligned} \tag{2.46}
$$

We continue to simplify the last two terms by calculating the gradients. Observe that

$$
\begin{aligned}
\nabla_\lambda W_p^{r-1} &= (r-1)W_p^{r-2}(\nabla_\lambda W_p) \\
&= -(r-1)W_p^{r-2}\nabla_\lambda(u_\alpha p^\alpha) \\
&= -(r-1)W_p^{r-2}p^\alpha \nabla_\lambda u_\alpha \\
&= -(r-1)W_p^{r-2}(p^{\langle\alpha\rangle} + W_p u^\alpha)\nabla_\lambda u_\alpha \\
&= -(r-1)W_p^{r-2}p^{\langle\alpha\rangle}\nabla_\lambda u_\alpha
\end{aligned} \tag{2.47}
$$

using the normalization condition $u_\alpha u^\alpha = -1$. Plugging this into Eq. (2.46) gives

$$
\begin{aligned}
\Delta^{\mu_1...\mu_n}_{\nu_1...\nu_n} D\rho_r^{\nu_1...\nu_n} = &-n\int \frac{d^3p}{(2\pi)^3 p^0}\delta f W_p^{r+1} p^{\langle\mu_1}p^{\mu_2}...a^{\mu_n\rangle} \\
&- r a_\sigma \int \frac{d^3p}{(2\pi)^3 p^0}\delta f W_p^{r-1} p^{\langle\sigma}p^{\mu_1}p^{\mu_2}...p^{\mu_n\rangle} \\
&- r\frac{n}{2n+1}\int \frac{d^3p}{(2\pi)^3 p^0}\delta f W_p^{r-1}(W_p^2 - m^2) p^{\langle\mu_1}p^{\mu_2}...a^{\mu_n\rangle} \\
&+ \int \frac{d^3p}{(2\pi)^3 p^0} C[f] W_p^{r-1} p^{\langle\mu_1}p^{\mu_2}...p^{\mu_n\rangle} \\
&- \int \frac{d^3p}{(2\pi)^3 p^0} (\partial_\lambda f_0) W_p^{r-1} p^\lambda p^{\langle\mu_1}p^{\mu_2}...p^{\mu_n\rangle} \\
&- \Delta^{\mu_1...\mu_n}_{\nu_1...\nu_n}\nabla_\lambda \int \frac{d^3p}{(2\pi)^3 p^0}\delta f W_p^{r-1} p^{\langle\lambda\rangle} p^{\langle\nu_1}p^{\nu_2}...p^{\nu_n\rangle} \\
&+ \Delta^{\mu_1...\mu_n}_{\nu_1...\nu_n} \int \frac{d^3p}{(2\pi)^3 p^0}\delta f W_p^{r-1} p^{\langle\lambda\rangle} (\nabla_\lambda p^{\langle\nu_1}p^{\nu_2}...p^{\nu_n\rangle}) \\
&- \theta \int \frac{d^3p}{(2\pi)^3 p^0} W_p^r \delta f p^{\langle\mu_1}p^{\mu_2}...p^{\mu_n\rangle} \\
&- (r-1) \int \frac{d^3p}{(2\pi)^3 p^0}\delta f W_p^{r-2} (\nabla_\lambda u_\alpha) p^{\langle\alpha\rangle} p^{\langle\lambda\rangle} p^{\langle\mu_1}p^{\mu_2}...p^{\mu_n\rangle}
\end{aligned}
\tag{2.48}
$$

Now, using Eq. (A.11) proven in Appendix A, the third-last term on the right-hand side can be written as

$$
\begin{aligned}
&\Delta^{\mu_1...\mu_n}_{\nu_1...\nu_n} \int \frac{d^3p}{(2\pi)^3 p^0}\delta f W_p^{r-1} p^{\langle\lambda\rangle} (\nabla_\lambda p^{\langle\nu_1}p^{\nu_2}...p^{\nu_n\rangle}) \\
&\quad = -n \int \frac{d^3p}{(2\pi)^3 p^0} W_p^r \delta f p^{\langle\lambda\rangle} p^{\langle\mu_1}p^{\mu_2}...\nabla_\lambda u^{\mu_n\rangle}
\end{aligned}
\tag{2.49}
$$

Eq. (2.48) now becomes

$$
\begin{aligned}
\Delta^{\mu_1\cdots\mu_n}_{\nu_1\cdots\nu_n} D\rho_r^{\nu_1\cdots\nu_n} = &-n\int \frac{d^3p}{(2\pi)^3p^0}\delta f W_p^{r+1} p^{\langle\mu_1}p^{\mu_2}...a^{\mu_n\rangle} \\
&- r a_\sigma \int \frac{d^3p}{(2\pi)^3p^0}\delta f W_p^{r-1} p^{\langle\sigma}p^{\mu_1}p^{\mu_2}...p^{\mu_n\rangle} \\
&- r\frac{n}{2n+1}\int \frac{d^3p}{(2\pi)^3p^0}\delta f W_p^{r-1}(W_p^2-m^2) p^{\langle\mu_1}p^{\mu_2}...a^{\mu_n\rangle} \\
&+ \int \frac{d^3p}{(2\pi)^3p^0} C[f] W_p^{r-1} p^{\langle\mu_1}p^{\mu_2}...p^{\mu_n\rangle} \\
&- \int \frac{d^3p}{(2\pi)^3p^0}(\partial_\lambda f_0) W_p^{r-1} p^\lambda p^{\langle\mu_1}p^{\mu_2}...p^{\mu_n\rangle} \\
&- \Delta^{\mu_1\cdots\mu_n}_{\nu_1\cdots\nu_n}\nabla_\lambda \int \frac{d^3p}{(2\pi)^3p^0}\delta f W_p^{r-1} p^{\langle\lambda\rangle}p^{\langle\nu_1}p^{\nu_2}...p^{\nu_n\rangle} \\
&- n\int \frac{d^3p}{(2\pi)^3p^0} W_p^r \delta f p^{\langle\lambda\rangle}p^{\langle\mu_1}p^{\mu_2}...\nabla_\lambda u^{\mu_n\rangle} \\
&- \theta\int \frac{d^3p}{(2\pi)^3p^0} W_p^r \delta f p^{\langle\mu_1}p^{\mu_2}...p^{\mu_n\rangle} \\
&- (r-1)\int \frac{d^3p}{(2\pi)^3p^0}\delta f W_p^{r-2}(\nabla_\lambda u_\alpha) p^{\langle\alpha\rangle}p^{\langle\lambda\rangle}p^{\langle\mu_1}p^{\mu_2}...p^{\mu_n\rangle}
\end{aligned}
\tag{2.50}
$$

Applying Eq. (2.39) again to the sixth term on the right-hand side, we get

$$
\begin{aligned}
&- \Delta^{\mu_1\cdots\mu_n}_{\nu_1\cdots\nu_n}\nabla_\lambda \int \frac{d^3p}{(2\pi)^3p^0}\delta f W_p^{r-1} p^{\langle\lambda\rangle}p^{\langle\nu_1}p^{\nu_2}...p^{\nu_n\rangle} \\
&= -\Delta^{\mu_1\cdots\mu_n}_{\nu_1\cdots\nu_n}\nabla_\lambda \int \frac{d^3p}{(2\pi)^3p^0}\delta f W_p^{r-1} p^{\langle\lambda}p^{\nu_1}p^{\nu_2}...p^{\nu_n\rangle} \\
&\quad - \frac{n}{2n+1}\Delta^{\mu_1\cdots\mu_n}_{\nu_1\cdots\nu_n}\nabla_\lambda \int \frac{d^3p}{(2\pi)^3p^0}\delta f W_p^{r-1}(W_p^2-m^2) p^{\langle\nu_1}p^{\nu_2}...\Delta^{\nu_n\rangle\lambda}
\end{aligned}
\tag{2.51}
$$

Plugging this back into Eq. (2.50) gives us

$$\begin{aligned}
\Delta^{\mu_1...\mu_n}_{\nu_1...\nu_n} D\rho_r^{\nu_1...\nu_n} = &\int \frac{d^3p}{(2\pi)^3 p^0} C[f] W_p^{r-1} p^{\langle\mu_1} p^{\mu_2} ... p^{\mu_n\rangle} \\
&- \int \frac{d^3p}{(2\pi)^3 p^0} (\partial_\lambda f_0) W_p^{r-1} p^\lambda p^{\langle\mu_1} p^{\mu_2} ... p^{\mu_n\rangle} \\
&- n \int \frac{d^3p}{(2\pi)^3 p^0} \delta f W_p^{r+1} p^{\langle\mu_1} p^{\mu_2} ... a^{\mu_n\rangle} \\
&- r \frac{n}{2n+1} \int \frac{d^3p}{(2\pi)^3 p^0} \delta f W_p^{r-1} (W_p^2 - m^2) p^{\langle\mu_1} p^{\mu_2} ... a^{\mu_n\rangle} \\
&- r a_\sigma \int \frac{d^3p}{(2\pi)^3 p^0} \delta f W_p^{r-1} p^{\langle\sigma} p^{\mu_1} p^{\mu_2} ... p^{\mu_n\rangle} \\
&- \Delta^{\mu_1...\mu_n}_{\nu_1...\nu_n} \nabla_\lambda \int \frac{d^3p}{(2\pi)^3 p^0} \delta f W_p^{r-1} p^{\langle\lambda} p^{\nu_1} p^{\nu_2} ... p^{\nu_n\rangle} \\
&- \frac{n}{2n+1} \Delta^{\mu_1...\mu_n}_{\nu_1...\nu_n} \nabla_\lambda \int \frac{d^3p}{(2\pi)^3 p^0} \delta f W_p^{r-1} (W_p^2 - m^2) p^{\langle\nu_1} p^{\nu_2} ... \Delta^{\nu_n\rangle\lambda} \\
&- n \int \frac{d^3p}{(2\pi)^3 p^0} W_p^r \delta f p^{\langle\lambda\rangle} p^{\langle\mu_1} p^{\mu_2} ... \nabla_\lambda u^{\mu_n\rangle} \\
&- \theta \int \frac{d^3p}{(2\pi)^3 p^0} W_p^r \delta f p^{\langle\mu_1} p^{\mu_2} ... p^{\mu_n\rangle} \\
&- (r-1) \int \frac{d^3p}{(2\pi)^3 p^0} \delta f W_p^{r-2} (\nabla_\lambda u_\alpha) p^{\langle\alpha\rangle} p^{\langle\lambda\rangle} p^{\langle\mu_1} p^{\mu_2} ... p^{\mu_n\rangle}
\end{aligned} \tag{2.52}$$

Using the definition of the moments, we get

$$
\begin{aligned}
\Delta^{\mu_1\ldots\mu_n}_{\nu_1\ldots\nu_n} D\rho_r^{\nu_1\ldots\nu_n} = & \int \frac{d^3p}{(2\pi)^3 p^0} C[f] W_p^{r-1} p^{\langle\mu_1} p^{\mu_2} \ldots p^{\mu_n\rangle} \\
& - \int \frac{d^3p}{(2\pi)^3 p^0} (\partial_\lambda f_0) W_p^{r-1} p^\lambda p^{\langle\mu_1} p^{\mu_2} \ldots p^{\mu_n\rangle} \\
& - \theta \rho_r^{\mu_1\cdots\mu_n} \\
& - \Delta^{\mu_1\ldots\mu_n}_{\nu_1\ldots\nu_n} \nabla_\lambda \rho_{r-1}^{\lambda\nu_1\cdots\nu_n} \\
& - \frac{n}{2n+1} \left(\nabla^{\langle\mu_1} \rho_{r+1}^{\mu_2\cdots\mu_n\rangle} - m^2 \nabla^{\langle\mu_1} \rho_{r-1}^{\mu_2\cdots\mu_n\rangle} \right) \\
& - r a_\alpha \rho_{r-1}^{\alpha\mu_1\cdots\mu_n} \\
& + r \frac{n}{2n+1} m^2 \rho_{r-1}^{\langle\mu_1\cdots\mu_{n-1}} a^{\mu_n\rangle} \\
& - \frac{n(r+2n+1)}{2n+1} \rho_{r+1}^{\langle\mu_1\cdots\mu_{n-1}} a^{\mu_n\rangle} \\
& - n \int \frac{d^3p}{(2\pi)^3 p^0} W_p^r \delta f p^{\langle\lambda\rangle} p^{\langle\mu_1} p^{\mu_2} \ldots \nabla_\lambda u^{\mu_n\rangle} \\
& - (r-1) \int \frac{d^3p}{(2\pi)^3 p^0} \delta f W_p^{r-2} (\nabla_\lambda u_\alpha) p^{\langle\alpha\rangle} p^{\langle\lambda\rangle} p^{\langle\mu_1} p^{\mu_2} \ldots p^{\mu_n\rangle}
\end{aligned}
\tag{2.53}
$$

Now, we can further expand the term $-n \int \frac{d^3p}{(2\pi)^3 p^0} W_p^r \delta f p^{\langle\lambda\rangle} p^{\langle\mu_1} p^{\mu_2} \ldots \nabla_\lambda u^{\mu_n\rangle}$ as the following:

$$
\begin{aligned}
& - n \int \frac{d^3p}{(2\pi)^3 p^0} W_p^r \delta f p^{\langle\lambda\rangle} p^{\langle\mu_1} p^{\mu_2} \ldots \nabla_\lambda u^{\mu_n\rangle} \\
& = - \int \frac{d^3p}{(2\pi)^3 p^0} W_p^r \delta f \left(\sum_{i=1}^{n} (\nabla_\lambda u^{\mu_i}) p^{\langle\lambda\rangle} p^{\langle\mu_1\cdots} p^{\mu_{i-1}} p^{\mu_{i+1}\cdots} p^{\mu_n\rangle} \right) \\
& \quad + \frac{2}{2n-1} \int \frac{d^3p}{(2\pi)^3 p^0} W_p^r \delta f \left(\sum_{i\neq j}^{n} \Delta^{\mu_i\mu_j} (\nabla_\lambda u_\alpha) p^{\langle\lambda\rangle} p^{\langle\alpha} p^{\mu_1\cdots} p^{\mu_{i-1}} p^{\mu_{i+1}\cdots} p^{\mu_{j-1}} p^{\mu_{j+1}\cdots} p^{\mu_n\rangle} \right)
\end{aligned}
\tag{2.54}
$$

where we used

$$p^{\langle\mu_1\cdots}p^{\mu_{n-1}}a^{\mu_n\rangle} = \frac{1}{n}\sum_{i=1}^{n} a^{\mu_i}p^{\langle\mu_1\cdots}p^{\mu_{i-1}}p^{\mu_{i+1}\cdots}p^{\mu_n\rangle} - \frac{2}{n(2n-1)}\sum_{i\neq j}^{n}\Delta^{\mu_i\mu_j}a_\lambda p^{\langle\lambda}p^{\mu_1\cdots}p^{\mu_{i-1}}p^{\mu_{i+1}\cdots}p^{\mu_{j-1}}p^{\mu_{j+1}\cdots}p^{\mu_n\rangle} \tag{2.55}$$

in which a^μ is an arbitrary vector, which can be easily replaced by a rank-2 tensor by fixing one of the two indices. Using Eq. (2.39) to combine the angular brackets, we can further expand Eq. (2.54) as

$$\begin{aligned}
&-n\int\frac{d^3p}{(2\pi)^3p^0}W_p^r\delta f p^{\langle\lambda\rangle}p^{\langle\mu_1}p^{\mu_2}\ldots\nabla_\lambda u^{\mu_n\rangle}\\
&=-\int\frac{d^3p}{(2\pi)^3p^0}W_p^r\delta f\sum_{i=1}^{n}(\nabla_\lambda u^{\mu_i})p^{\langle\lambda}p^{\mu_1\cdots}p^{\mu_{i-1}}p^{\mu_{i+1}\cdots}p^{\mu_n\rangle}\\
&\quad-\frac{n-1}{2n-1}\int\frac{d^3p}{(2\pi)^3p^0}W_p^r\delta f\sum_{i=1}^{n}(\nabla_\lambda u^{\mu_i})(W_p^2-m^2)p^{\langle\mu_1\cdots}p^{\mu_{i-1}}p^{\mu_{i+1}\cdots}\Delta^{\mu_n\rangle\lambda}\\
&\quad+\frac{2}{2n-1}\int\frac{d^3p}{(2\pi)^3p^0}W_p^r\delta f\sum_{i\neq j}^{n}\Delta^{\mu_i\mu_j}(\nabla_\lambda u_\alpha)p^{\langle\lambda}p^\alpha p^{\mu_1\cdots}p^{\mu_{i-1}}p^{\mu_{i+1}\cdots}p^{\mu_{j-1}}p^{\mu_{j+1}\cdots}p^{\mu_n\rangle}\\
&\quad+\frac{2(n-1)}{(2n-1)^2}\int\frac{d^3p}{(2\pi)^3p^0}W_p^r\delta f\sum_{i\neq j}^{n}\Delta^{\mu_i\mu_j}(\nabla_\lambda u_\alpha)(W_p^2-m^2)p^{\langle\alpha}p^{\mu_1\cdots}p^{\mu_{i-1}}p^{\mu_{i+1}\cdots}p^{\mu_{j-1}}p^{\mu_{j+1}\cdots}\Delta^{\mu_n\rangle\lambda}
\end{aligned} \tag{2.56}$$

which can be written in terms of the moments:

$$
\begin{aligned}
& -n\int \frac{d^3p}{(2\pi)^3p^0} W_p^r \delta f p^{\langle\lambda\rangle} p^{\langle\mu_1} p^{\mu_2} ... \nabla_\lambda u^{\mu_n\rangle} \\
&= -\sum_{i=1}^{n} (\nabla_\lambda u^{\mu_i}) \rho_r^{\lambda\mu_1\cdots\mu_{i-1}\mu_{i+1}\cdots\mu_n} \\
&\quad + \frac{2}{2n-1}\sum_{i\neq j}^{n} \Delta^{\mu_i\mu_j} (\nabla_\lambda u_\alpha) \rho_r^{\lambda\alpha\mu_1\cdots\mu_{i-1}\mu_{i+1}\cdots\mu_{j-1}\mu_{j+1}\cdots\mu_n} \\
&\quad - \frac{n-1}{2n-1}\sum_{i=1}^{n} \rho_{r+2}^{\langle\mu_1\cdots\mu_{i-1}\mu_{i+1}\cdots\mu_{n-1}} \nabla^{\mu_n\rangle} u^{\mu_i} \\
&\quad + \frac{2(n-1)}{(2n-1)^2}\sum_{i\neq j}^{n} \Delta^{\mu_i\mu_j} \rho_{r+2}^{\langle\alpha\mu_1\cdots\mu_{i-1}\mu_{i+1}\cdots\mu_{j-1}\mu_{j+1}\cdots\mu_{n-1}} \nabla^{\mu_n\rangle} u_\alpha \\
&\quad + \frac{m^2(n-1)}{2n-1}\sum_{i=1}^{n} \rho_{r}^{\langle\mu_1\cdots\mu_{i-1}\mu_{i+1}\cdots\mu_{n-1}} \nabla^{\mu_n\rangle} u^{\mu_i} \\
&\quad - \frac{2m^2(n-1)}{(2n-1)^2}\sum_{i\neq j}^{n} \Delta^{\mu_i\mu_j} \rho_{r}^{\langle\alpha\mu_1\cdots\mu_{i-1}\mu_{i+1}\cdots\mu_{j-1}\mu_{j+1}\cdots\mu_{n-1}} \nabla^{\mu_n\rangle} u_\alpha \\
&= -\sum_{i=1}^{n} \nabla_\lambda u^{\langle\mu_i} \rho_r^{\mu_1\cdots\mu_{i-1}\mu_{i+1}\cdots\mu_n\rangle\lambda} \\
&\quad - \frac{n-1}{2n-1}\sum_{i=1}^{n} \rho_{r+2}^{\langle\mu_1\cdots\mu_{i-1}\mu_{i+1}\cdots\mu_{n-1}} \sigma^{\mu_n\mu_i\rangle} \\
&\quad + \frac{m^2(n-1)}{2n-1}\sum_{i=1}^{n} \rho_{r}^{\langle\mu_1\cdots\mu_{i-1}\mu_{i+1}\cdots\mu_{n-1}} \sigma^{\mu_n\mu_i\rangle}
\end{aligned}
\tag{2.57}
$$

where

$$
\sigma^{\mu\nu} = \nabla^{\langle\mu} u^{\nu\rangle} \tag{2.58}
$$

is the symmetric Navier-Stokes shear tensor. Since the angular bracket represents the traceless and symmetric combination of the Lorentz indices, all permutations of the Lorentz indices inside the bracket give the same term. Thus

$$\begin{aligned}
& -n\int \frac{d^3p}{(2\pi)^3p^0}W_p^r\delta f p^{\langle\lambda\rangle}p^{\langle\mu_1}p^{\mu_2}...\nabla_\lambda u^{\mu_n\rangle} \\
& = -n\rho_r^{\lambda\langle\mu_1\ldots\mu_{n-1}}\nabla_\lambda u^{\mu_n\rangle} - \frac{n(n-1)}{2n-1}\rho_{r+2}^{\langle\mu_1\ldots\mu_{n-2}}\sigma^{\mu_{n-1}\mu_n\rangle} \\
& \quad + \frac{m^2(n-1)n}{2n-1}\rho_r^{\langle\mu_1\ldots\mu_{n-2}}\sigma^{\mu_{n-1}\mu_n\rangle}
\end{aligned} \tag{2.59}$$

Here, we can replace $\nabla_\lambda u^{\mu_n}$ using

$$\nabla^\lambda u^\mu = \sigma^{\mu\nu} + \omega^{\mu\nu} + \frac{\theta}{3}\Delta^{\mu\nu} \tag{2.60}$$

where

$$\omega^{\mu\nu} = \frac{1}{2}\bigg(\nabla^\mu u^\nu - \nabla^\nu u^\mu\bigg) \tag{2.61}$$

is the anti-symmetric vorticity tensor. Doing so gives us

$$\begin{aligned}
& -n\int \frac{d^3p}{(2\pi)^3p^0}W_p^r\delta f p^{\langle\lambda\rangle}p^{\langle\mu_1}p^{\mu_2}...\nabla_\lambda u^{\mu_n\rangle} \\
& = -n\rho_r^{\lambda\langle\mu_1\ldots\mu_{n-1}}\sigma_\lambda^{\mu_n\rangle} - n\rho_r^{\lambda\langle\mu_1\ldots\mu_{n-1}}\omega_\lambda^{\mu_n\rangle} - \frac{n}{3}\theta\rho_r^{\mu_1\ldots\mu_n} \\
& \quad - \frac{n(n-1)}{2n-1}\rho_{r+2}^{\langle\mu_1\ldots\mu_{n-2}}\sigma^{\mu_{n-1}\mu_n\rangle} + \frac{m^2(n-1)n}{2n-1}\rho_r^{\langle\mu_1\ldots\mu_{n-2}}\sigma^{\mu_{n-1}\mu_n\rangle}
\end{aligned} \tag{2.62}$$

Now let's go back to the general moment equation Eq. (2.53) and take a look at the term $-(r-1)\int \frac{d^3p}{(2\pi)^3p^0}\delta f W_p^{r-2}(\nabla_\lambda u_\alpha)p^{\langle\alpha\rangle}p^{\langle\lambda\rangle}p^{\langle\mu_1}p^{\mu_2}...p^{\mu_n\rangle}$. Using Eq. (2.60), this term can be written as

$$\begin{aligned}
&-(r-1)\int \frac{d^3p}{(2\pi)^3p^0}\delta f W_p^{r-2}(\nabla_\lambda u_\alpha)p^{\langle\alpha\rangle}p^{\langle\lambda\rangle}p^{\langle\mu_1}p^{\mu_2}...p^{\mu_n\rangle} \\
&=-(r-1)\sigma_{\lambda\alpha}\int \frac{d^3p}{(2\pi)^3p^0}\delta f W_p^{r-2}p^{\langle\alpha\rangle}p^{\langle\lambda\rangle}p^{\langle\mu_1}p^{\mu_2}...p^{\mu_n\rangle} \\
&\quad-\frac{(r-1)}{3}\theta\int \frac{d^3p}{(2\pi)^3p^0}\delta f W_p^{r-2}(W_p^2-m^2)p^{\langle\mu_1}p^{\mu_2}...p^{\mu_n\rangle} \\
&=-(r-1)\sigma_{\lambda\alpha}\int \frac{d^3p}{(2\pi)^3p^0}\delta f W_p^{r-2}p^{\langle\alpha\rangle}p^{\langle\lambda\rangle}p^{\langle\mu_1}p^{\mu_2}...p^{\mu_n\rangle} \\
&\quad-\frac{(r-1)}{3}\theta\rho_r^{\mu_1...\mu_n}+\frac{(r-1)m^2}{3}\theta\rho_{r-2}^{\mu_1...\mu_n}
\end{aligned} \tag{2.63}$$

Note that the term with $\omega_{\lambda\alpha}$ vanishes due to its anti-symmetric property. We then proceed to expand the first term on the right-hand side using the following identity analogous to Eq. (2.39):

$$\begin{aligned}
&p^{\langle\alpha\rangle}p^{\langle\lambda\rangle}p^{\langle\mu_1}\cdots p^{\mu_{n-1}}p^{\mu_n\rangle} \\
&=p^{\langle\alpha}p^{\lambda}p^{\mu_1}\cdots p^{\mu_{n-1}}p^{\mu_n\rangle} \\
&\quad+\frac{1}{(2n+3)}\left(W_p^2-m^2\right)\left(\sum_{i=1}^{n}\Delta^{\mu_i\alpha}p^{\langle\lambda}p^{\mu_1}\cdots p^{\mu_{i-1}}p^{\mu_{i+1}}\cdots p^{\mu_n\rangle}\right. \\
&\quad\left.-\frac{2}{(2n-1)}\sum_{i\neq j}^{n}\Delta^{\mu_i\mu_j}p^{\langle\alpha}p^{\lambda}p^{\mu_1}\cdots p^{\mu_{i-1}}p^{\mu_{i+1}}\cdots p^{\mu_{j-1}}p^{\mu_{j+1}}\cdots p^{\mu_n\rangle}\right) \\
&\quad+\frac{1}{(2n+3)}\left(W_p^2-m^2\right)\left(\sum_{i=1}^{n}\Delta^{\mu_i\lambda}p^{\langle\alpha}p^{\mu_1}\cdots p^{\mu_{i-1}}p^{\mu_{i+1}}\cdots p^{\mu_n\rangle}\right. \\
&\quad\left.-\frac{2}{(2n-1)}\sum_{i\neq j}^{n}\Delta^{\mu_i\mu_j}p^{\langle\alpha}p^{\lambda}p^{\mu_1}\cdots p^{\mu_{i-1}}p^{\mu_{i+1}}\cdots p^{\mu_{j-1}}p^{\mu_{j+1}}\cdots p^{\mu_n\rangle}\right) \\
&\quad+\frac{1}{(2n+3)}\left(W_p^2-m^2\right)\left(\Delta^{\lambda\alpha}p^{\langle\mu_1}\cdots p^{\mu_n\rangle}\right) \\
&\quad+\frac{n(n-1)}{(2n+1)(2n-1)}\left(W_p^2-m^2\right)^2\left(p^{\langle\mu_1}\cdots p^{\mu_{n-2}}\Delta_{\alpha'}^{\mu_{n-1}}\Delta_{\lambda'}^{\mu_n\rangle}\right)\Delta^{\alpha\alpha'}\Delta^{\lambda\lambda'}
\end{aligned} \tag{2.64}$$

which is obtained by considering all the possible symmetric combinations of the momenta and projectors. This leads to

$$
\begin{aligned}
&-(r-1)\sigma_{\lambda\alpha}\int\frac{d^3p}{(2\pi)^3p^0}\delta f W_p^{r-2}p^{\langle\alpha\rangle}p^{\langle\lambda\rangle}p^{\langle\mu_1}p^{\mu_2}...p^{\mu_n\rangle} \\
&=-(r-1)\sigma_{\lambda\alpha}\rho_{r-2}^{\alpha\lambda\mu_1\dots\mu_n} \\
&\quad-\frac{2(r-1)}{2n+3}\sum_{i=1}^{n}\sigma_{\alpha}^{\mu_i}\rho_r^{\alpha\mu_1\dots\mu_{i-1}\mu_{i+1}\dots\mu_n} \\
&\quad+\frac{4(r-1)}{(2n+3)(2n-1)}\sum_{i\neq j}^{n}\Delta^{\mu_i\mu_j}\sigma_{\lambda\alpha}\rho_r^{\alpha\lambda\mu_1\dots\mu_{i-1}\mu_{i+1}\dots\mu_{j-1}\mu_{j+1}\dots\mu_n} \\
&\quad+\frac{2m^2(r-1)}{2n+3}\sum_{i=1}^{n}\sigma_{\alpha}^{\mu_i}\rho_{r-2}^{\alpha\mu_1\dots\mu_{i-1}\mu_{i+1}\dots\mu_n} \\
&\quad-\frac{4m^2(r-1)}{(2n+3)(2n-1)}\sum_{i\neq j}^{n}\Delta^{\mu_i\mu_j}\sigma_{\lambda\alpha}\rho_{r-2}^{\alpha\lambda\mu_1\dots\mu_{i-1}\mu_{i+1}\dots\mu_{j-1}\mu_{j+1}\dots\mu_n} \\
&\quad-\frac{(r-1)(n-1)n}{(2n+1)(2n-1)}\rho_{r+2}^{\langle\mu_1\dots\mu_{n-2}}\sigma^{\mu_{n-1}\mu_n\rangle} \\
&\quad+\frac{2m^2(r-1)(n-1)n}{(2n+1)(2n-1)}\rho_{r}^{\langle\mu_1\dots\mu_{n-2}}\sigma^{\mu_{n-1}\mu_n\rangle} \\
&\quad-\frac{m^4(r-1)(n-1)n}{(2n+1)(2n-1)}\rho_{r-2}^{\langle\mu_1\dots\mu_{n-2}}\sigma^{\mu_{n-1}\mu_n\rangle}
\end{aligned}
\tag{2.65}
$$

Note that each pair of summations give the traceless and symmetric combination of $\sigma_{\alpha}^{\mu_i}$ and $\rho_r^{\alpha\mu_1\cdots\mu_{i-1}\mu_{i+1}\cdots\mu_n}$. Thus this reduces to

$$\begin{aligned}
&-(r-1)\sigma_{\lambda\alpha}\int\frac{d^3p}{(2\pi)^3p^0}\delta f W_p^{r-2}p^{\langle\alpha\rangle}p^{\langle\lambda\rangle}p^{\langle\mu_1}p^{\mu_2}...p^{\mu_n\rangle}\\
&=-(r-1)\sigma_{\lambda\alpha}\rho_{r-2}^{\alpha\lambda\mu_1\cdots\mu_n}\\
&\quad-\frac{2(r-1)}{2n+3}\sum_{i=1}^{n}\sigma_{\alpha}^{\langle\mu_i}\rho_r^{\mu_1\cdots\mu_{i-1}\mu_{i+1}\cdots\mu_n\rangle\alpha}\\
&\quad+\frac{2m^2(r-1)}{2n+3}\sum_{i=1}^{n}\sigma_{\alpha}^{\langle\mu_i}\rho_{r-2}^{\mu_1\cdots\mu_{i-1}\mu_{i+1}\cdots\mu_n\rangle\alpha}\\
&\quad-\frac{(r-1)(n-1)n}{(2n+1)(2n-1)}\rho_{r+2}^{\langle\mu_1\cdots\mu_{n-2}}\sigma^{\mu_{n-1}\mu_n\rangle}\\
&\quad+\frac{2m^2(r-1)(n-1)n}{(2n+1)(2n-1)}\rho_{r}^{\langle\mu_1\cdots\mu_{n-2}}\sigma^{\mu_{n-1}\mu_n\rangle}\\
&\quad-\frac{m^4(r-1)(n-1)n}{(2n+1)(2n-1)}\rho_{r-2}^{\langle\mu_1\cdots\mu_{n-2}}\sigma^{\mu_{n-1}\mu_n\rangle}
\end{aligned}\tag{2.66}$$

Since all permutations of the Lorentz indices inside the angular brackets give the same term, this can be simplified to

$$\begin{aligned}
&-(r-1)\sigma_{\lambda\alpha}\int\frac{d^3p}{(2\pi)^3p^0}\delta f W_p^{r-2}p^{\langle\alpha\rangle}p^{\langle\lambda\rangle}p^{\langle\mu_1}p^{\mu_2}...p^{\mu_n\rangle}\\
&=-(r-1)\sigma_{\lambda\alpha}\rho_{r-2}^{\alpha\lambda\mu_1\cdots\mu_n}\\
&\quad-\frac{2(r-1)n}{2n+3}\rho_r^{\alpha\langle\mu_1\cdots\mu_{n-1}}\sigma_{\alpha}^{\mu_n\rangle}\\
&\quad+\frac{2m^2(r-1)n}{2n+3}\rho_{r-2}^{\alpha\langle\mu_1\cdots\mu_{n-1}}\sigma_{\alpha}^{\mu_n\rangle}\\
&\quad-\frac{(r-1)(n-1)n}{(2n+1)(2n-1)}\rho_{r+2}^{\langle\mu_1\cdots\mu_{n-2}}\sigma^{\mu_{n-1}\mu_n\rangle}\\
&\quad+\frac{2m^2(r-1)(n-1)n}{(2n+1)(2n-1)}\rho_{r}^{\langle\mu_1\cdots\mu_{n-2}}\sigma^{\mu_{n-1}\mu_n\rangle}\\
&\quad-\frac{m^4(r-1)(n-1)n}{(2n+1)(2n-1)}\rho_{r-2}^{\langle\mu_1\cdots\mu_{n-2}}\sigma^{\mu_{n-1}\mu_n\rangle}
\end{aligned}\tag{2.67}$$

Plugging all the above results back into Eq. (2.53), and expressing everything in terms of the moments, we arrive at the final form of the general moment equation:

$$
\begin{aligned}
\Delta^{\mu_1\dots\mu_n}_{\nu_1\dots\nu_n} D\rho_r^{\nu_1\dots\nu_n} = & \int \frac{d^3p}{(2\pi)^3 p^0} C[f] W_p^{r-1} p^{\langle\mu_1} p^{\mu_2} \dots p^{\mu_n\rangle} \\
& - \int \frac{d^3p}{(2\pi)^3 p^0} (\partial_\lambda f_0) W_p^{r-1} p^\lambda p^{\langle\mu_1} p^{\mu_2} \dots p^{\mu_n\rangle} \\
& - \frac{n(2n+r+1)}{2n+1} \rho_{r+1}^{\langle\mu_1\dots\mu_{n-1}} a^{\mu_n\rangle} \\
& + rm^2 \frac{n}{2n+1} \rho_{r-1}^{\langle\mu_1\dots\mu_{n-1}} a^{\mu_n\rangle} \\
& - r a_\lambda \rho_{r-1}^{\lambda\mu_1\dots\mu_n} \\
& - \Delta^{\mu_1\dots\mu_n}_{\nu_1\dots\nu_n} \nabla_\lambda \rho_{r-1}^{\lambda\nu_1\dots\nu_n} \\
& - \frac{n}{2n+1} \nabla^{\langle\mu_1} \rho_{r+1}^{\mu_2\dots\mu_n\rangle} \\
& + m^2 \frac{n}{2n+1} \nabla^{\langle\mu_1} \rho_{r-1}^{\mu_2\dots\mu_n\rangle} \\
& - \frac{n+r+2}{3} \theta \rho_r^{\mu_1\dots\mu_n} \\
& - (r-1) \sigma_{\lambda\alpha} \rho_{r-2}^{\alpha\lambda\mu_1\dots\mu_n} \\
& + \frac{(r-1)m^2}{3} \theta \rho_{r-2}^{\mu_1\dots\mu_n} \\
& - \frac{n(2n+2r+1)}{2n+3} \rho_r^{\lambda\langle\mu_1\dots\mu_{n-1}} \sigma_\lambda^{\mu_n\rangle} \\
& - n \rho_r^{\lambda\langle\mu_1\dots\mu_{n-1}} \omega_\lambda^{\mu_n\rangle} \\
& - \frac{(2n+r)(n-1)n}{(2n-1)(2n+1)} \rho_{r+2}^{\langle\mu_1\dots\mu_{n-2}} \sigma^{\mu_{n-1}\mu_n\rangle} \\
& + 2m^2 \frac{(r-1)n}{2n+3} \rho_{r-2}^{\lambda\langle\mu_1\dots\mu_{n-1}} \sigma_\lambda^{\mu_n\rangle} \\
& - m^4 \frac{(r-1)(n-1)n}{(2n+1)(2n-1)} \rho_{r-2}^{\langle\mu_1\dots\mu_{n-2}} \sigma^{\mu_{n-1}\mu_n\rangle} \\
& + m^2 \frac{(2n+2r-1)(n-1)n}{(2n+1)(2n-1)} \rho_r^{\langle\mu_1\dots\mu_{n-2}} \sigma^{\mu_{n-1}\mu_n\rangle}
\end{aligned}
\tag{2.68}
$$

By letting $n = 0, 1, 2$, this result agrees with the general equations of motion displayed in [63], in which the local equilibrium term is expanded in terms of the hydrodynamic variables.

Chapter 3

Second-Order Regularized Hydrodynamics

In this chapter, we will extend the non-relativistic regularized 13-moment hydrodynamics to the relativistic regularized second-order 14-moment hydrodynamics (R14). We will then conduct a series of linear stability and causality analyses on both the longitudinal and transverse components of the evolution equations with some assumptions. The derivation and analysis of the third-order equations will be addressed in the subsequent chapter.

3.1 Second-Order Moment Equations

The 14 moments in "R14" encompass energy density ε, particle number density ν, fluid flow velocity u^μ, shear stress tensor $\pi^{\mu\nu}$, bulk viscous pressure Π, and diffusion current q^μ. Due to the traceless and symmetric properties, the number of independent moments in a rank-n tensor is $2n+1$. One can verify that the total number of the above moments is indeed 14. As already mentioned earlier, the evolution equations for ϵ, ν, and u^μ are given by the conservation of energy, particle number, and momentum respectively. The thermal pressure P_0, on the other hand, depends on ε and ν, as specified by the equation of state. Thus, at this point, we need to derive the evolution equations for all the other moments, which are Π, q^μ, and $\pi^{\mu\nu}$, using the general moment equation Eq. (2.68). Upon closer examination of the general moment equation, it becomes apparent that numerous energy-momentum moments appear on the right-hand side. Specifically, the equation for $\rho_r^{\mu_1\cdots\mu_n}$ can include energy orders ranging from $r-2$ to $r+2$ and momentum orders from $n-2$ to $n+2$. Consequently, the 14-moment equations are not closed, and a means of linking additional moments to the existing 14 moments (i.e., the closure problem) must be devised to generate a well-defined set of hydrodynamic equations.

In a series of papers [50–53], Struchtrup and Torrilhon developed a novel method that combines the method of moments and the Chapman-Enskog expansion. This technique commences by utilizing the general evolution equations for the energy-momentum moments (Eq.(2.68)), then applying a Chapman-Enskog-like expansion directly to the moments instead of δf, excluding the 14 moments that are left intact. This is because, as we shall see later, the 14 moments are of first-order in the expansion and their corresponding moment equations do not generate evolution equations at the lowest order. By using this technique, there is no room for arbitrariness in choosing the closure conditions, and it systematically produces a unique set of equations at any order in the expansion parameter ϵ. We will demonstrate this technique in the following sections.

3.1.1 Equilibrium Term

In the general moment equation Eq.(2.68), the leading order $O(1)$ contribution comes from the equilibrium density term (the second term on the right-hand side)

$$F_r^{\mu_1\cdots\mu_n} = \int \frac{d^3p}{(2\pi)^3 p^0} W_p^r p^{\langle\mu_1} \cdots p^{\mu_{n-1}} p^{\mu_n\rangle} p^\lambda \partial_\lambda f_0 \tag{3.1}$$

where $f_0 = e^{-\beta W_p + \alpha}$ is the local equilibrium density function. The temperature, chemical potential, and fluid velocity are all functions of position and time. Following Eq. (2.43), the space-time derivative can be decomposed as

$$p^{\lambda}\partial_{\lambda} = p^{\langle\lambda\rangle}\nabla_{\lambda} + W_p D \tag{3.2}$$

It is then clear that $p^{\lambda}\partial_{\lambda} f_0 = f_0 p^{\lambda}\partial_{\lambda}(\alpha - W_p\beta)$ can contain only $1, p^{\langle\mu_1\rangle}, p^{\langle\mu_1}p^{\mu_2\rangle}$. Hence the orthogonality of $p^{\langle\mu_1}\cdots p^{\mu_n\rangle}$ (i.e. Eq. (16) in [63]) demands that

$$F_r^{\mu_1\cdots\mu_n} = 0 \quad \text{for } n \geq 3 \tag{3.3}$$

For $n = 0, 1, 2$, we get

$$F_r = \phi_{r|0}\theta + \phi^{q}_{r|1}\partial_{\mu}q^{\mu} + \phi^{\pi\Pi}_{r|1}(\pi^{\gamma\rho}\sigma_{\gamma\rho} + \theta\Pi) \tag{3.4}$$

$$F_r^{\mu} = \psi_{r|0}\nabla^{\mu}\alpha + \psi_{r|1}\left(\Delta^{\mu}_{\gamma}\partial_{\rho}\pi^{\rho\gamma} + (\nabla^{\mu}\Pi) + a^{\mu}\Pi\right) \tag{3.5}$$

$$F_r^{\mu\nu} = \varphi_{r|0}\sigma^{\mu\nu} \tag{3.6}$$

where the coefficient functions ϕ, ψ and φ are functions of α and β only. Recall that $\theta = \nabla_{\mu}u^{\mu}$ is the expansion rate of the fluid cell. Observe that F_r, F_r^{μ} and $F_r^{\mu\nu}$ all involve gradients and time derivatives of the hydrodynamic variables. Consequently, they can be physically described as the forces that are driving the evolution of the system. In deriving the above expressions, we have used the conservation laws Eqs. (2.4) and (2.6) to express any time derivative in terms of spatial derivatives. Details can be found in Appendix B. From now on, the index preceded by a vertical bar on any quantity indicates the order in the formal expansion parameter ϵ. For instance, $\psi_{r|0}$ is the $O(1)$ coefficient of F_r^{μ}. The notation $F_{r|0}^{\mu_1\cdots\mu_n}$ is for the $O(1)$ part of $F_r^{\mu_1\cdots\mu_n}$ and $F_{r|1}^{\mu_1\cdots\mu_n}$ is the collective $O(\epsilon)$ part. As we will see in the next section, Π, q^{μ} and $\pi^{\mu\nu}$ are all $O(\epsilon)$.

3.1.2 Power Counting in ϵ

In the Chapman-Enskog method, the collision term is scaled as $C[f] \to (1/\epsilon)C[f]$ and the non-equilibrium part of the phase space density is expanded as

$$\delta f = \sum_{n=1}^{\infty} \epsilon^n \delta f_{|n} \tag{3.7}$$

These are then plugged into the Boltzmann equation. Collecting terms having the same power of ϵ, the n-th order piece $\delta f_{|n}$ can be found iteratively at each order of ϵ. This in turn determines $\delta T^{\mu\nu}_{|n}$ and $q^{\mu}_{|n}$ which are expressed solely in terms of $\alpha, \beta, \mathbf{u}$ and their derivatives. As such, the Chapman-Enskog procedure does not yield separate evolution equations for $\delta T^{\mu\nu}$ and q^{μ}. The resulting equations are often acausal and can lead to instability [38–43]. To obtain the evolution equations for $\delta T^{\mu\nu}$ and q^{μ} within the Chapman-Enskog method, one needs to substitute time derivatives of $\delta T^{\mu\nu}_{|n}$ and $q^{\mu}_{|n}$ with the equivalent time derivatives of δT and q^{μ} without spoiling the ϵ accuracy. For instance, in [60], this procedure was carried out up to $O(\epsilon^2)$.

In the R14 method, instead of δf, the energy-momentum moments of δf are expanded in powers of ϵ

$$\rho_r^{\mu_1\cdots\mu_n} = \sum_{n=1}^{\infty} \epsilon^n \rho_{r|n}^{\mu_1\cdots\mu_n} \tag{3.8}$$

Working out the order-by-order solution by putting Eq.(3.8) in Eq.(2.68) would be completely equivalent to iteratively finding $\delta f_{|n}$. What we would like to do differently, however, is *not* to expand the bulk pressure, $\rho_0 = -\Pi(3/m^2)$, the dissipative current $\rho_0^{\mu} = q^{\mu}$ and the shear tensor $\rho_0^{\mu\nu} = \pi^{\mu\nu}$ whenever they occur while expanding all other moments. In this way, the evolution equations for these quantities will naturally result in closed evolution equations for them while all other energy-momentum moments are expressed in terms of the 14 moments. The purpose of this dissertation is to derive these evolution equations up to and including the $O(\epsilon^2)$ terms (the third order). This subsection establishes the ϵ-order of energy-momentum moments.

To be concrete, we use the relaxation time approximation for the collision term

$$C[f] = -\frac{W_p}{\epsilon\,\tau_R}\delta f(x,p) \tag{3.9}$$

where we have explicitly indicated the expansion parameter ϵ. The relaxation time τ_R is a function of β and α only. The parameter ϵ stands for the Knudsen number and at the end of the calculations, ϵ is set to 1. The relaxation time approximation has a significant physical meaning: when a system in local thermal equilibrium undergoes slight perturbations, it will eventually return to its original equilibrium state, with a time scale determined by the relaxation time τ_R. Putting Eqs. (3.8) and (3.9) into the general moment equation Eq. (2.68) and collecting the $O(1)$ terms, we get

$$\rho_{r|1}^{\mu_1\cdots\mu_n} = -\tau_R F_{r-1|0}^{\mu_1\cdots\mu_n} \tag{3.10}$$

where $F_{r-1|0}^{\mu_1\cdots\mu_n}$ is the $O(1)$ part of $F_{r-1}^{\mu_1\cdots\mu_n}$. Since $F_r^{\mu_1\cdots\mu_n} = 0$ for $n \geq 3$ (e.g. Eq.(3.3)), it is clear that $\rho_{r|1}^{\mu_1\cdots\mu_n} = 0$ for $n \geq 3$. Hence

$$\rho_r, \rho_r^{\mu}, \rho_r^{\mu_1\mu_2} = O(\epsilon) \tag{3.11}$$

$$\rho_r^{\mu_1\cdots\mu_n} = O(\epsilon^2) \quad \text{for } n \geq 3 \tag{3.12}$$

In fact, only $n = 3$ and $n = 4$ moments are $O(\epsilon^2)$. Note that in Eq.(2.68), the lowest momentum order on the right-hand side is $n-2$. Hence, for $n = 5, 6$, the lowest momentum order appearing on the right-hand side is $n = 3$ and $n = 4$ respectively. This implies that the right-hand sides for $n = 5, 6$ are at most $O(\epsilon^2)$, which further implies that $\rho_{r|2}^{\mu_1\cdots\mu_n}/\tau_R = 0$ for $n = 5, 6$ since there are no $O(\epsilon)$ terms in the right hand side of Eq.(2.68). Equivalently,

$$\rho_r^{\mu_1\cdots\mu_n} = O(\epsilon^3) \ \text{ for } \ n = 5, 6 \tag{3.13}$$

Continuing this way, it can be established that in general

$$\rho_r^{\mu_1 \cdots \mu_n} = O(\epsilon^{\lceil n/2 \rceil}) \;\text{ for }\; n \geq 1 \tag{3.14}$$

where $\lceil n/2 \rceil$ is the closest integer that is larger than or equal to $n/2$. Since we have now established the ϵ-order of the energy-momentum moments, we do not have to carry ϵ around from here on although we will keep referring to ϵ-order for specific terms. For the relaxation time approximation, the ϵ-order is the same as the number of τ_R factors. Note that the dissipative currents $\pi^{\mu\nu}, q^\mu$ and the bulk viscous pressure Π are all $O(\epsilon)$.

3.1.3 Moment Equations for Π, q^μ, and $\pi^{\mu\nu}$

Equation for Π

We now proceed to derive the second-order moment equations for the bulk viscous pressure Π, diffusion current q^μ, and shear-stress tensor $\pi^{\mu\nu}$. We will start with the equation for Π first. Taking $r = 0$ and $n = 0$ in Eq. (2.68):

$$\begin{aligned} D\rho_0 = &\int \frac{d^3p}{(2\pi)^3 p^0} C[f] W_p^{-1} - \int \frac{d^3p}{(2\pi)^3 p^0} p^\lambda (\partial_\lambda f_0) W_p^{-1} \\ &- \nabla_\lambda \rho_{-1}^\lambda - \frac{2}{3}\theta\rho_0 + \sigma_{\lambda\alpha}\rho_{-2}^{\lambda\alpha} - \frac{m^2}{3}\theta\rho_{-2} \end{aligned} \tag{3.15}$$

Using the definition of Π in Eq. (2.30):

$$\Pi = -\frac{m^2}{3}\int \frac{d^3p}{(2\pi)^3 p^0}\delta f = -\frac{m^2}{3}\rho_0 \tag{3.16}$$

Eq. (3.15) is equivalent to

$$\begin{aligned} D\Pi = &\frac{m^2}{3} F_{-1} - \frac{m^2}{3}\int \frac{d^3p}{(2\pi)^3 p^0} C[f] W_p^{-1} + \frac{m^2}{3}\nabla_\lambda \rho_{-1}^\lambda - \frac{2}{3}\theta\Pi - \frac{m^2}{3}\sigma_{\lambda\alpha}\rho_{-2}^{\lambda\alpha} \\ &+ \frac{m^4}{9}\theta\rho_{-2} \end{aligned} \tag{3.17}$$

To get the second-order equation, we need to know ρ_{-2}, ρ^{μ}_{-1}, $\rho^{\mu\nu}_{-2}$ up to and including $O(\epsilon)$. One obvious way to do so is to use Eqs. (3.4) – (3.6) and (3.10), along with the relaxation time approximation Eq. (3.9):

$$\begin{aligned} D\Pi = & \frac{m^2}{3}\left[\phi_{-1|0}\theta + \phi^{q}_{-1|1}\partial_\mu q^\mu + \phi^{\pi\Pi}_{-1|1}\left(\theta\Pi + \pi^{\gamma\rho}\sigma_{\gamma\rho}\right)\right] \\ & - \frac{\Pi}{\tau_R} - \frac{m^2}{3}\tau_R\nabla_\lambda\left(\psi_{-2|0}\nabla^\lambda\alpha\right) - \frac{2}{3}\theta\Pi + \frac{m^2}{3}\tau_R\varphi_{-3|0}\sigma_{\lambda\alpha}\sigma^{\lambda\alpha} - \frac{m^4}{9}\tau_R\phi_{-3|0}\theta^2 \end{aligned} \tag{3.18}$$

This expression poses a problem because the second-order terms on the right-hand side are all second-order in the spatial derivative, while the left-hand side is first-order in the time derivative, which is a typical characteristic of parabolic equations. If a Lorentz boost is applied, terms with second-order time derivatives will be introduced on the right-hand side, altering the mathematical structure of the equation. This can result in issues such as instability and acausality in the solutions. However, these problems can be resolved by using the first-order constitutive relationship

$$\Pi_{|1} = \frac{m^2}{3}\tau_R\phi_{-1|0}\theta \tag{3.19}$$

$$q^{\mu}_{|1} = -\tau_R\psi_{-1|0}\nabla^\mu\alpha \tag{3.20}$$

$$\pi^{\mu\nu}_{|1} = -\tau_R\varphi_{-1|0}\sigma^{\mu\nu} \tag{3.21}$$

obtained using again Eqs. (3.4) – (3.6) and (3.10), to replace the terms with second-order spatial derivatives. The scalar equation now becomes

$$\begin{aligned} D\Pi = & -\frac{\Pi}{\tau_R} - \frac{2}{3}\theta\Pi + \frac{m^2}{3}\left[\phi_{-1|0}\theta + \phi^{q}_{-1|1}\partial_\mu q^\mu + \phi^{\pi\Pi}_{-1|1}\left(\theta\Pi + \pi^{\gamma\rho}\sigma_{\gamma\rho}\right)\right] \\ & + \frac{m^2}{3}\nabla_\lambda\left(\frac{\psi_{-2|0}}{\psi_{-1|0}}q^\lambda\right) - \frac{m^2}{3}\left(\frac{\varphi_{-3|0}}{\varphi_{-1|0}}\right)\sigma_{\lambda\alpha}\pi^{\lambda\alpha} - \frac{m^2}{3}\left(\frac{\phi_{-3|0}}{\phi_{-1|0}}\right)\theta\Pi \end{aligned} \tag{3.22}$$

Equation for q^μ

For $n = 1$ and $r = 0$ and with relaxation time approximation, Eq. (2.68) becomes:

$$\begin{aligned}\Delta^\mu_\nu Dq^\nu = &-\frac{q^\mu}{\tau_R} - F^\mu_{-1} - \rho_1 a^\mu - \Delta^\mu_\nu \nabla_\lambda \rho^{\lambda\nu}_{-1} - \frac{1}{3}\nabla^\mu \rho_1 + \frac{m^2}{3}\nabla^\mu \rho_{-1}\\ &- \theta q^\mu + \sigma_{\lambda\alpha}\rho^{\lambda\alpha\mu}_{-2} - \frac{m^2}{3}\theta\rho^\mu_{-2} - \frac{3}{5}q^\lambda \sigma^\mu_\lambda - q^\lambda \omega^\mu_\lambda\\ &- \frac{2m^2}{5}\rho^\lambda_{-2}\sigma^\mu_\lambda\end{aligned} \tag{3.23}$$

Note that all the ρ_1 terms vanish due to Eq. (2.25). The $\rho^{\lambda\alpha\mu}_{-2}$ term does not contribute at the second order since $\rho^{\lambda\alpha\mu}_{-2}$ is $O(\epsilon^2)$. Again using the first-order constitutive relationship to replace the ρ terms on the right-hand side, we get

$$\begin{aligned}\Delta^\mu_\nu Dq^\nu = &-\frac{q^\mu}{\tau_R} - \psi_{-1|0}\nabla^\mu\alpha - \psi_{-1|1}\left(\Delta^\mu_\gamma \partial_\rho \pi^{\gamma\rho} + \nabla^\mu \Pi + a^\mu \Pi\right) - \Delta^\mu_\nu \nabla_\lambda \left(\frac{\varphi_{-2|0}}{\varphi_{-1|0}}\pi^{\lambda\nu}\right)\\ &- \nabla^\mu\left(\frac{\phi_{-2|0}}{\phi_{-1|0}}\Pi\right) - \theta q^\mu - \frac{m^2}{3}\left(\frac{\psi_{-3|0}}{\psi_{-1|0}}\right)\theta q^\mu - \frac{3}{5}q^\lambda\sigma^\mu_\lambda - q^\lambda\omega^\mu_\lambda\\ &- \frac{2m^2}{5}\sigma^\mu_\lambda\left(\frac{\psi_{-3|0}}{\psi_{-1|0}}\right)q^\lambda\end{aligned} \tag{3.24}$$

which is the second-order q^μ equation.

Equation for $\pi^{\mu\nu}$

Taking $n = 2$ and $r = 0$ along with relaxation time approximation in Eq. (2.68), we get

$$\begin{aligned}\Delta^{\mu\nu}_{\alpha\beta}D\pi^{\alpha\beta} = &-\frac{\pi^{\mu\nu}}{\tau_R} - F^{\mu\nu}_{-1} - 2\rho^{\langle\mu}_1 a^{\nu\rangle} - \Delta^{\mu\nu}_{\alpha\beta}\nabla_\lambda \rho^{\lambda\alpha\beta}_{-1} - \frac{2}{5}\nabla^{\langle\mu}\rho^{\nu\rangle}_1\\ &+ \frac{2m^2}{5}\nabla^{\langle\mu}\rho^{\nu\rangle}_{-1} - \frac{4}{3}\theta\pi^{\mu\nu} + \sigma_{\lambda\alpha}\rho^{\alpha\lambda\mu\nu}_{-2} - \frac{m^2}{3}\theta\rho^{\mu\nu}_{-2}\\ &- \frac{10}{7}\pi^{\lambda\langle\mu}\sigma^{\nu\rangle}_\lambda - 2\pi^{\lambda\langle\mu}\omega^{\nu\rangle}_\lambda - \frac{8}{15}\rho_2\sigma^{\mu\nu}\\ &- \frac{4m^2}{7}\rho^{\lambda\langle\mu}_{-2}\sigma^{\nu\rangle}_\lambda + \frac{2m^4}{15}\rho_{-2}\sigma^{\mu\nu} + \frac{2m^2}{5}\rho_0\sigma^{\mu\nu}\end{aligned} \tag{3.25}$$

Observe that all the ρ_1 and ρ_2 terms vanish due to matching conditions $\rho_1 = \rho_2 = \rho^\mu_1 = 0$. Just as before, the second-order equation for $\pi^{\mu\nu}$ is obtained using the first-order constitutive relationship and rejecting all the $O(\epsilon^2)$ terms:

$$\begin{aligned}\Delta^{\mu\nu}_{\alpha\beta} D\pi^{\alpha\beta} = &-\frac{\pi^{\mu\nu}}{\tau_R} - \varphi_{-1|0}\sigma^{\mu\nu} + \frac{2m^2}{5}\nabla^{\langle\mu}\left(\frac{\psi_{-2|0}}{\psi_{-1|0}}\right)q^{\nu\rangle} \\ &- \frac{4}{3}\theta\pi^{\mu\nu} - \frac{m^2}{3}\theta\left(\frac{\varphi_{-3|0}}{\varphi_{-1|0}}\right)\pi^{\mu\nu} - \frac{10}{7}\pi^{\lambda\langle\mu}\sigma^{\nu\rangle}_{\lambda} \\ &- 2\pi^{\lambda\langle\mu}\omega^{\nu\rangle}_{\lambda} - \frac{4m^2}{7}\left(\frac{\varphi_{-3|0}}{\varphi_{-1|0}}\right)\pi^{\lambda\langle\mu}\sigma^{\nu\rangle}_{\lambda} - \frac{2m^2}{5}\left(\frac{\phi_{-3|0}}{\phi_{-1|0}}\right)\Pi\sigma^{\mu\nu} \\ &- \frac{6}{5}\Pi\sigma^{\mu\nu}\end{aligned} \tag{3.26}$$

3.2 Linear Stability and Causality Analysis

The previous section provided us with the second-order moment equations. However, it is crucial to ensure that these equations lead to stable and causal solutions since these properties dictate the usability of the equations in numerical computations. Generally speaking, analyzing the stability and causality of non-linear partial differential equations is a challenging task. Therefore, the best course of action in this scenario is to *linearize* the equations before conducting any analysis. This is achieved by considering small fluctuations in hydrodynamic variables from the local equilibrium and retaining only the terms that are linear in these small fluctuations. The analysis of stability and causality performed on these linearized equations is referred to as *linear stability/causality analysis*. To simplify matters, we will assume that the particles are massless (i.e. $m = 0$), and we will not assume the conservation of particle number throughout the analysis. As we will see, these assumptions reduce the R14 theory to the R9 theory.

3.2.1 Linearized Second-Order R9 Equations

Our analysis of second-order moment equations will commence by linearizing them. Notably, in the case of massless particles, the bulk viscous pressure Π vanishes. Additionally, since there is no conservation of particle number (i.e., Eq. (2.6) does not hold), q^μ and ν do not contribute to our analysis, therefore, the only relevant dissipative quantity for our study is the shear-stress tensor $\pi^{\mu\nu}$, reducing the total number of moments from 14 to 9. Consequently, we only need to linearize the $\pi^{\mu\nu}$ equation, along with the conservation laws, by considering small fluctuations in the energy density ϵ, fluid 4-velocity u^μ, and shear-stress tensor $\pi^{\mu\nu}$:

$$\epsilon = \epsilon_0 + \delta\epsilon, \;\; u^\mu = u_0^\mu + \delta u^\mu, \;\; \pi^{\mu\nu} = \delta\pi^{\mu\nu} \tag{3.27}$$

Setting $m = 0$ and keeping only terms that are linear in small perturbations, Eq. (3.26) reduces to

$$D_0\delta\pi^{\mu\nu} + \frac{\delta\pi^{\mu\nu}}{\tau_R} + \frac{8}{5\pi^2\beta^4}\sigma^{\mu\nu} = 0 \tag{3.28}$$

where $D_0 = u_0^\mu\partial_\mu$ and we have used Eq. (B.39) in B.2 to express $\varphi_{-1|0}$. Now, since we are dealing with only one particle species in this analysis, the chemical potential term in f_0 vanishes, and Eq. (2.19) reduces to

$$\begin{aligned}
\epsilon &= \int \frac{d^3p}{(2\pi)^3} p^0 e^{-\beta p^0} \\
&= \int \frac{d^3p}{(2\pi)^3} |\mathbf{p}| e^{-\beta|\mathbf{p}|} \\
&= \frac{4\pi}{(2\pi)^3}\int_0^\infty p^3 e^{-\beta p} dp \\
&= \frac{1}{2\pi^2}\frac{3!}{\beta^4} \\
&= \frac{3}{\pi^2\beta^4}
\end{aligned} \tag{3.29}$$

Thus Eq. (3.28) becomes

$$D_0\delta\pi^{\mu\nu} + \frac{\delta\pi^{\mu\nu}}{\tau_R} + \frac{8\epsilon_0}{15}\sigma^{\mu\nu} = 0 \tag{3.30}$$

which is the linearized $\pi^{\mu\nu}$ equation. Now, we also need to linearize the energy-momentum conservation laws. To obtain these laws, we can simply take the longitudinal and transverse components of Eq. (2.4) with respect to the fluid velocity u^μ:

$$\begin{aligned}
u_\nu\partial_\mu T^{\mu\nu} &= D\epsilon + (\epsilon + P_0)\theta + \pi^{\alpha\beta}\sigma_{\alpha\beta} = 0 \\
\Delta^\lambda_\nu\partial_\mu T^{\mu\nu} &= (\epsilon + P_0)Du^\lambda + \nabla^\lambda P_0 + \pi^{\lambda\beta}Du_\beta + \Delta^\lambda_\nu\nabla_\mu\pi^{\mu\nu} = 0
\end{aligned} \tag{3.31}$$

Here, we can replace the thermal pressure P_0 by the equation of state $P_0 = \frac{1}{3}\epsilon$ (obtained from Eq. (2.19) and (2.22)). The linearized conservation laws are straightforward to get:

$$\begin{aligned}
&D_0\delta\epsilon + \frac{4}{3}\epsilon_0\nabla_{\mu,0}\delta u^\mu = 0 \\
&D_0(\epsilon_0\delta u^\mu) + \frac{1}{4}\nabla_0^\mu\delta\epsilon + \frac{3}{4}\nabla_{\lambda,0}\delta\pi^{\lambda\mu} = 0
\end{aligned} \tag{3.32}$$

where we define $\Delta_0^{\mu\nu} = g^{\mu\nu} + u_0^\mu u_0^\nu$ and $\nabla_0^\mu = \Delta_0^{\mu\nu}\partial_\nu$. It is convenient to express the above equations in Fourier space. We will use the following format of Fourier transform:

$$\begin{aligned}\widetilde{f}(k) &= \int_{-\infty}^{\infty} d^4x\, e^{-ik_\mu x^\mu} f(x) \\ f(x) &= \int_{-\infty}^{\infty} \frac{d^4k}{(2\pi)^4} e^{ik_\mu x^\mu} \widetilde{f}(k)\end{aligned} \tag{3.33}$$

Here, $k^\mu = (\omega, \mathbf{k})$ is the wave 4-vector. Therefore, we can express each Fourier component of the variables in the linearized equations as a plane wave multiplied by a complex amplitude $\widetilde{\phi}$:

$$\phi = \widetilde{\phi} e^{ik_\mu x^\mu} = \widetilde{\phi} e^{i(\mathbf{k}\cdot\mathbf{x} - \omega t)} \tag{3.34}$$

Note that since $g^{\mu\nu} = diag(-1, 1, 1, 1)$, we have $k_\mu x^\mu = \mathbf{k} \cdot \mathbf{x} - \omega t$. Furthermore, we shall rewrite the linearized equations in terms of the Lorentz-covariant variables defined below:

$$\begin{aligned}\Omega &\equiv u_0^\mu k_\mu \\ \kappa^\mu &\equiv \Delta_0^{\mu\nu} k_\nu\end{aligned} \tag{3.35}$$

which correspond to the angular frequency and wave vector in the local rest frame of the background system, respectively. We also define the covariant wave number κ as

$$\kappa \equiv \sqrt{\kappa^\mu \kappa_\mu} \tag{3.36}$$

In terms of the covariant variables, the linearized conservation laws Eq. (3.32) can now be rewritten as

$$\begin{aligned}&\Omega \delta\widetilde{\epsilon} + \frac{4}{3}\epsilon_0 \kappa_\mu \delta\widetilde{u}^\mu = 0 \\ &\Omega \epsilon_0 \delta\widetilde{u}^\mu + \frac{1}{4}\kappa^\mu \delta\widetilde{\epsilon} + \frac{3}{4}\kappa_\alpha \delta\widetilde{\pi}^{\alpha\mu} = 0\end{aligned} \tag{3.37}$$

and the linearized $\pi^{\mu\nu}$ equation becomes

$$\left(i\Omega + \frac{1}{\tau_R}\right)\delta\widetilde{\pi}^{\mu\nu} + \frac{4}{15} i\epsilon_0 \left(\kappa^\mu \delta\widetilde{u}^\nu + \kappa^\nu \delta\widetilde{u}^\mu - \frac{2}{3}\Delta_0^{\mu\nu}\kappa_\alpha \delta\widetilde{u}^\alpha\right) = 0 \tag{3.38}$$

From now on, we will assume that all linearized equations are expressed in Fourier space and will therefore omit the tilde. Furthermore, Ω and κ are also assumed to be properly scaled using the relaxation time to become dimensionless quantities.

The linear stability and causality analysis presented in this dissertation adheres to the procedure outlined in [5, 64]. This involves decomposing the linearized equations in Fourier space into longitudinal (parallel to κ^μ) and transverse (orthogonal to κ^μ) components. This method offers the advantage of decoupling the equations in the linear regime, allowing them to be solved independently and simplifying the calculations [5]. Thus, it is beneficial to introduce a projector that is analogous to $\Delta^{\mu\nu}$ but with respect to κ^μ:

$$\Delta_\kappa^{\mu\nu} = g^{\mu\nu} - \frac{\kappa^\mu \kappa^\nu}{\kappa^2} \tag{3.39}$$

where κ^2 is introduced to ensure normalization. Then, any 4-vector A^μ can be decomposed into a linear combination of the longitudinal and transverse parts:

$$A^\mu = A_{||} \frac{\kappa^\mu}{\kappa} + A_\perp^\mu \tag{3.40}$$

where $A_{||} = \kappa_\mu A^\mu / \kappa$ and $A_\perp^\mu = \Delta_\kappa^{\mu\nu} A_\nu$. Similarly, a rank-2 tensor $A^{\mu\nu}$ can also be decomposed as

$$A^{\mu\nu} = A_{||} \frac{\kappa^\mu \kappa^\nu}{\kappa^2} + \frac{1}{3} A_\perp \Delta_\kappa^{\mu\nu} + A_\perp^\mu \frac{\kappa^\nu}{\kappa} + + A_\perp^\nu \frac{\kappa^\mu}{\kappa} + A_\perp^{\mu\nu} \tag{3.41}$$

where $A_{||} = \kappa_\mu \kappa_\nu A^{\mu\nu}/\kappa^2$, $A_\perp = \Delta_\kappa^{\mu\nu} A_{\mu\nu}$, $A_\perp^\mu = \kappa^\lambda \Delta_\kappa^{\mu\nu} A_{\lambda\nu}/\kappa$, and $A_\perp^{\mu\nu} = \Delta_\kappa^{\mu\nu\alpha\beta} A_{\alpha\beta}$. Here, we defined the rank-2 κ-projector to be

$$\Delta_\kappa^{\mu\nu\alpha\beta} = \frac{1}{2}\left(\Delta_\kappa^{\mu\alpha} \Delta_\kappa^{\nu\beta} + \Delta_\kappa^{\mu\beta} \Delta_\kappa^{\nu\alpha} - \frac{2}{3} \Delta_\kappa^{\mu\nu} \Delta_\kappa^{\alpha\beta} \right) \tag{3.42}$$

3.2.2 Transverse Modes

In this section, we will analyze the linear stability and causality of the transverse components of second-order R9 hydrodynamics. We will discuss two cases: in the first, the wave vector **k** is parallel to the background fluid velocity **V**, while in the second, the wave vector is orthogonal to **V**.

Case 1: k is parallel to V

For simplicity and without loss of generality, we will assume that **k** and **V** are both in the x-axis:

$$\begin{aligned} u_0^\mu &= \gamma(1, V, 0, 0) \\ k^\mu &= (\omega, k, 0, 0) \end{aligned} \tag{3.43}$$

It immediately follows that

$$\begin{aligned} \Omega &= \gamma(Vk - \omega) \\ \kappa^2 &= \gamma^2(k - V\omega)^2 \end{aligned} \tag{3.44}$$

Now, note that the first equation in Eq. (3.37), which corresponds to the energy conservation law, is a scalar equation. Thus it is purely longitudinal and does not contribute to the transverse analysis. The transverse component of the momentum conservation law and the $\pi^{\mu\nu}$ equation can be easily obtained by applying the projector $\Delta_\kappa^{\mu\nu}$ and κ^μ. Doing so gives us

$$\begin{aligned} &\Omega\epsilon_0\delta u_\perp^\mu + \frac{3}{4}\kappa\delta\pi_\perp^\mu = 0 \\ &\left(i\Omega + \frac{1}{\tau_R}\right)\delta\pi_\perp^\mu + \frac{4}{15}i\epsilon_0\kappa\delta u_\perp^\mu = 0 \end{aligned} \tag{3.45}$$

This system of equations can be written in the following matrix form:

$$\begin{pmatrix} \Omega & \frac{3}{4}\kappa \\ \frac{4}{15}i\kappa & i\Omega + \frac{1}{\tau_R} \end{pmatrix} \begin{pmatrix} \epsilon_0\delta u_\perp^\mu \\ \delta\pi_\perp^\mu \end{pmatrix} = 0 \tag{3.46}$$

To obtain a non-trivial solution, we require that the determinant of the 2×2 matrix M to be zero:

$$det(M) = \Omega(i\Omega + \frac{1}{\tau_R}) - \frac{1}{5}i\kappa^2 = 0 \tag{3.47}$$

which is the dispersion relation. Note that the dispersion relation implies a quadratic order for Ω, indicating that we should anticipate obtaining two modes. Indeed, the solutions to the dispersion relation are

$$\omega_{1,2} = \frac{5i - 8k\gamma\tau_R V \pm i\sqrt{25 + 20ik\gamma\tau_R V(V^2-1) - 20k^2\gamma^2\tau_R^2(V^2-1)^2}}{2\gamma\tau_R(V^2-5)} \tag{3.48}$$

To determine whether these solutions are linearly stable, we first take a look at the plane waves formula (Eq. (3.34)):

$$\phi \sim e^{i(kx-\omega t)} = e^{ikx}e^{-i\omega_r t}e^{\omega_i t} \tag{3.49}$$

where $\omega = \omega_r + i\omega_i$ is complex. Note that the first two exponential terms are simply oscillating waves, therefore only the third term contributes to the damping, and thus, stability. To ensure exponential suppression of Eq. (3.49) for $t \geq 0$, it is necessary that ω_i be less than or equal to zero. Thus, in general, stability requires

$$\omega_i \leq 0 \tag{3.50}$$

for all $t \geq 0$. In practice, it is sufficient to show that this requirement is satisfied for small wave number k. This is because hydrodynamics is in essence a macroscopic and large wavelength theory, and is therefore associated with small wave numbers. In the limit of small k, we can Taylor-expand Eq. (3.48):

$$\begin{aligned} \omega_1 &= Vk - \frac{1}{5}i\gamma\tau_R(V^2-1)^2k^2 + O(k^3) \\ \omega_2 &= -\frac{5i}{\gamma\tau_R(5-V^2)} - \frac{V(V^2+3)}{V^2-5}k + \frac{1}{5}i\gamma\tau_R(V^2-1)^2k^2 + O(k^3) \end{aligned} \tag{3.51}$$

It is clear that for small k, both ω_1 and ω_2 have non-positive imaginary parts since $0 \leq V \leq 1$. Thus, according to Eq. (3.50), we can conclude that the second-order R9 equations have linearly stable transverse modes when the fluid velocity vector is parallel to the

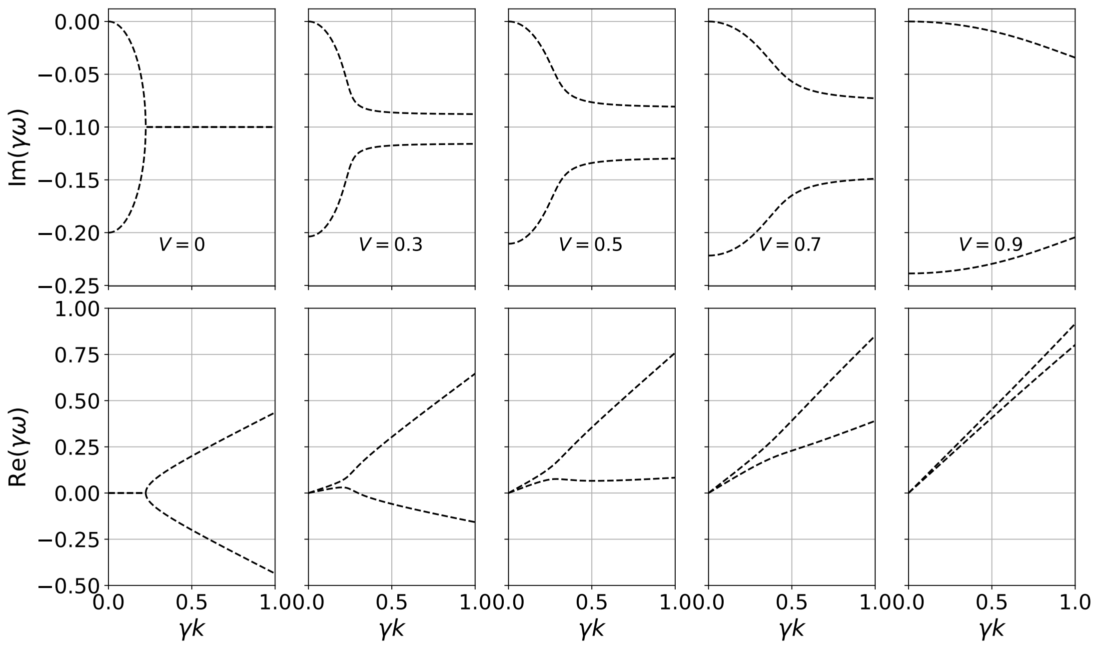

Figure 3.1: Real and Imaginary parts of the transverse modes of the massless second-order R9 hydrodynamics, in the case of fluid velocity vector being parallel to the wave vector. The relaxation time is chosen to be $\tau_R = 5$ [5,6].

wave vector. Fig. (3.1) shows the plots of both modes with different values of background fluid velocity V and with $\tau_R = 5$ [5,6]. This particular value for the shear relaxation time τ_R is calculated from the Boltzmann equation in the ultra-relativistic limit, using the 14 moments approximation. Clearly, one can see that the imaginary parts of both solutions are non-positive for small k. But in fact, one can show that these imaginary parts are non-positive for *all* $k \geq 0$. Fig. (3.2) shows the imaginary parts of both modes for $V = 0.9$ and $\tau_R = 5$, but for a much larger range of k. One can see that the curves demonstrate asymptotic behavior as k increases. We claim that this result also holds for any other values of V.

The modes displayed in Eq. (3.48) also encode the physical information of the propagating sound waves. For example, as we will see very soon, $\partial Re(\omega)/\partial k$ is the group velocity of the sound waves, where ω is the temporal frequency and k is the correspond-

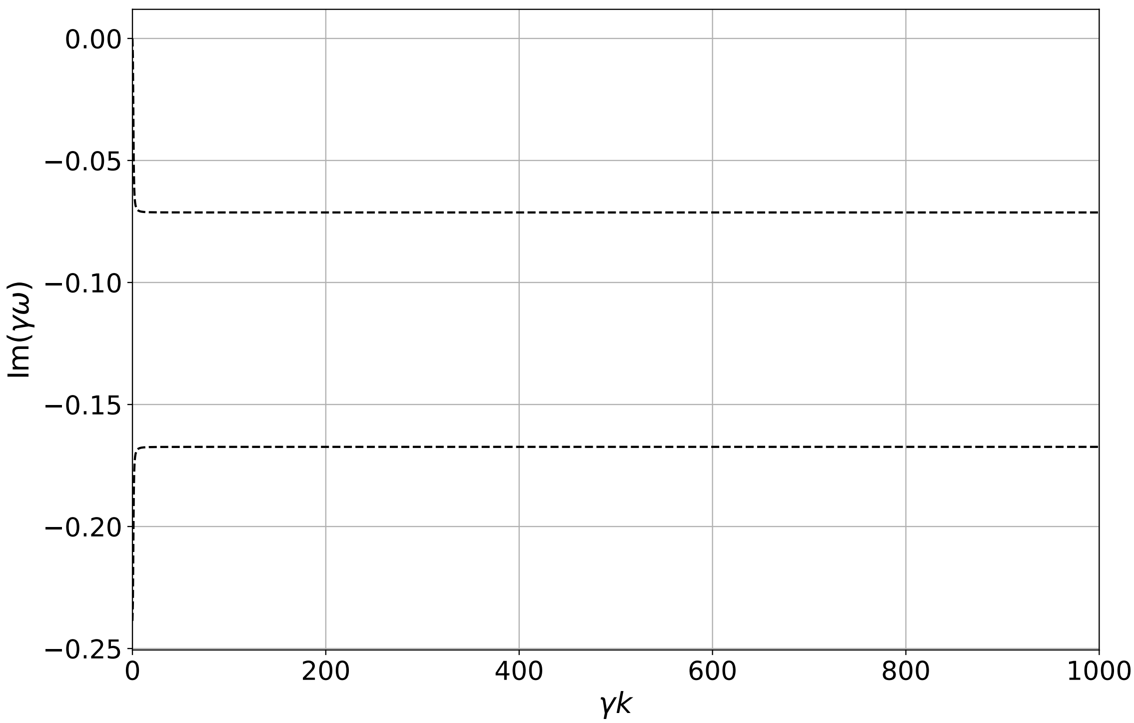

Figure 3.2: The imaginary parts of the transverse modes of the massless second-order R9 hydrodynamics, in the case of fluid velocity vector being parallel to the wave vector, for $V = 0.9$ and with relaxation time $\tau_R = 5$. Note that a large range of k is chosen to demonstrate the asymptotic behavior of the curves.

ing wave number. In this particular case, Eq. (3.48) contains information on how the waves propagate in the transverse direction.

To conduct the causality analysis, we shall first Taylor-expand Eq. (3.48) again but under the assumption of large k this time. The results are

$$\begin{aligned} \omega_1 &= -\frac{4V + \sqrt{5}(V^2-1)}{V^2-5}k + \frac{i(5+\sqrt{5}V)}{2\gamma\tau_R(V^2-5)} - \frac{\sqrt{5}}{8k\gamma^2\tau_R^2(V^2-1)} + O\left(\frac{1}{k^2}\right) \\ \omega_2 &= -\frac{4V - \sqrt{5}(V^2-1)}{V^2-5}k - \frac{i(-5+\sqrt{5}V)}{2\gamma\tau_R(V^2-5)} + \frac{\sqrt{5}}{8k\gamma^2\tau_R^2(V^2-1)} + O\left(\frac{1}{k^2}\right) \end{aligned} \tag{3.52}$$

Observe that the constant imaginary parts of both solutions are still negative in the large-k limit, since $V^2 \leq 1$. Causality requires that the asymptotic group velocity of the plane wave must be subliminal [65]:

$$\lim_{k\to\infty}\left|\frac{\partial Re(\omega)}{\partial k}\right| \leq 1 \tag{3.53}$$

From Eq. (3.52), we get

$$\lim_{k\to\infty}\left|\frac{\partial Re(\omega_{1,2})}{\partial k}\right| = \left|\frac{4V \pm \sqrt{5}(V^2-1)}{V^2-5}\right| \leq 1 \quad \text{for all } 0 \leq V \leq 1. \tag{3.54}$$

Therefore, the transverse modes are also linearly causal.

Case 2: k is orthogonal to V

We will now discuss the second case in which the wave vector is orthogonal to the fluid velocity vector. Without loss of generality, we will assume that **V** is still in the x-axis, but **k** is now in the y-axis:

$$\begin{aligned} u_0^\mu &= \gamma(1, V, 0, 0) \\ k^\mu &= (\omega, 0, k, 0) \end{aligned} \tag{3.55}$$

It follows that

$$\begin{aligned} \Omega &= -\gamma\omega \\ \kappa^2 &= \gamma^2 V^2 \omega^2 + k^2 \end{aligned} \tag{3.56}$$

Plugging Eq. (3.56) into Eq. (3.47) and solving for ω, we obtain

$$\omega_{1,2} = \pm\frac{i(\pm 5 + \sqrt{25 + 4k^2\tau_R^2(V^2-5)})}{2\gamma\tau_R(V^2-5)} \tag{3.57}$$

Note that the square-root term is always smaller than 5 since $V^2 - 5 < 0$ for all $0 \leq V \leq 1$. In the limit of small wave number k, the solutions can be expanded as

$$\begin{aligned} \omega_1 &= \frac{5i}{\gamma\tau_R(V^2-5)} + \frac{i\tau_R k^2}{5\gamma} + O(k^3) \\ \omega_2 &= -\frac{i\tau_R k^2}{5\gamma} + O(k^3) \end{aligned} \tag{3.58}$$

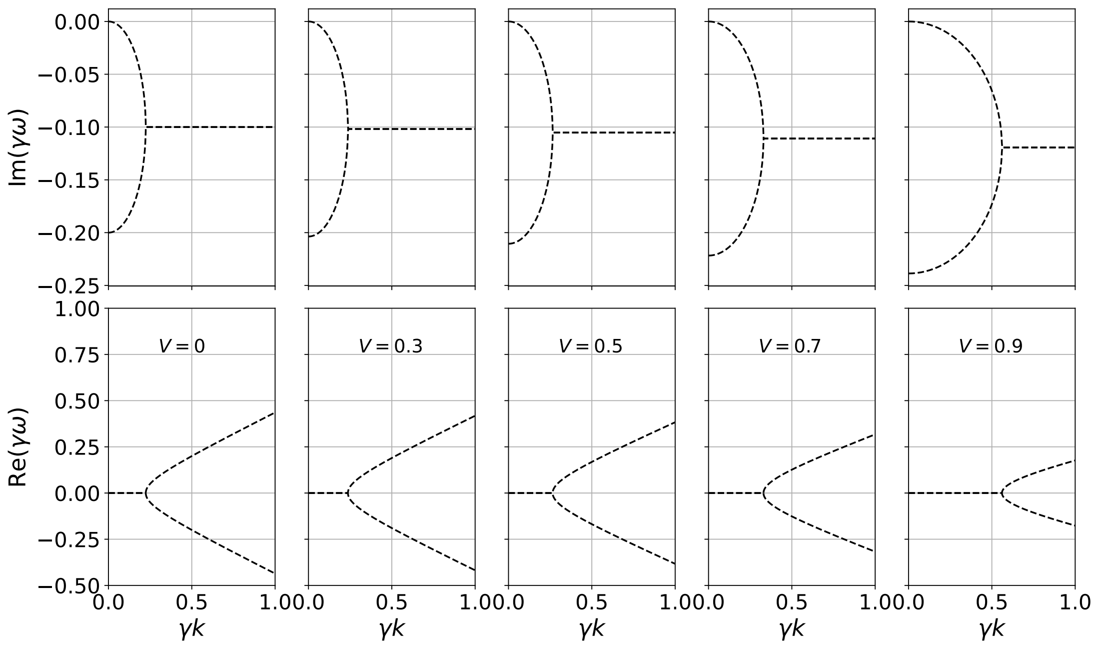

Figure 3.3: Real and Imaginary parts of the transverse modes of the massless second-order R9 hydrodynamics, in the case of fluid velocity vector being orthogonal to the wave vector. As before, the relaxation time is chosen to be $\tau_R = 5$.

Note that the first term in ω_1 is negative since $V^2 - 5 < 0$ for all $0 \leq V \leq 1$. Again, one can see that both solutions have non-positive imaginary parts, and therefore, are linearly stable. Indeed, we can draw the same conclusion from Fig. (3.3) by noticing that the imaginary parts of the modes are all non-positive for small k. Similar to case 1, one can obtain a stronger argument that the modes are linearly stable for *all* $k \geq 0$ by noticing the asymptotic behavior of the modes for large values of k, shown in Fig. (3.4), with $V = 0.9$ and $\tau_R = 5$.

To examine the causality of the above modes, we expand them around large values of k, just as before:

$$
\begin{aligned}
\omega_1 &= \frac{k}{\gamma\sqrt{5 - V^2}} - \frac{5i}{2\gamma\tau_R(5 - V^2)} + \frac{25i}{8\gamma\tau_R^2(V^2 - 5)^{3/2}k} + O\left(\frac{1}{k^3}\right) \\
\omega_2 &= -\frac{k}{\gamma\sqrt{5 - V^2}} - \frac{5i}{2\gamma\tau_R(5 - V^2)} + \frac{25}{8\gamma\tau_R^2(5 - V^2)^{3/2}k} + O\left(\frac{1}{k^3}\right)
\end{aligned}
\tag{3.59}
$$

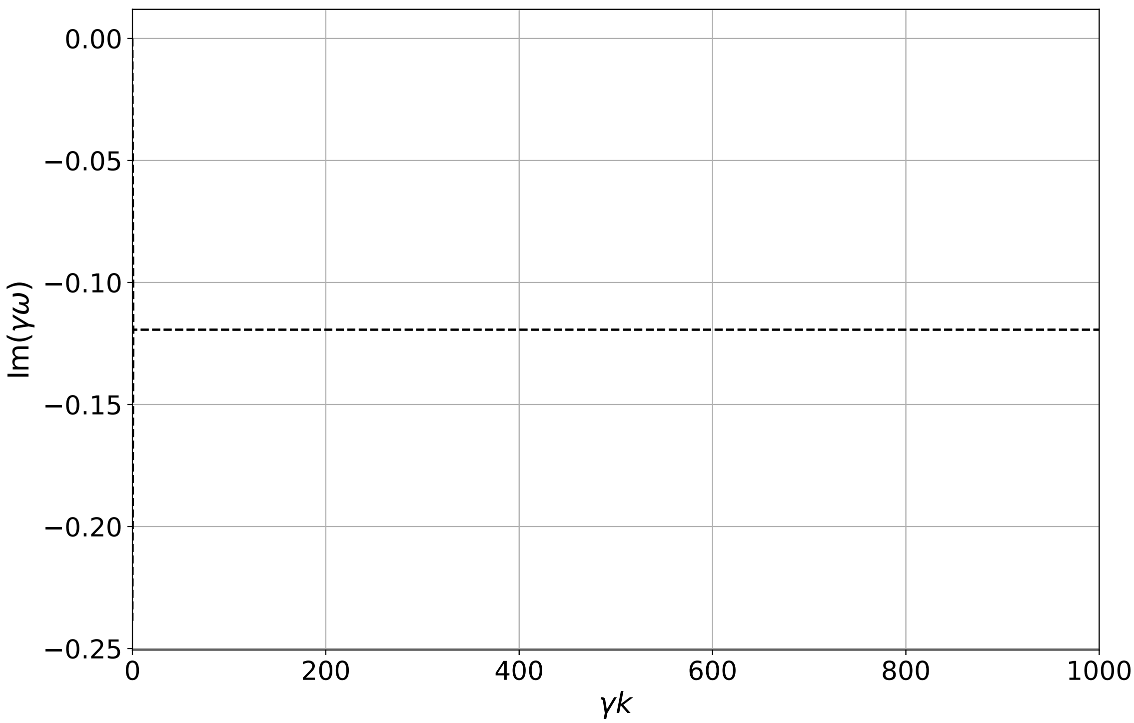

Figure 3.4: The imaginary parts of the transverse modes of the massless second-order R9 hydrodynamics plotted for a larger range of k, in the case of fluid velocity vector being orthogonal to the wave vector, for $V = 0.9$ and with relaxation time $\tau_R = 5$.

Then, it is straightforward to realize that

$$\lim_{k\to\infty}\left|\frac{\partial Re(\omega_{1,2})}{\partial k}\right| = \frac{1}{\gamma\sqrt{5-V^2}} = \sqrt{\frac{1-V^2}{5-V^2}} \leq 1 \tag{3.60}$$

for all $0 \leq V \leq 1$. At this point, we can conclude that the transverse modes are linearly causal when the fluid velocity vector is orthogonal to the wave vector.

3.2.3 Longitudinal Modes

In this section, we will perform the linear stability and causality analysis on the longitudinal components of the second-order R9 hydrodynamics. Similar to the transverse analysis done in the previous section, we will also discuss the two cases in which the fluid velocity vector is parallel and orthogonal to the wave vector, respectively.

Case 1: k is parallel to V

The first step of the analysis is to obtain the longitudinal components of the conservation laws and the $\pi^{\mu\nu}$ equation. To do this, we simply apply κ_μ and $\kappa_\mu\kappa_\nu$ to Eq. (3.37) and Eq. (3.38). Also, note that we need to include the purely-longitudinal energy conservation law this time. As before, we now have a system of linearized equations:

$$\begin{aligned}
&\Omega\delta\epsilon + \frac{4}{3}\epsilon_0\kappa\delta u_{||} = 0 \\
&\Omega\epsilon_0\delta u_{||} + \frac{1}{4}\kappa\delta\epsilon + \frac{3}{4}\kappa\delta\pi_{||} = 0 \\
&\left(i\Omega + \frac{1}{\tau_R}\right)\delta\pi_{||} + \frac{16}{45}i\epsilon_0\kappa\delta u_{||} = 0
\end{aligned} \tag{3.61}$$

which can be written in the following matrix form:

$$\begin{pmatrix} \Omega & \frac{4}{3}\kappa & 0 \\ \frac{1}{4}\kappa & \Omega & \frac{3}{4}\kappa \\ 0 & \frac{16}{45}i\kappa & i\Omega + \frac{1}{\tau_R} \end{pmatrix} \begin{pmatrix} \delta\epsilon \\ \epsilon_0\delta u_{||} \\ \delta\pi_{||} \end{pmatrix} = 0 \tag{3.62}$$

Again, by requiring the determinant of the 3×3 matrix M to be zero, we obtain the dispersion relation:

$$\begin{aligned}
det(M) = &-\frac{4}{15}i\gamma^3(kV-\omega)(k-V\omega)^2 \\
&+ \left(\frac{1}{\tau_R} + i\gamma(kV-\omega)\right)\left(\gamma^2(\omega-kV)^2 - \frac{1}{3}\gamma^2(k-V\omega)^2\right) \\
= &\ 0
\end{aligned} \tag{3.63}$$

Since ω is of cubic order in the dispersion relation, we should expect to get three modes. We address that the complete analytical expressions of the solutions are exceedingly complex. Nonetheless, for small values of k, we can utilize a series expansion to simplify the solutions and retain solely the $O(1)$ terms:

$$
\begin{aligned}
\omega_1 &= O(k) \\
\omega_2 &= -\frac{5i(V^2-3)}{3\gamma\tau_R(3V^2-5)} + O(k) \\
\omega_3 &= O(k)
\end{aligned}
\tag{3.64}
$$

Observe that when $k = 0$, ω_1 and ω_3 coincide at zero, while ω_2 has strictly negative imaginary parts for all $0 \leq V \leq 1$. It is then clear that they are all linearly stable solutions. Indeed, Fig. (3.5) shows that all modes have non-positive imaginary parts for small k, and we can extend this result to all $k \geq 0$ using Fig. (3.6), which guarantees linearly stability of the modes by demonstrating the asymptotic behavior of the modes for a larger range of k. As usual, we chose $\tau_R = 5$ for the numerical computation. Also, note that two of the modes have identical imaginary parts in the case of static fluids.

To confirm the causality of the modes, it seems natural to adopt the previous procedure of expanding the solutions in a series, assuming large values of k. However, even the zeroth-order term in such an expansion is forbiddingly complex to display when $V \neq 0$. Nevertheless, it suffices to demonstrate the causal nature of the modes for $V = 0$ since one can always shift to another reference frame with non-zero V through Lorentz boosts, which do not affect the causality of a solution. For $V = 0$, the large-k expansions of the solutions are

$$
\begin{aligned}
\omega_1 &= -\frac{5i}{9\tau_R} + O\left(\frac{1}{k}\right) \\
\omega_2 &= -\sqrt{\frac{3}{5}}k - \frac{2i}{9\tau_R} + O\left(\frac{1}{k}\right) \\
\omega_3 &= \sqrt{\frac{3}{5}}k - \frac{2i}{9\tau_R} + O\left(\frac{1}{k}\right)
\end{aligned}
\tag{3.65}
$$

It then follows that

$$
\begin{aligned}
\lim_{k\to\infty}\left|\frac{\partial Re(\omega_1)}{\partial k}\right| &= 0 \leq 1 \\
\lim_{k\to\infty}\left|\frac{\partial Re(\omega_{2,3})}{\partial k}\right| &= \sqrt{\frac{3}{5}} \leq 1
\end{aligned}
\tag{3.66}
$$

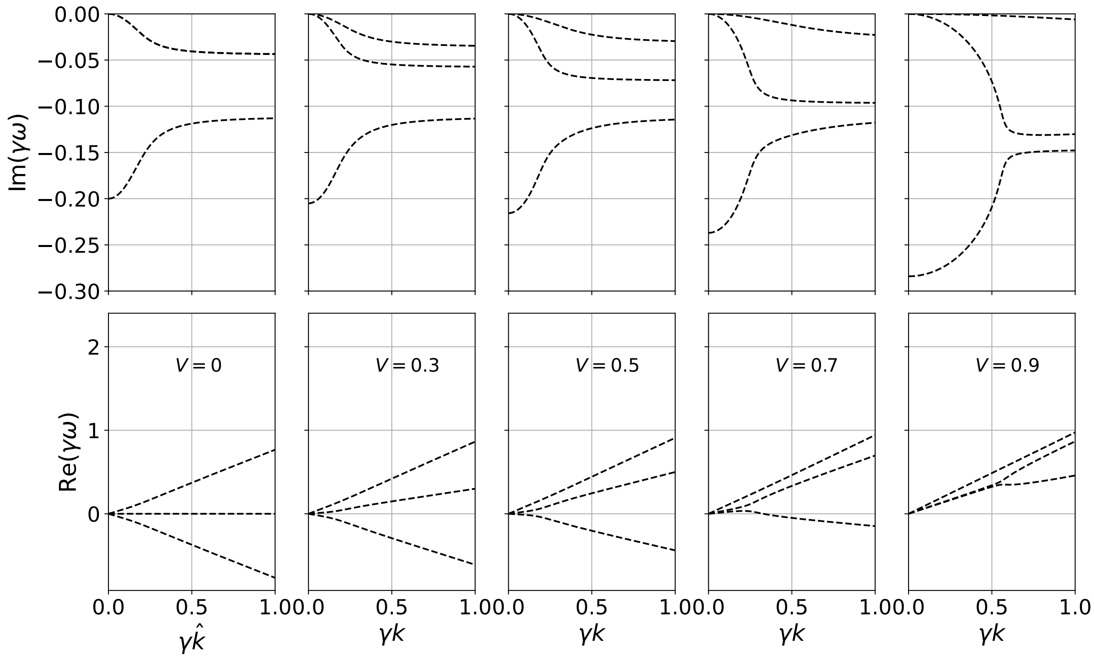

Figure 3.5: Real and Imaginary parts of the longitudinal modes of the massless second-order R9 hydrodynamics, in the case of fluid velocity vector being parallel to the wave vector and $\tau_R = 5$.

Thus, all the modes are causal when $V = 0$, and therefore, for all $0 \leq V \leq 1$. In particular, ω_1 corresponds to a static mode in the fluid rest frame since its group velocity is zero.

Case 2: k is orthogonal to V

With Eq. (3.56), the dispersion relation becomes

$$k^2(9i\gamma\tau_R\omega - 5) + \gamma^2\omega^2(15 - 15i\gamma\tau_R\omega + V^2(9i\gamma\tau_R\omega - 5)) = 0 \tag{3.67}$$

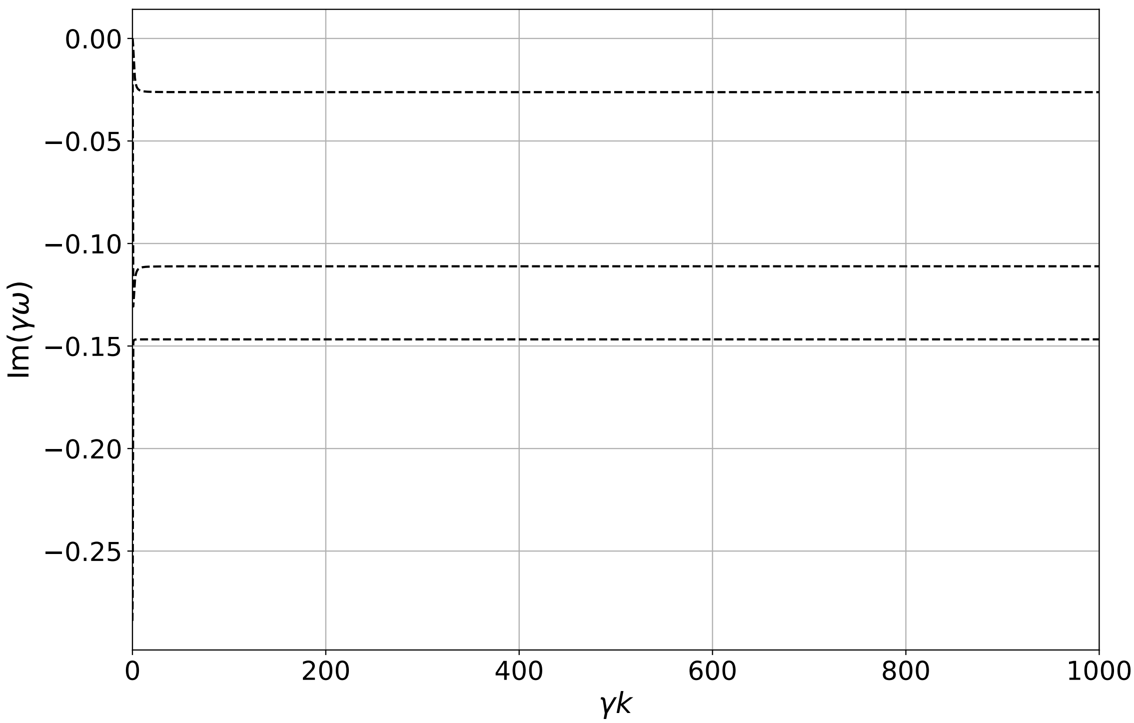

Figure 3.6: The imaginary parts of the longitudinal modes of the massless second-order R9 hydrodynamics plotted for a larger range of k, in the case of fluid velocity vector being parallel to the wave vector, for $V = 0.9$ and with relaxation time $\tau_R = 5$.

In the limit of small k, the $O(1)$ terms in the series expansion of the modes are

$$\begin{aligned} \omega_1 &= O(k) \\ \omega_2 &= -\frac{5i(V^2-3)}{3\gamma\tau_R(3V^2-5)} + O(k) \\ \omega_3 &= O(k) \end{aligned} \tag{3.68}$$

Note that these terms are the same as those in Case 1 (Eq. (3.64)). This is expected because when $k \approx 0$, it is irrelevant whether the wave vector is parallel or orthogonal to the fluid velocity vector, resulting in the same outcome. As a result, the solutions remain linearly stable, as in the previous case. The same conclusion can also be inferred from Fig. (3.7), as the numerically-computed imaginary parts of the modes are all non-positive for small k.

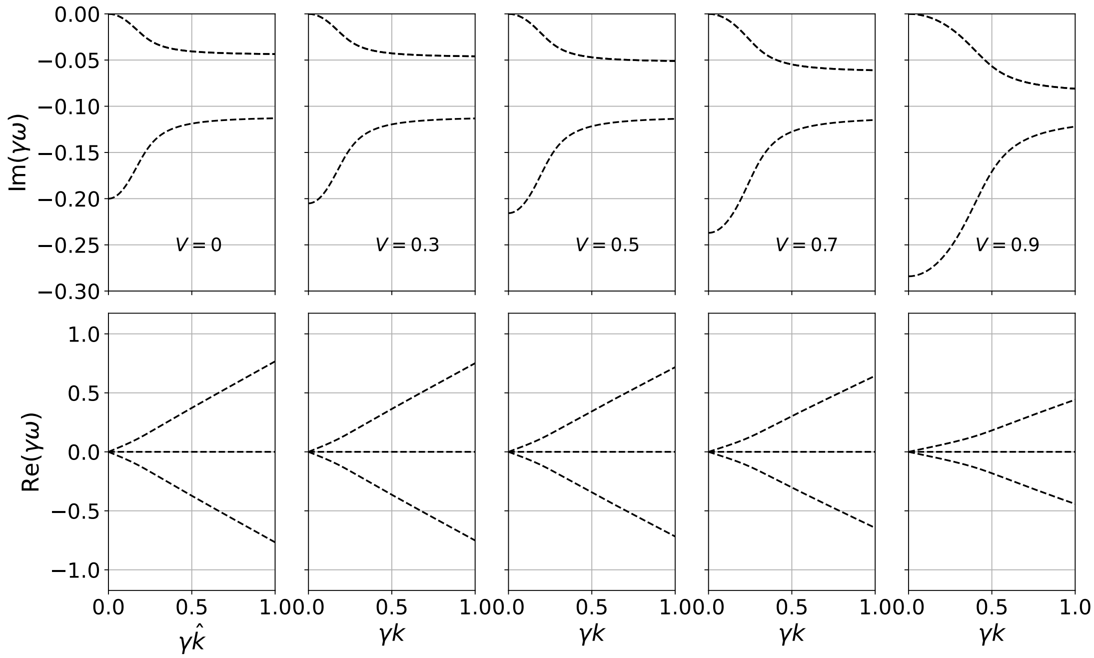

Figure 3.7: Real and Imaginary parts of the longitudinal modes of the massless second-order R9 hydrodynamics, in the case of fluid velocity vector being orthogonal to the wave vector and $\tau_R = 5$.

The asymptotic behavior of the modes for a larger range of k in Fig. (3.8) further extends the linear stability of the modes to all $k \geq 0$. Also observe that the imaginary components of two out of the three modes are identical, regardless of the background fluid velocity.

For the causality analysis, we will follow the same procedure as in Case 1, in which we restrict the fluid velocity V to zero. The large-k expansion then gives

$$\begin{aligned}
\omega_1 &= -\frac{5i}{9\tau_R} + O\left(\frac{1}{k}\right) \\
\omega_2 &= -\sqrt{\frac{3}{5}}k - \frac{2i}{9\tau_R} + O\left(\frac{1}{k}\right) \\
\omega_3 &= \sqrt{\frac{3}{5}}k - \frac{2i}{9\tau_R} + O\left(\frac{1}{k}\right)
\end{aligned} \tag{3.69}$$

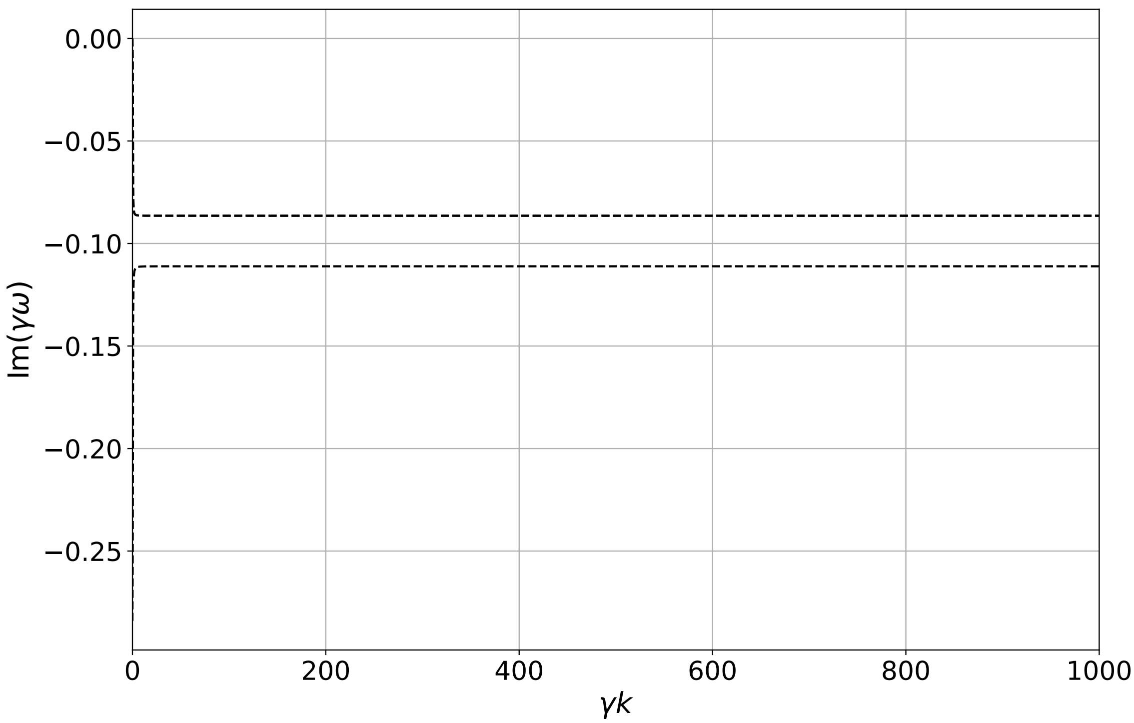

Figure 3.8: The imaginary parts of the longitudinal modes of the massless second-order R9 hydrodynamics plotted for a larger range of k, in the case of fluid velocity vector being orthogonal to the wave vector, for $V = 0.9$ and with relaxation time $\tau_R = 5$.

As expected, this is again identical to Case 1 (Eq. (3.65)) because $V = 0$ has no impact in either scenario. Therefore, we can deduce that the solutions are also causal in this instance.

3.3 Discussion

The previous sections have demonstrated the linear stability and causality of both the longitudinal and transverse components of the second-order R9 theory, the massless second-order R14 theory without particle number conservation. However, there remains a question as to whether this theory is compatible with the Israel-Stewart theory, which is also a second-order theory. According to [43], there are various ways to derive second-order relativistic viscous hydrodynamics, but their disparities lie only in the non-linear terms. Such differences arise from the way δf is represented in terms of the 14 moments in each theory, as well as the truncation process used to close the set of evolution equations. Nonetheless, the R9/R14 theory does not suffer from this issue. Its hydrodynamic equations are derived systematically and uniquely, without any arbitrariness involved in the process. For the purpose of linear stability analysis, however, all second-order theories should yield the same set of linearized hydrodynamic equations. Indeed, the linearized $\pi^{\mu\nu}$ equation for the Israel-Stewart theory is given by Eq. (2.58) in [66]:

$$D_0 \delta\pi^{\mu\nu} + \frac{\pi^{\mu\nu}}{\tau_\pi} - 2\frac{\eta}{\tau_\pi}\sigma^{\mu\nu} = 0 \tag{3.70}$$

where τ_π is the relaxation time associated with the shear-stress tensor $\pi^{\mu\nu}$ and η is the shear viscosity. It is evident that this equation takes on a similar form to Eq. (3.30), with differences appearing in the transport coefficients and the sign in front of the last terms, which can be attributed to the choice of the Minkowski metric. Because of the similarities between these two equations, it is reasonable to expect that the IS and R9 theories will demonstrate similar properties in linear stability and causality analysis. In fact, when $\tau_\pi = 5$, both theories produce almost identical curves for transverse and longitudinal modes if not the same (see Fig. (3) and (5) in [66]).

Another issue worth mentioning is that although the regularization technique provides a set of systematically and uniquely derived hydrodynamic equations, it is not clear whether this theory is more "correct" than the others using arguments based on first principles. However, since we just showed that the R9/R14 theory has linearly stable and causal modes, we can at least conclude that this theory leads to more physically reasonable results than other approaches such as Chapman-Enskog expansion, which results in linearly unstable modes [5].

To conclude this section, we have established the linear stability and causality of the longitudinal and transverse components of the second-order R9 hydrodynamics in both parallel and orthogonal cases of wave vector $\mathbf{k}$ and fluid velocity vector $\mathbf{V}$. Subsequently, we will derive the equations for the third-order regularized hydrodynamics, which is anticipated to be more complex yet more intriguing. Following this, we will conduct a series of linear stability and causality analyses akin to the second-order scenario presented in this section.

Chapter 4

Third-Order Regularized Hydrodynamics

In this chapter, we will proceed to the derivation and analysis of the third-order R14 hydrodynamics. To get the third-order equations, we need to obtain the $O(\epsilon^2)$ components of the energy-momentum moments with $n = 0, 1, 2, 3, 4$ except Π, q^μ, and $\pi^{\mu\nu}$, then plug them back into Eqs. (3.17), (3.23), and (3.25). Similar to the second-order scenario, a series of linear stability and causality analysis on the longitudinal and transverse components of the third-order theory will be presented, following the derivation of the third-order R14 equations.

4.1 Third-Order Moment Equations

Setting $n = 0$ in Eq. (2.68), we get the general moment equation for scalar moments:

$$\begin{aligned}
D\rho_r = &- \frac{\rho_r}{\tau_R} - F_{r-1} \\
&- \frac{2+r}{3}\theta\rho_r + m^2(r-1)\frac{\theta}{3}\rho_{r-2} \\
&- \nabla_\lambda \rho^\lambda_{r-1} - r a_\lambda \rho^\lambda_{r-1} \\
&- (r-1)\sigma_{\lambda\alpha}\rho^{\alpha\lambda}_{r-2}
\end{aligned} \tag{4.1}$$

Collecting all the $O(\epsilon)$ terms, the $O(\epsilon^2)$ components of the scalar moments can be expressed as

$$
\begin{aligned}
\frac{\rho_{r|2}}{\tau_R} = &- D\rho_{r|1} - F_{r-1|1} \\
&- \frac{(r+2)}{3}\theta\rho_{r|1} + \frac{(r-1)}{3}\theta m^2 \rho_{r-2|1} \\
&- r a_\lambda \rho^\lambda_{r-1|1} - \nabla_\lambda \rho^\lambda_{r-1|1} \\
&- (r-1)\sigma_{\lambda\alpha}\rho^{\lambda\alpha}_{r-2|1}
\end{aligned}
\tag{4.2}
$$

Once again, we emphasize that Π, q^μ, and $\pi^{\mu\nu}$ should not be expanded if they appear in the expression. The time derivative can be calculated as the following:

$$
\begin{aligned}
-D\rho_{r|1} &= D\left(\tau_R F_{r-1|0}\right) \\
&= \left(\frac{\partial\left(\tau_R\phi_{r-1|0}\right)}{\partial\alpha}\chi_{\alpha|0}\theta + \frac{\partial\left(\tau_R\phi_{r-1|0}\right)}{\partial\beta}\chi_{\beta|0}\theta\right)\theta + \left(\tau_R\phi_{r-1|0}\right)\left(\nabla_\gamma a^\gamma_{|0} + a^\gamma_{|0}a_{|0\gamma}\right)
\end{aligned}
\tag{4.3}
$$

where we have used $F_{r-1|0} = \phi_{r-1|0}\theta, D\theta = \nabla_\gamma a^\gamma_{|0} + a^\gamma_{|0}a_{|0\gamma}, (D\alpha)_{|0} = \chi_{\alpha|0}\theta$, and $(D\beta)_{|0} = \chi_{\beta|0}\theta$. The leading order acceleration $a^\gamma_{|0}$ is given by

$$
a^\gamma_{|0} = -\frac{\nabla^\gamma P}{\varepsilon + P}
\tag{4.4}
$$

Details are included in Appendix B. In summary, the scalar moments up to $O(\epsilon^2)$ are given by:

$$
\begin{aligned}
\rho_r = &-\tau_R F_{r-1} \\
&+\tau_R\Bigg[\left(\frac{\partial\left(\tau_R\phi_{r-1|0}\right)}{\partial\alpha}\chi_{\alpha|0}\theta + \frac{\partial\left(\tau_R\phi_{r-1|0}\right)}{\partial\beta}\chi_{\beta|0}\theta\right)\theta \\
&\quad + \left(\tau_R\phi_{r-1|0}\right)\left(\nabla_\gamma a^\gamma_{|0} + a^\gamma_{|0}a_{|0\gamma}\right) \\
&\quad - \frac{(r+2)}{3}\theta\rho_{r|1} + \frac{(r-1)}{3}\theta m^2\rho_{r-2|1} \\
&\quad - r a_{|0\lambda}\rho^\lambda_{r-1|1} - \nabla_\lambda\rho^\lambda_{r-1|1} \\
&\quad - (r-1)\sigma_{\lambda\alpha}\rho^{\lambda\alpha}_{r-2|1}\Bigg] + O\left(\epsilon^3\right)
\end{aligned}
\tag{4.5}
$$

Similarly, for the vector moments, setting $n = 1$ in Eq. (2.68) gives us

$$\begin{aligned}
\Delta^{\mu_1}_{\nu_1} D\rho^{\nu_1}_r =& -\frac{\rho^{\mu_1}_r}{\tau_R} - F^{\mu_1}_{r-1} \\
& - \frac{3+r}{3}\theta\rho^{\mu_1}_r + m^2(r-1)\frac{\theta}{3}\rho^{\mu_1}_{r-2} \\
& - \Delta^{\mu_1}_{\nu_1}\nabla_\lambda\rho^{\lambda\nu_1}_{r-1} - ra_\alpha\rho^{\alpha\mu_1}_{r-1} \\
& - \frac{1}{3}\left(\nabla^{\mu_1}\rho_{r+1} - m^2\nabla^{\mu_1}\rho_{r-1}\right) \\
& - \frac{(r+3)}{3}\rho_{r+1}a^{\mu_1} + r\frac{1}{3}m^2\rho_{r-1}a^{\mu_1} \\
& - (r-1)\sigma_{\lambda\alpha}\rho^{\alpha\lambda\mu_1}_{r-2} \\
& - \frac{(2r+3)}{5}\sigma^{\mu_1}_{\lambda}\rho^{\lambda}_r \\
& + m^2(r-1)\frac{2}{5}\sigma^{\mu_1}_{\lambda}\rho^{\lambda}_{r-2} \\
& - \omega^{\mu_1}_{\lambda}\rho^{\lambda}_r
\end{aligned} \tag{4.6}$$

Collecting all the terms up to $O(\epsilon^2)$, we have

$$\begin{aligned}
\rho^\mu_r =& -\tau_R F^\mu_{r-1} \\
& +\tau_R\Bigg[-\Delta^\mu_\nu D\rho^\nu_{r|1} \\
& + \frac{\theta}{3}\left(m^2(r-1)\rho^\mu_{r-2|1} - (r+3)\rho^\mu_{r|1}\right) \\
& - \frac{3+2r}{5}\sigma^\mu_\lambda\rho^\lambda_{r|1} + \frac{2}{5}(r-1)\sigma^\mu_\lambda m^2\rho^\lambda_{r-2|1} - \omega^\mu_\lambda\rho^\lambda_{r|1} \\
& + r\frac{1}{3}m^2\rho_{r-1|1}a^\mu_{|0} - \frac{(r+3)}{3}\rho_{r+1|1}a^\mu_{|0} \\
& - \frac{1}{3}\left(\nabla^\mu\rho_{r+1|1} - m^2\nabla^\mu\rho_{r-1|1}\right) \\
& - ra_{|0\lambda}\rho^{\lambda\mu}_{r-1|1} - \Delta^\mu_\nu\nabla_\lambda\rho^{\lambda\nu}_{r-1|1}\Bigg] + O\left(\epsilon^3\right)
\end{aligned} \tag{4.7}$$

where the time derivative is given by

$$-\Delta^{\mu}_{\nu} D\rho^{\nu}_{r|1} = \left(\frac{\partial\left(\tau_R\psi_{r-1|0}\right)}{\partial\alpha}\chi_{\alpha|0}\theta + \frac{\partial\left(\tau_R\psi_{r-1|0}\right)}{\partial\beta}\chi_{\beta|0}\theta\right)\left(\nabla^{\mu}\alpha\right) \\ + \left(\tau_R\psi_{r-1|0}\right) a^{\mu}_{|0}\chi_{\alpha|0}\theta + \left(\tau_R\psi_{r-1|0}\right)\nabla^{\mu}\left(\chi_{\alpha|0}\theta\right) \tag{4.8}$$

in which we have used $\Delta^{\mu}_{\nu} D\nabla^{\nu}\alpha = \nabla^{\mu}(D\alpha) + a^{\mu}D\alpha$. Using the same methodology, the rank-2 general moment equation is

$$\begin{aligned}
&\Delta^{\mu_1\mu_2}_{\nu_1\nu_2} D\rho^{\nu_1\nu_2}_{r} \\
&= -\frac{\rho^{\mu_1\mu_2}_{r}}{\tau_R} - F^{\mu_1\mu_2}_{r-1} \\
&\quad - \frac{4+r}{3}\theta\rho^{\mu_1\mu_2}_{r} + m^2(r-1)\frac{\theta}{3}\rho^{\mu_1\mu_2}_{r-2} \\
&\quad - \Delta^{\mu_1\mu_2}_{\nu_1\nu_2}\nabla_{\lambda}\rho^{\lambda\nu_1\nu_2}_{r-1} - r a_{\alpha}\rho^{\alpha\mu_1\mu_2}_{r-1} \\
&\quad - \frac{2}{5}\left(\nabla^{\langle\mu_1}\rho^{\mu_2\rangle}_{r+1} - m^2\nabla^{\langle\mu_1}\rho^{\mu_2\rangle}_{r-1}\right) \\
&\quad + r\frac{2}{5}m^2\rho^{\langle\mu_1}_{r-1}a^{\mu_2\rangle} - \frac{2(r+5)}{5}\rho^{\langle\mu_1}_{r+1}a^{\mu_2\rangle} \\
&\quad - (r-1)\sigma_{\lambda\alpha}\rho^{\alpha\lambda\mu_1\mu_2}_{r-2} \\
&\quad - \frac{2(2r+5)}{7}\sigma^{\langle\mu_1}_{\lambda}\rho^{\mu_2\rangle\lambda}_{r} \\
&\quad + m^2(r-1)\frac{4}{7}\sigma^{\langle\mu_1}_{\lambda}\rho^{\mu_2\rangle\lambda}_{r-2} \\
&\quad - \frac{2(4+r)}{15}\rho_{r+2}\sigma^{\mu_1\mu_2} \\
&\quad + m^2\frac{2(2r+3)}{15}\rho_{r}\sigma^{\mu_1\mu_n} \\
&\quad - m^4\frac{(r-1)2}{15}\rho_{r-2}\sigma^{\mu_1\mu_2} \\
&\quad - 2\omega^{\langle\mu_1}_{\lambda}\rho^{\mu_2\rangle\lambda}_{r}
\end{aligned} \tag{4.9}$$

Collecting all the terms up to $O(\epsilon^2)$, we have

$$
\begin{aligned}
\rho_r^{\mu_1\mu_2} =& -\tau_R F_{r-1}^{\mu_1\mu_2} \\
&+ \tau_R \Bigg[-\Delta^{\mu_1\mu_2}_{\nu_1\nu_2} D\rho^{\nu_1\nu_2}_{r|1} - \frac{\theta}{3}\left((4+r)\rho^{\mu_1\mu_2}_{r|1} - (r-1)m^2\rho^{\mu_1\mu_2}_{r-2|1}\right) \\
&+ \frac{2}{7}\left(-(2r+5)\sigma^{\langle\mu_2}_{\lambda}\rho^{\mu_1\rangle\lambda}_{r|1} + (2r-2)m^2\sigma^{\langle\mu_2}_{\lambda}\rho^{\mu_1\rangle\lambda}_{r-2|1}\right) - 2\omega^{\langle\mu_2}_{\lambda}\rho^{\mu_1\rangle\lambda}_{r|1} \\
&+ \frac{2}{15}\sigma^{\mu_1\mu_2}\left(-(4+r)\rho_{r+2|1} + (2r+3)m^2\rho_{r|1} - (r-1)m^4\rho_{r-2|1}\right) \\
&+ \frac{2}{5}\left(rm^2\rho^{\langle\mu_1}_{r-1|1}a^{\mu_2\rangle}_{|0} - (r+5)\rho^{\langle\mu_1}_{r+1|1}a^{\mu_2\rangle}_{|0}\right) - \frac{2}{5}\left(\nabla^{\langle\mu_1}\rho^{\mu_2\rangle}_{r+1|1} - m^2\nabla^{\langle\mu_1}\rho^{\mu_2\rangle}_{r-1|1}\right)\Bigg] \\
&+ O\left(\epsilon^3\right)
\end{aligned}
\tag{4.10}
$$

with the time derivative being

$$
\begin{aligned}
-\Delta^{\mu_1\mu_2}_{\nu_1\nu_2} D\rho^{\nu_1\nu_2}_{r|1} =& \Delta^{\mu_1\mu_2}_{\nu_1\nu_2} D\left(\tau_R F^{\nu_1\nu_2}_{r-1|0}\right) \\
=& \left(\frac{\partial\left(\tau_R\varphi_{r-1|0}\right)}{\partial\alpha}\chi_{\alpha|0}\theta + \frac{\partial\left(\tau_R\varphi_{r-1|0}\right)}{\partial\beta}\chi_{\beta|0}\theta\right)\sigma^{\mu_1\mu_2} \\
&+ \tau_R\varphi_{r-1|0}\nabla^{\langle\mu_1}a^{\mu_2\rangle}_{|0} + \tau_R\varphi_{r-1|0}a^{\langle\mu_1}_{|0}a^{\mu_2\rangle}_{|0}
\end{aligned}
\tag{4.11}
$$

where we have used $\Delta^{\mu_1\mu_2}_{\nu_1\nu_2} D\sigma^{\nu_1\nu_2} = \nabla^{\langle\mu_1} a^{\mu_2\rangle} + a^{\langle\mu_1} a^{\mu_2\rangle}$. We also need the rank-3 and rank-4 moment equations:

$$
\begin{aligned}
&\Delta^{\mu_1\mu_2\mu_3}_{\nu_1\nu_2\nu_3} D\rho_r^{\nu_1\nu_2\nu_3} \\
&= -\frac{\rho_r^{\mu_1\mu_2\mu_3}}{\tau_R} \\
&\quad - \frac{6(6+r)}{35}\rho_{r+2}^{\langle\mu_1}\sigma^{\mu_2\mu_3\rangle} \\
&\quad + m^2\frac{6(2r+5)}{35}\rho_r^{\langle\mu_1}\sigma^{\mu_2\mu_3\rangle} \\
&\quad - m^4\frac{(r-1)6}{35}\rho_{r-2}^{\langle\mu_1}\sigma^{\mu_2\mu_3\rangle} \\
&\quad - \frac{3}{7}\left(\nabla^{\langle\mu_1}\rho_{r+1}^{\mu_2\mu_3\rangle} - m^2\nabla^{\langle\mu_1}\rho_{r-1}^{\mu_2\mu_3\rangle}\right) \\
&\quad + r\frac{3}{7}m^2\rho_{r-1}^{\langle\mu_1\mu_2} a^{\mu_3\rangle} - \frac{3(r+7)}{7}\rho_{r+1}^{\langle\mu_1\mu_2} a^{\mu_3\rangle} \\
&\quad - \frac{5+r}{3}\theta\rho_r^{\mu_1\mu_2\mu_3} + m^2(r-1)\frac{\theta}{3}\rho_{r-2}^{\mu_1\mu_2\mu_3} \\
&\quad - \frac{3(2r+7)}{9}\sigma_\lambda^{\langle\mu_1}\rho_r^{\mu_2\mu_3\rangle\lambda} \\
&\quad + m^2(r-1)\frac{2}{3}\sigma_\lambda^{\langle\mu_1}\rho_{r-2}^{\mu_2\mu_3\rangle\lambda} \\
&\quad - 3\omega_\lambda^{\langle\mu_1}\rho_r^{\mu_2\mu_3\rangle\lambda} \\
&\quad - \Delta^{\mu_1\mu_2\mu_3}_{\nu_1\nu_2\nu_3}\nabla_\lambda\rho_{r-1}^{\lambda\nu_1\nu_2\nu_3} - ra_\alpha\rho_{r-1}^{\alpha\mu_1\mu_2\mu_3} \\
&\quad - (r-1)\sigma_{\lambda\alpha}\rho_{r-2}^{\alpha\lambda\mu_1\mu_2\mu_3}
\end{aligned}
\tag{4.12}
$$

$$
\begin{aligned}
\Delta^{\mu_1\mu_2\mu_3\mu_4}_{\nu_1\nu_2\nu_3\nu_4} D\rho_r^{\nu_1\nu_2\nu_3\nu_4} = &- \frac{\rho_r^{\mu_1\mu_2\mu_3\mu_4}}{\tau_R} \\
&- \frac{4(8+r)}{21}\rho_{r+2}^{\langle\mu_1\mu_2}\sigma^{\mu_3\mu_4\rangle} \\
&+ m^2\frac{4(2r+7)}{21}\rho_r^{\langle\mu_1\mu_2}\sigma^{\mu_3\mu_4\rangle} \\
&- m^4\frac{(r-1)4}{21}\rho_{r-2}^{\langle\mu_1\mu_2}\sigma^{\mu_3\mu_4\rangle} \\
&- \frac{4}{9}\left(\nabla^{\langle\mu_1}\rho_{r+1}^{\mu_2\mu_3\mu_4\rangle} - m^2\nabla^{\langle\mu_1}\rho_{r-1}^{\mu_2\mu_3\mu_4\rangle}\right) \\
&+ r\frac{4}{9}m^2\rho_{r-1}^{\langle\mu_1\mu_2\mu_3}a^{\mu_4\rangle} - \frac{4(r+9)}{9}\rho_{r+1}^{\langle\mu_1\mu_2\mu_3}a^{\mu_4\rangle} \\
&- \frac{4(2r+9)}{11}\sigma_\lambda^{\langle\mu_1}\rho_r^{\mu_2\mu_3\mu_4\rangle\lambda} \\
&+ m^2(r-1)\frac{8}{11}\sigma_\lambda^{\langle\mu_1}\rho_{r-2}^{\mu_2\mu_3\mu_4\rangle\lambda} \\
&- 4\omega_\lambda^{\langle\mu_1}\rho_r^{\mu_2\mu_3\mu_4\rangle\lambda} \\
&- \frac{6+r}{3}\theta\rho_r^{\mu_1\mu_2\mu_3\mu_n} + m^2(r-1)\frac{\theta}{3}\rho_{r-2}^{\mu_1\mu_2\mu_3\mu_4} \\
&- \Delta^{\mu_1\mu_2\mu_3\mu_\lambda}_{\nu_1\nu_2\nu_3\nu_4}\nabla_\lambda\rho_{r-1}^{\lambda\nu_1\nu_2\nu_3\nu_4} - ra_\alpha\rho_{r-1}^{\alpha\mu_1\mu_2\mu_3\mu_4} \\
&- (r-1)\sigma_{\lambda\alpha}\rho_{r-2}^{\alpha\lambda\mu_1\mu_2\mu_3\mu_4}
\end{aligned}
\tag{4.13}
$$

As before, collecting all the terms up to $O(\epsilon^2)$ gives us:

$$
\begin{aligned}
\rho_r^{\mu_1\mu_2\mu_3} = \tau_R\Big[&- \frac{3}{7}\left(\nabla^{\langle\mu_1}\rho_{r+1|1}^{\mu_2\mu_3\rangle} - m^2\nabla^{\langle\mu_1}\rho_{r-1|1}^{\mu_2\mu_3\rangle}\right) \\
&+ r\frac{3}{7}m^2\rho_{r-1|1}^{\langle\mu_1\mu_2}a^{\mu_3\rangle} - \frac{3(r+7)}{7}\rho_{r+1|1}^{\langle\mu_1\mu_2}a^{\mu_3\rangle} \\
&- (r+6)\frac{6}{35}\rho_{r+2|1}^{\langle\mu_1}\sigma^{\mu_2\mu_3\rangle} + (5+2r)\frac{6}{35}m^2\rho_{r|1}^{\langle\mu_1}\sigma^{\mu_2\mu_3\rangle} \\
&- (r-1)m^4\frac{6}{35}\rho_{r+2|1}^{\langle\mu_1}\sigma^{\mu_2\mu_3\rangle}\Big] + O\left(\epsilon^3\right)
\end{aligned}
\tag{4.14}
$$

and

$$
\begin{aligned}
\rho_r^{\mu_1\mu_2\mu_3\mu_4} = \tau_R\Big[&-(8+r)\frac{4}{21}\rho_{r+2|1}^{\langle\mu_1\mu_2}\sigma^{\mu_3\mu_4\rangle} + (7+2r)\frac{4}{21}m^2\rho_{r|1}^{\langle\mu_1\mu_2}\sigma^{\mu_3\mu_4\rangle} \\
&-(r-1)\frac{4}{21}m^4\rho_{r-2|1}^{\langle\mu_1\mu_2}\sigma^{\mu_3\mu_4\rangle}\Big] + O\left(\epsilon^3\right)
\end{aligned}
\tag{4.15}
$$

Note that the time derivatives vanish at $O(\epsilon)$ for $n = 3, 4$. Inserting all the previous results back into Eqs. (3.17), (3.23), and (3.25) to replace all the moments except Π, q^μ, and $\pi^{\mu\nu}$ gives us the third-order R14 theory.

4.2 Third-Order R25 Hydrodynamics

Analogous to the second-order case, for simplicity, we will assume massless particles without particle number conservation throughout the linear stability and causality analysis that will be presented in the next section. In this section, we will derive the corresponding reduced third-order theory based on the R14 theory, so that they can be used in the next section. With $m = 0$, the only dissipative quantity left is the shear-stress tensor $\pi^{\mu\nu}$, as already mentioned in the previous chapter. Therefore, the total number of moments reduces to 9, akin to the second-order case. Setting $m = 0$ in Eq. (3.25) gives

$$\begin{aligned} \Delta^{\mu\nu}_{\alpha\beta} D\pi^{\alpha\beta} = &-\frac{\pi^{\mu\nu}}{\tau_R} - \varphi_{-1|0}\sigma^{\mu\nu} - \Delta^{\mu\nu}_{\alpha\beta}\nabla_\lambda \rho^{\lambda\alpha\beta}_{-1} \\ &- \frac{4}{3}\theta\pi^{\mu\nu} + \sigma_{\lambda\alpha}\rho^{\alpha\lambda\mu\nu}_{-2} - \frac{10}{7}\pi^{\lambda\langle\mu}\sigma^{\nu\rangle}_{\lambda} - 2\pi^{\lambda\langle\mu}\omega^{\nu\rangle}_{\lambda} \end{aligned} \tag{4.16}$$

At this point, it seems natural to insert the results in Section 4.1 back into Eq. (4.16) to replace $\rho^{\lambda\mu\nu}_{-1}$ and $\rho^{\alpha\beta\mu\nu}_{-2}$ in order to get the third-order $\pi^{\mu\nu}$ equations. However, careful observation reveals that doing this results in second-order spatial gradients in the third-order equations. For example, the first term in Eq. (4.14) will become $\sim \frac{3}{7}\nabla^{\langle\lambda}\pi^{\alpha\beta\rangle}$ for $r = -1$, when being plugged back into Eq. (4.16), the corresponding term will become second-order in gradient. Under a Lorentz boost, this term produces second-order time derivatives and turns the original parabolic equation into a hyperbolic one. This usually introduces extra modes in Fourier space, which are often linearly unstable and acausal. To solve this problem, we need to promote $\rho^{\lambda\mu\nu}_{-1}$ and $\rho^{\alpha\beta\mu\nu}_{-2}$ to hydrodynamic variables with their own equations of evolution given by Eqs. (4.12) and (4.13) with $r = -1$ and $r = -2$, respectively. All the moments with order $n > 4$ are also rejected since they are $O(\epsilon^3)$.

Doing this raises the total number of moments from 9 to 25. Now, let

$$\begin{aligned}
\xi^{\lambda\mu\nu} &= \rho_{-1}^{\lambda\mu\nu} \\
\varsigma^{\alpha\beta\mu\nu} &= \rho_{-2}^{\alpha\beta\mu\nu}
\end{aligned} \tag{4.17}$$

Setting $m = 0$ and $r = -1$ in Eq. (4.12) along with relaxation time approximation, we obtain the $\xi^{\lambda\mu\nu}$ equation:

$$\begin{aligned}
\Delta^{\lambda\mu\nu}_{\rho\alpha\beta} D\xi^{\rho\alpha\beta} = &-\frac{1}{\tau_\xi}\xi^{\lambda\mu\nu} - \frac{18}{7}\pi^{\langle\lambda\mu}a^{\nu\rangle} + a_\rho\varsigma^{\rho\lambda\mu\nu} - \Delta^{\lambda\mu\nu}_{\rho\alpha\beta}\nabla_\omega\varsigma^{\omega\rho\alpha\beta} \\
&- \frac{3}{7}\nabla^{\langle\lambda}\pi^{\mu\nu\rangle} - \frac{4}{3}\theta\xi^{\lambda\mu\nu} + 2\sigma_{\alpha\beta}\rho_{-3}^{\alpha\beta\lambda\mu\nu} \\
&- \frac{5}{3}\xi^{\alpha\langle\lambda\mu}\sigma^{\nu\rangle}_\alpha - 3\xi^{\alpha\langle\lambda\mu}\omega^{\nu\rangle}_\alpha - \frac{6}{7}\rho_1^{\langle\lambda}\sigma^{\mu\nu\rangle}
\end{aligned} \tag{4.18}$$

where τ_ξ is the relaxation time associated with $\xi^{\lambda\mu\nu}$, and the $\rho_1^{\langle\lambda}\sigma^{\mu\nu\rangle}$ term vanishes due to the matching conditions. Note that we have used Eq. (3.3) to eliminate $F_{-2}^{\lambda\mu\nu}$. We will also reject the $\rho_{-3}^{\omega\alpha\lambda\mu\nu}$ term since it is $O(\epsilon^3)$.

To get the equation for $\varsigma^{\alpha\beta\mu\nu}$, we set $m = 0$ and $r = -2$ in Eq. (4.13) along with relaxation time approximation:

$$\begin{aligned}
\Delta^{\alpha\beta\mu\nu}_{\rho\lambda\omega\gamma} D\varsigma^{\rho\lambda\omega\gamma} = &-\frac{1}{\tau_\varsigma}\varsigma^{\alpha\beta\mu\nu} - \frac{28}{9}\xi^{\langle\alpha\beta\mu}a^{\nu\rangle} + 2a_\lambda\rho_{-3}^{\lambda\alpha\beta\mu\nu} - \Delta^{\alpha\beta\mu\nu}_{\rho\lambda\omega\gamma}\nabla_\theta\rho_{-3}^{\theta\rho\lambda\omega\gamma} \\
&- \frac{4}{9}\nabla^{\langle\alpha}\xi^{\beta\mu\nu\rangle} - \frac{4}{3}\theta\varsigma^{\alpha\beta\mu\nu} + 3\sigma_{\lambda\rho}\rho_{-4}^{\lambda\rho\alpha\beta\mu\nu} \\
&- \frac{20}{11}\varsigma^{\lambda\langle\alpha\beta\mu}\sigma^{\nu\rangle}_\lambda - 4\varsigma^{\lambda\langle\alpha\beta\mu}\omega^{\nu\rangle}_\lambda - \frac{8}{7}\pi^{\langle\alpha\beta}\sigma^{\mu\nu\rangle}
\end{aligned} \tag{4.19}$$

where we reject all the $\rho_{-3}^{\omega\alpha\lambda\mu\nu}$ and $\rho_{-4}^{\omega\lambda\alpha\beta\mu\nu}$ terms since they are $O(\epsilon^3)$.

4.3 Linear Stability and Causality Analysis

In this section, we will examine the linear stability and causality of the third-order R25 theory derived in the previous section. Similar to the analyses done in the previous chapter, we will decompose the evolution equations into longitudinal and transverse parts, and then analyze them independently.

4.3.1 Linearized Third-Order Equations

Akin to the second-order analysis, we reject all the higher-order terms in Eq. (4.16) and keep only the terms that are linear in small fluctuations to obtain the linearized $\pi^{\mu\nu}$ equation:

$$\Delta^{\mu\nu}_{\alpha\beta,0} D_0 \pi^{\alpha\beta} + \frac{1}{\tau_\pi}\pi^{\mu\nu} + \varphi_{-1|0}\sigma^{\mu\nu} + \Delta^{\mu\nu}_{\alpha\beta,0}\nabla_{\lambda,0}\xi^{\lambda\alpha\beta} = 0 \tag{4.20}$$

Again, using Eq. (3.29) and (B.39), and expressing the hydrodynamic variables in Fourier space lead us to the following:

$$\left(i\Omega + \frac{1}{\tau_\pi}\right)\delta\pi^{\mu\nu} + \frac{4i\epsilon_0}{15}\left(\kappa^\mu \delta u^\nu + \kappa^\nu \delta u^\mu - \frac{2}{3}\kappa_\alpha \delta u^\alpha \Delta_0^{\mu\nu}\right) + i\kappa_\lambda \xi^{\lambda\mu\nu} = 0 \tag{4.21}$$

Similarly, the linearized equation for $\xi^{\lambda\mu\nu}$ is:

$$\Delta^{\lambda\mu\nu}_{\alpha\beta\gamma,0} D_0 \xi^{\alpha\beta\gamma} + \frac{1}{\tau_\xi}\xi^{\lambda\mu\nu} + \frac{3}{7}\Delta^{\lambda\mu\nu}_{\alpha\beta\gamma,0}\nabla_0^\alpha \delta\pi^{\beta\gamma} + \Delta^{\lambda\mu\nu}_{\alpha\beta\gamma,0}\nabla_{\omega,0}\varsigma^{\omega\alpha\beta\gamma} = 0 \tag{4.22}$$

which becomes

$$\begin{aligned}
&\left(i\Omega + \frac{1}{\tau_\xi}\right)\xi^{\lambda\mu\nu} + \frac{i}{7}\left(\kappa^\lambda \delta\pi^{\mu\nu} + \kappa^\mu \delta\pi^{\nu\lambda} + \kappa^\nu \delta\pi^{\mu\lambda}\right) \\
&- \frac{2i}{35}\left(\Delta_0^{\lambda\mu}\kappa^\omega \delta\pi^\nu_\omega + \Delta_0^{\lambda\nu}\kappa^\omega \delta\pi^\mu_\omega + \Delta_0^{\mu\nu}\kappa^\omega \delta\pi^\lambda_\omega\right) + i\kappa_\omega \varsigma^{\omega\lambda\mu\nu} = 0
\end{aligned} \tag{4.23}$$

in the Fourier space after taking the derivatives D_0 and $\nabla_{\lambda,0}$. To derive the above expression, we have used the following explicit expression of the rank-3 projector [66]:

$$\begin{aligned}
\Delta^{\mu\nu\lambda}_{\alpha\beta\rho} \equiv\, & \frac{1}{6}\left[\Delta^\mu_\alpha\left(\Delta^\nu_\beta\Delta^\lambda_\rho + \Delta^\nu_\rho\Delta^\lambda_\beta\right) + \Delta^\mu_\beta\left(\Delta^\nu_\alpha\Delta^\lambda_\rho + \Delta^\nu_\rho\Delta^\lambda_\alpha\right) + \Delta^\mu_\rho\left(\Delta^\nu_\alpha\Delta^\lambda_\beta + \Delta^\nu_\beta\Delta^\lambda_\alpha\right)\right] \\
& - \frac{1}{15}\left[\Delta^{\mu\nu}\left(\Delta^\lambda_\alpha\Delta_{\beta\rho} + \Delta^\lambda_\beta\Delta_{\alpha\rho} + \Delta^\lambda_\rho\Delta_{\alpha\beta}\right) + \Delta^{\mu\lambda}\left(\Delta^\nu_\alpha\Delta_{\beta\rho} + \Delta^\nu_\beta\Delta_{\alpha\rho} + \Delta^\nu_\rho\Delta_{\alpha\beta}\right)\right. \\
& \left. + \Delta^{\nu\lambda}\left(\Delta^\mu_\alpha\Delta_{\beta\rho} + \Delta^\mu_\beta\Delta_{\alpha\rho} + \Delta^\mu_\rho\Delta_{\alpha\beta}\right)\right]
\end{aligned} \tag{4.24}$$

The linearized equation for $\varsigma^{\alpha\beta\mu\nu}$ is also straightforward to obtain:

$$\Delta^{\alpha\beta\mu\nu}_{\lambda\gamma\rho\theta,0} D_0 \varsigma^{\lambda\gamma\rho\theta} + \frac{1}{\tau_\varsigma}\varsigma^{\alpha\beta\mu\nu} + \frac{4}{9}\Delta^{\alpha\beta\mu\nu}_{\lambda\gamma\rho\theta,0}\nabla^{\lambda}_{0}\xi^{\gamma\rho\theta} = 0 \tag{4.25}$$

which becomes

$$\left(i\Omega + \frac{1}{\tau_\varsigma}\right)\varsigma^{\alpha\beta\mu\nu} + \frac{4i}{9}\Delta^{\alpha\beta\mu\nu}_{\lambda\gamma\rho\theta,0}\kappa^{\lambda}\xi^{\gamma\rho\theta} = 0 \tag{4.26}$$

in the Fourier space after taking the derivatives. Using Eq. (A.1), one can show that

$$\begin{aligned}
\Delta^{\alpha\beta\mu\nu}_{\lambda\gamma\rho\theta,0}\kappa^{\lambda}\xi^{\gamma\rho\theta} = {} & \frac{1}{4}\left(\kappa^{\alpha}\xi^{\beta\mu\nu} + \kappa^{\beta}\xi^{\alpha\mu\nu} + \kappa^{\mu}\xi^{\alpha\beta\nu} + \kappa^{\nu}\xi^{\alpha\mu\beta}\right) \\
& - \frac{1}{20}\Big(\Delta_0^{\beta\mu}\kappa_\lambda\xi^{\alpha\nu\lambda} + \Delta_0^{\beta\nu}\kappa_\lambda\xi^{\alpha\mu\lambda} + \Delta_0^{\mu\nu}\kappa_\lambda\xi^{\alpha\beta\lambda} \\
& \quad + \Delta_0^{\alpha\mu}\kappa_\lambda\xi^{\beta\nu\lambda} + \Delta_0^{\alpha\nu}\kappa_\lambda\xi^{\beta\mu\lambda} + \Delta_0^{\alpha\beta}\kappa_\lambda\xi^{\mu\nu\lambda}\Big) \\
& - \frac{3}{140}\Big(\Delta_0^{\alpha\beta}\kappa_\lambda\xi^{\lambda\mu\nu} + \Delta_0^{\alpha\mu}\kappa_\lambda\xi^{\lambda\beta\nu} + \Delta_0^{\alpha\nu}\kappa_\lambda\xi^{\lambda\beta\mu} \\
& \quad + \Delta_0^{\beta\mu}\kappa_\lambda\xi^{\lambda\alpha\nu} + \Delta_0^{\beta\nu}\kappa_\lambda\xi^{\lambda\mu\alpha} + \Delta_0^{\mu\nu}\kappa_\lambda\xi^{\lambda\alpha\beta}\Big)
\end{aligned} \tag{4.27}$$

Plugging this back into Eq. (4.26) gives the complete linearized evolution equation for $\varsigma^{\alpha\beta\mu\nu}$.

4.3.2 Transverse Modes

Case 1: k is parallel to V

As before, the background fluid velocity and the wave vector are given by Eq. (3.43), and it follows that the covariant variables are then given by Eq. (3.44). The energy conservation law is purely longitudinal and therefore will not contribute to the transverse analysis. The transverse components of the equations for $\pi^{\mu\nu}$, $\xi^{\lambda\mu\nu}$, $\varsigma^{\alpha\beta\mu\nu}$, and the momentum conservation law can be obtained by applying $\Delta^{\mu\nu}_{\kappa}$ and κ^{μ} to the linearized equations:

$$\begin{aligned}
&\Omega\epsilon_0\delta u^{\mu}_{\perp} + \frac{3}{4}\kappa\delta\pi^{\mu}_{\perp} = 0 \\
&\left(i\Omega + \frac{1}{\tau_\pi}\right)\delta\pi^{\mu}_{\perp} + \frac{4}{15}i\kappa\epsilon_0\delta u^{\mu}_{\perp} + i\kappa\xi^{\mu}_{\perp} = 0 \\
&\left(i\Omega + \frac{1}{\tau_\xi}\right)\xi^{\mu}_{\perp} + \frac{8}{35}i\kappa\delta\pi^{\mu}_{\perp} + i\kappa\varsigma^{\mu}_{\perp} = 0 \\
&\left(i\Omega + \frac{1}{\tau_\varsigma}\right)\varsigma^{\mu}_{\perp} + \frac{5}{21}i\kappa\xi^{\mu}_{\perp} = 0
\end{aligned} \tag{4.28}$$

where we defined $\xi^{\mu}_{\perp} = \kappa_\alpha\kappa_\lambda\Delta^{\mu}_{\nu,\kappa}\xi^{\alpha\lambda\nu}/\kappa^2$ and $\varsigma^{\mu}_{\perp} = \kappa_\alpha\kappa_\beta\kappa_\lambda\Delta^{\mu}_{\nu,\kappa}\varsigma^{\alpha\beta\lambda\nu}/\kappa^3$. This can be written in the following matrix form:

$$\begin{pmatrix} \Omega & \frac{3}{4}\kappa & 0 & 0 \\ \frac{4}{15}i\kappa & i\Omega + \frac{1}{\tau_\pi} & i\kappa & 0 \\ 0 & \frac{8}{35}i\kappa & i\Omega + \frac{1}{\tau_\xi} & i\kappa \\ 0 & 0 & \frac{5}{21}i\kappa & i\Omega + \frac{1}{\tau_\varsigma} \end{pmatrix} \begin{pmatrix} \epsilon_0\delta u^{\mu}_{\perp} \\ \delta\pi^{\mu}_{\perp} \\ \xi^{\mu}_{\perp} \\ \varsigma^{\mu}_{\perp} \end{pmatrix} = 0 \tag{4.29}$$

For simplicity, from now on we will assume that the corresponding relaxation time for each moment is the same throughout the analysis:

$$\tau_R = \tau_\pi = \tau_\xi = \tau_\varsigma \tag{4.30}$$

We require that the determinant of the 4×4 matrix be zero to obtain non-trivial solutions, the resulting equation is the dispersion relation, just as before. However, we should note that the dispersion relation is extremely complicated, even displaying the leading-order terms is not feasible. Therefore, we will only present the numerical solutions to the dispersion relation shown in Fig. (4.1), assuming $\tau_R = 5$ as always.

Since the M matrix is 4×4, and entries with ω are situated along the diagonal only, we can conclude that the dispersion relation is of fourth-order in ω and thus we should expect to obtain four solutions. Recall that in the second-order case, only two modes were

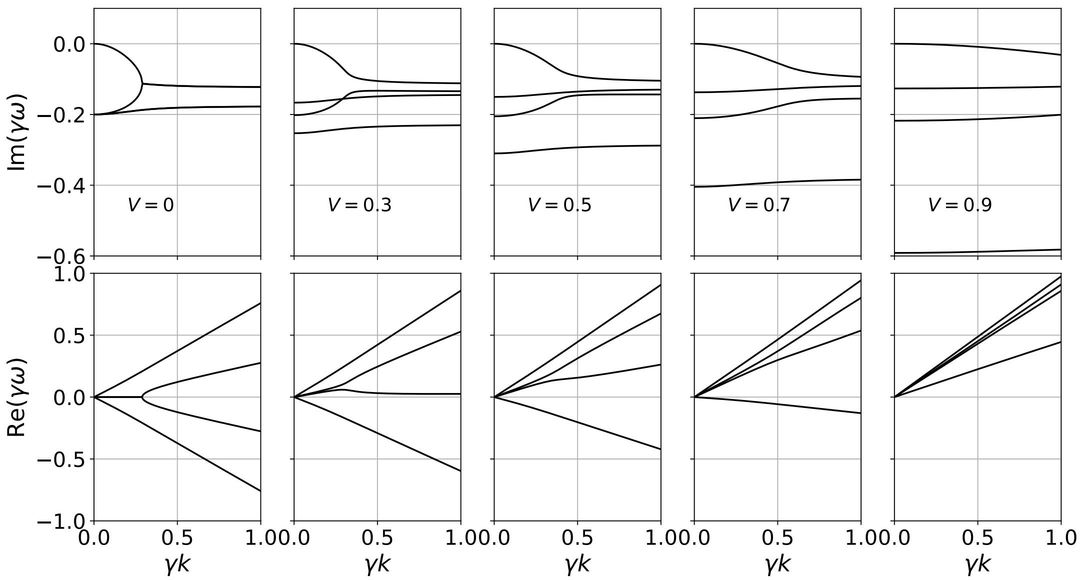

Figure 4.1: Real and Imaginary parts of the transverse modes of the massless third-order R25 hydrodynamics, in the case of fluid velocity vector being parallel to the wave vector. The relaxation time is chosen to be $\tau_R = 5$ as usual.

obtained (see Eq. (3.48)). The presence of additional modes can be attributed to the extra degrees of freedom in the hydrodynamic variables, which are $\xi_\perp^\mu$ and $\varsigma_\perp^\mu$. Indeed, Fig. (4.1) shows four distinct curves, two of which have the same imaginary parts for static fluids, i.e. $V = 0$. As one can easily see, all the modes have non-positive imaginary parts for small k and therefore are linearly stable. Similar to the second-order R14 theory, we can show that the modes are in fact linearly stable for all $k \geq 0$, proven by the asymptotic behavior of the modes for $V = 0.9$ and $\tau_R = 5$ shown in Fig. (4.2). We claim that the same conclusion can be obtained for any other values of V.

As for the causality analysis, similar problems arise when we try to expand the solutions in the limit of large wave number k: writing down the leading-order terms is not feasible. Therefore, taking the numerical approach is more practical. In the large ω and k limit, solving the dispersion relation is equivalent to solving the following series

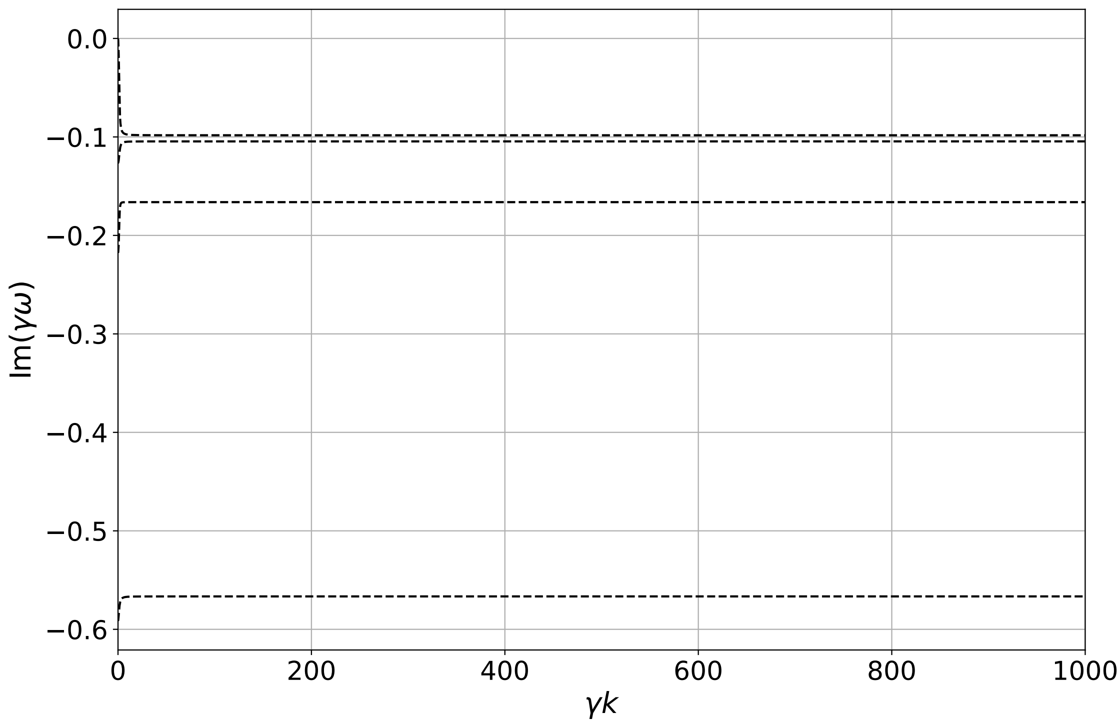

Figure 4.2: The imaginary parts of the transverse modes of the massless third-order R25 hydrodynamics plotted for a larger range of k, in the case of fluid velocity vector being parallel to the wave vector, for $V = 0.9$ and with relaxation time $\tau_R = 5$.

expansion:

$$-5ik^4\tau_R^3(1 - 14V^2 + 21V^4) - 5i\tau_R^3 V^4\omega^4 + O(k^3) + O(\omega^3) = 0 \tag{4.31}$$

where we omit the terms under $O(k^3)$ and $O(\omega^3)$ for display, but they are included in the actual numerical computation. The corresponding large-k solutions are obtained by solving the above equation numerically. Figure (4.3) displays the magnitude of the group velocities corresponding to these modes, as a function of the fluid velocity V. As we can see, in the large-k limit, the group velocity for each mode is subliminal, and thus causal. Furthermore, One can verify that the curves in Fig. (4.3) obey the relativistic velocity

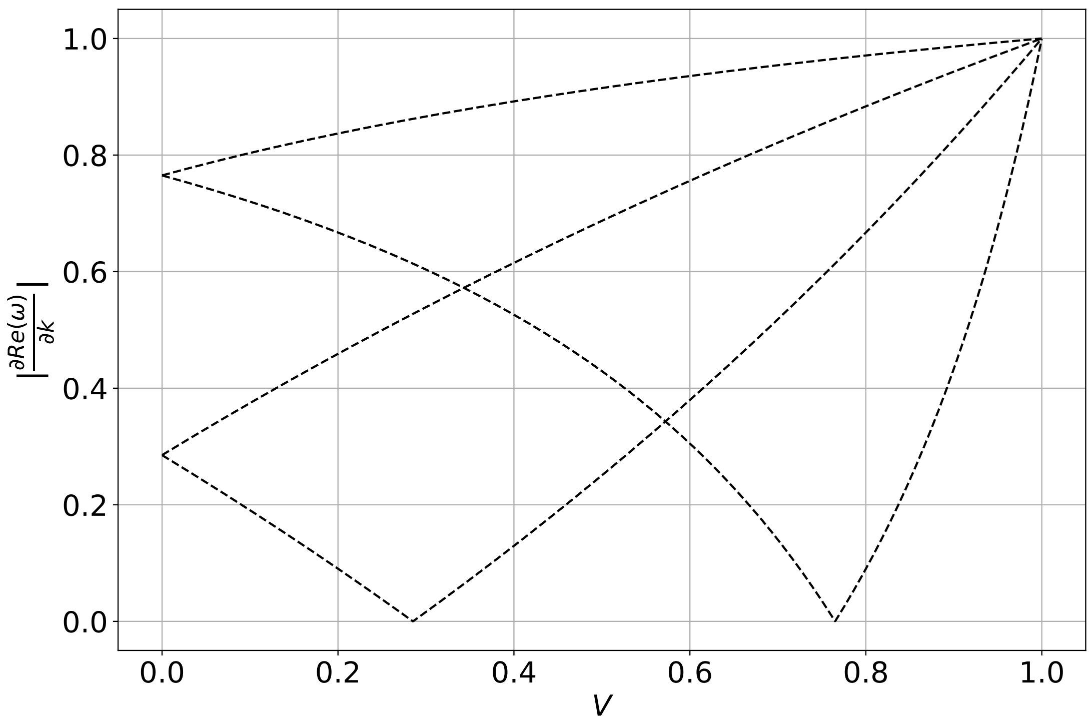

Figure 4.3: Magnitude of the group velocity for the transverse modes of the massless third-order R25 hydrodynamics, as a function of the fluid velocity V in the large k limit and with $\tau_R = 5$, in the case of fluid velocity vector being parallel to the wave vector.

addition formula:

$$u = \frac{v + u'}{1 + vu'} \tag{4.32}$$

Case 2: k is orthogonal to V

It is straightforward to obtain the solutions for this case by substituting Eq. (3.56) into the dispersion relation and then solving it numerically. The results are shown in Fig. (4.4). From the figure, we can again see that all the modes are linearly stable as their imaginary parts are always non-positive for small k, regardless of the background fluid velocity. Just as before,c we can further extend the linear stability of the modes to all $k \geq 0$ from the asymptotic behavior of the modes in Fig. (4.5), for $V = 0.9$ and $\tau_R = 5$.

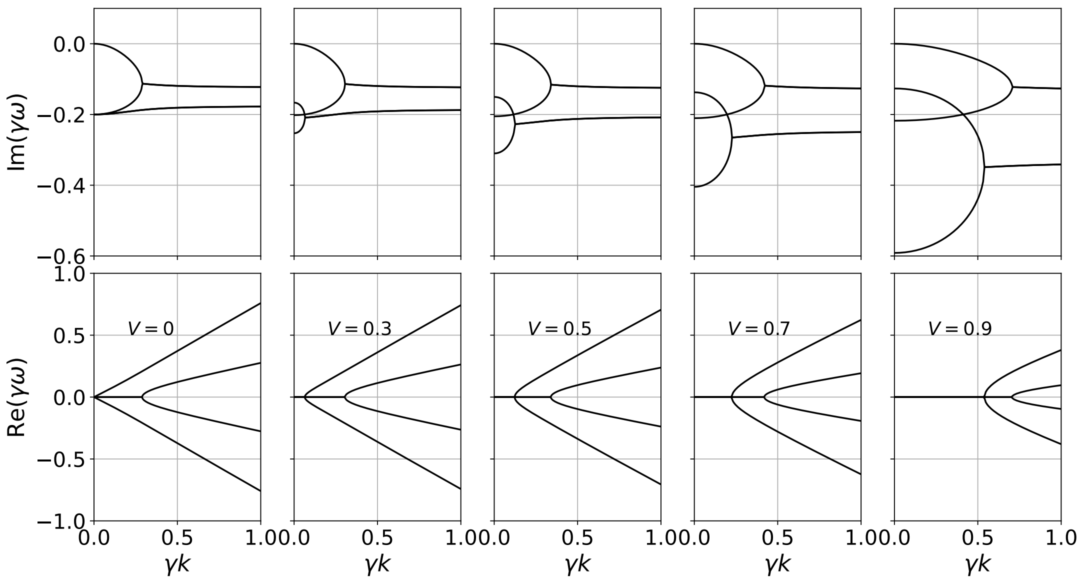

Figure 4.4: Real and Imaginary parts of the transverse modes of the massless third-order R25 hydrodynamics, in the case of fluid velocity vector being orthogonal to the wave vector and with $\tau_R = 5$.

Now, in the large-k limit, the dispersion relation can be expanded as

$$-5ik^4 - \frac{5iV^4\omega^4}{(V^2-1)^2} + O(k^2) + O(\omega^3) = 0 \tag{4.33}$$

Again, we should emphasize that although the $O(k^2)$ and $O(\omega^3)$ terms are not displayed, they are included in the numerical computation. Fig. (4.6) shows the corresponding group velocity as a function of V. Note that there are only two curves for four solutions. This is because the group velocities for each pair of solutions are only off by a sign. Since the y-axis is the absolute value of the group velocity, both solutions coincide in this case. Also, note that both curves approach zero when the fluid velocity reaches the speed of light. This is expected since the plane wave propagates in the orthogonal direction with respect to the fluid flow. As the fluid moves faster and faster, the wave is eventually "dragged" by the fluid flow under the effect of shear viscosity and moves in the fluid flow direction eventually, resulting in zero group velocity in the orthogonal direction.

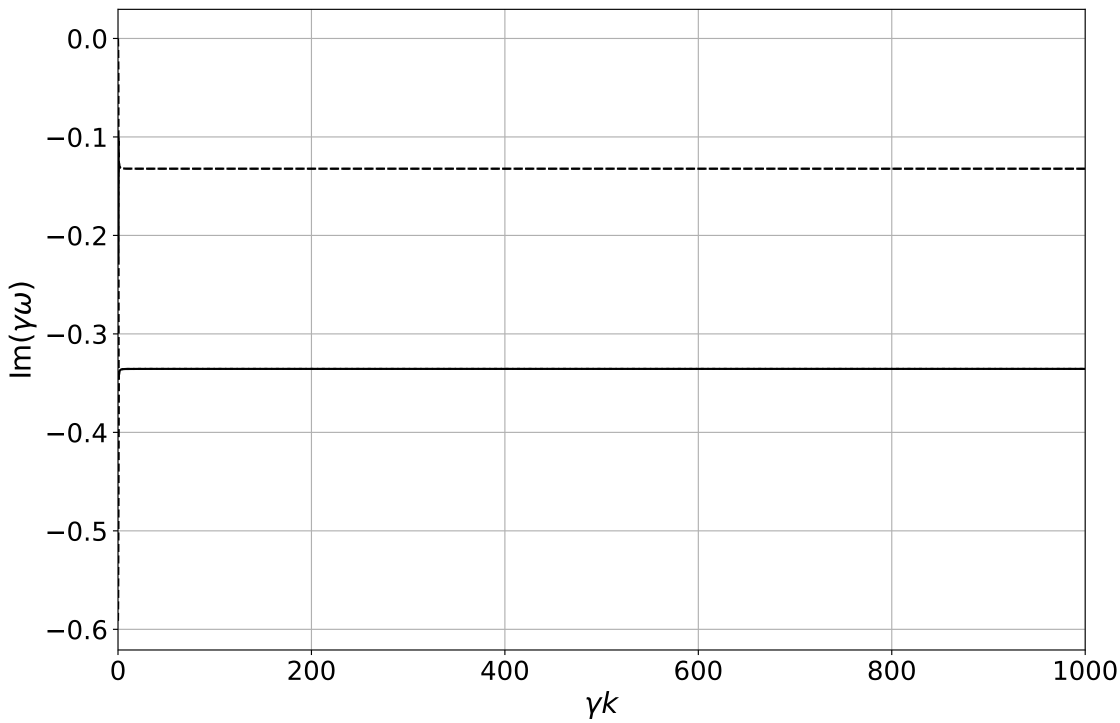

Figure 4.5: The imaginary parts of the transverse modes of the massless third-order R25 hydrodynamics plotted for a larger range of k, in the case of fluid velocity vector being orthogonal to the wave vector, for $V = 0.9$ and with relaxation time $\tau_R = 5$.

4.3.3 Longitudinal Modes

Case 1: k is parallel to V

Similar to the second-order case, the first step is to obtain the longitudinal components of the conservation laws and the equations for $\pi^{\mu\nu}$, $\xi^{\lambda\mu\nu}$, and $\varsigma^{\alpha\beta\mu\nu}$. Applying $\kappa^\mu\kappa^\nu$ and κ^μ to

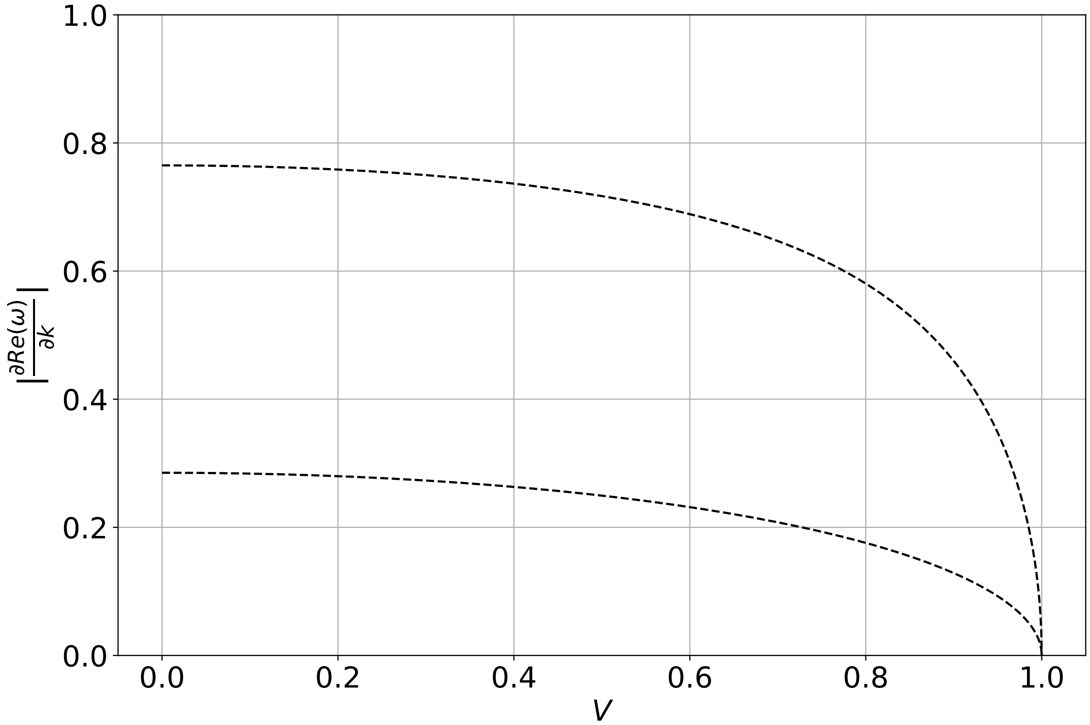

Figure 4.6: Magnitude of the group velocity for the transverse modes of the massless third-order R25 hydrodynamics, as a function of the fluid velocity V in the large k limit and with $\tau_R = 5$, in the case of fluid velocity vector being orthogonal to the wave vector.

the corresponding equations, we get

$$
\begin{aligned}
&\Omega\delta\epsilon + \frac{4}{3}\epsilon_0\kappa\delta u_{||} = 0 \\
&\Omega\epsilon_0\delta u_{||} + \frac{1}{4}\kappa\delta\epsilon + \frac{3}{4}\kappa\delta\pi_{||} = 0 \\
&\left(i\Omega + \frac{1}{\tau_R}\right)\delta\pi_{||} + \frac{16}{45}i\epsilon_0\kappa\delta u_{||} + i\kappa\xi_{||} = 0 \\
&\left(i\Omega + \frac{1}{\tau_R}\right)\xi_{||} + \frac{9}{35}i\kappa\delta\pi_{||} + i\kappa\varsigma_{||} = 0 \\
&\left(i\Omega + \frac{1}{\tau_R}\right)\varsigma_{||} + \frac{16}{63}i\kappa\xi_{||} = 0
\end{aligned}
\tag{4.34}
$$

where we defined $\xi_{||} = \kappa_\alpha\kappa_\beta\kappa_\lambda\xi^{\alpha\beta\lambda}/\kappa^3$ and $\varsigma_{||} = \kappa_\alpha\kappa_\beta\kappa_\mu\kappa_\nu\varsigma^{\alpha\beta\mu\nu}/\kappa^4$. Note that we have included the purely-longitudinal energy conservation law in this system of equations.

Written in the matrix form, this is equivalent to

$$\begin{pmatrix} \Omega & \frac{4}{3}\kappa & 0 & 0 & 0 \\ \frac{\kappa}{4} & \Omega & \frac{3}{4}\kappa & 0 & 0 \\ 0 & \frac{16}{45}i\kappa & i\Omega+\frac{1}{\tau_R} & i\kappa & 0 \\ 0 & 0 & \frac{9}{35}i\kappa & i\Omega+\frac{1}{\tau_R} & i\kappa \\ 0 & 0 & 0 & \frac{16}{63}i\kappa & i\Omega+\frac{1}{\tau_R} \end{pmatrix} \begin{pmatrix} \delta\epsilon \\ \epsilon_0\delta u_{||} \\ \delta\pi_{||} \\ \xi_{||} \\ \varsigma_{||} \end{pmatrix} = 0 \tag{4.35}$$

Since Ω is of fifth-order in the determinant, we should expect to obtain five modes. Indeed, Fig. (4.7) shows that all five solutions are linearly stable since their imaginary parts are all non-positive for various background fluid velocities, with small k. We can further generalize this result to all $k \geq 0$ by noticing the asymptotic behavior of all the five modes for $V = 0.9$ and $\tau_R = 5$, shown in Fig. (4.8). The same conclusion can be drawn for any other values of V.

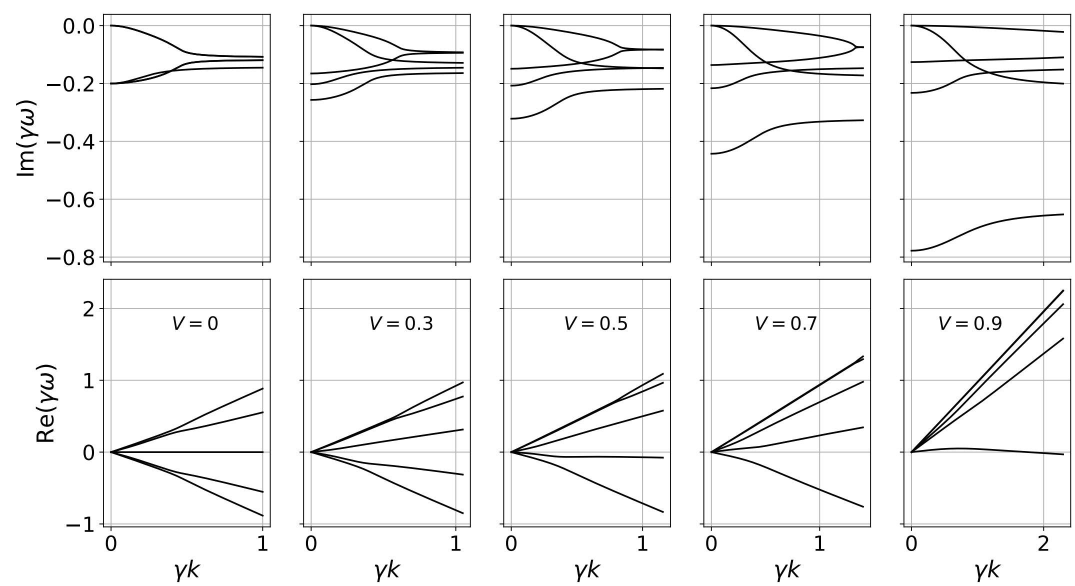

Figure 4.7: Real and Imaginary parts of the longitudinal modes of the massless third-order R25 hydrodynamics, in the case of fluid velocity vector being parallel to the wave vector and with $\tau_R = 5$.

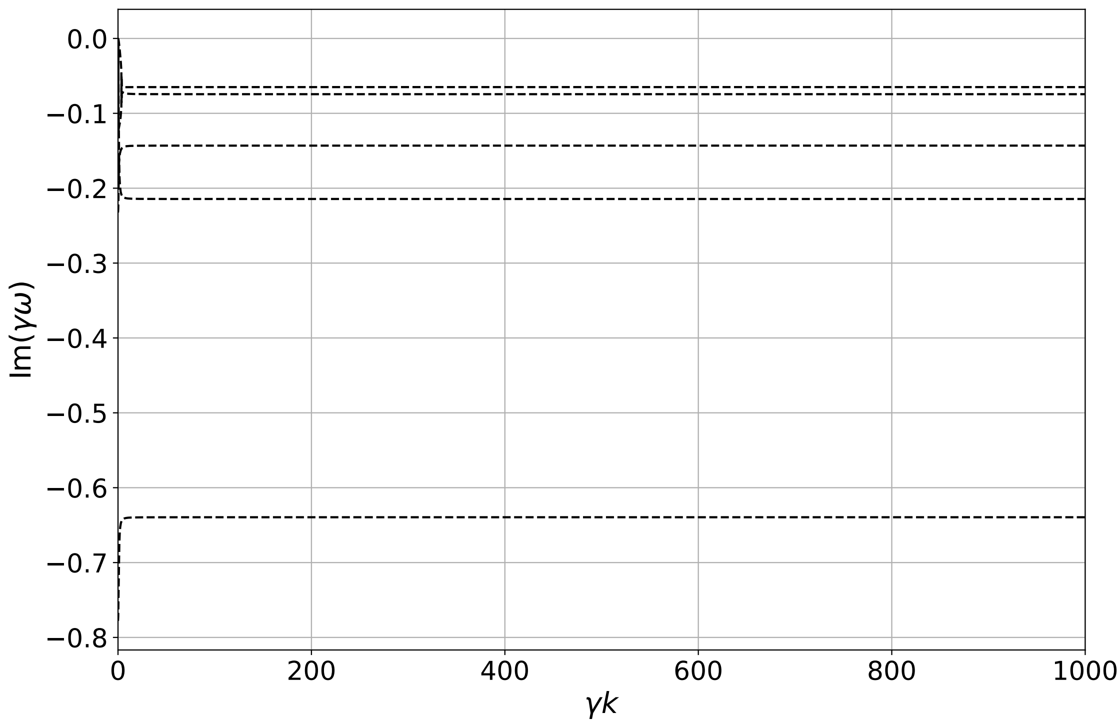

Figure 4.8: The imaginary parts of the longitudinal modes of the massless third-order R25 hydrodynamics plotted for a larger range of k, in the case of fluid velocity vector being parallel to the wave vector, for $V = 0.9$ and with relaxation time $\tau_R = 5$.

Now, in the large-k limit, the dispersion relation can be expanded as

$$-\frac{iV(15 - 70V^2 + 63V^4)}{63(1 - V^2)^{5/2}}k^5 + \frac{i\omega^5}{(1 - V^2)^{5/2}} + O(k^4) + O(\omega^4) = 0 \tag{4.36}$$

Again, since the full expression is complex, we will only show the leading-order term. However, all the terms are included when performing numerical calculations. The corresponding group velocities of the solutions to the dispersion relation are shown in Fig. (4.9), as a function of the fluid flow velocity V. One can see that all solutions are linearly causal since the magnitude of the group velocity is less than 1 for all of them, in the large-k limit. Also, note that the line in the middle of the figure corresponds to a stationary mode in the fluid rest frame since its group velocity is simply the fluid flow velocity.

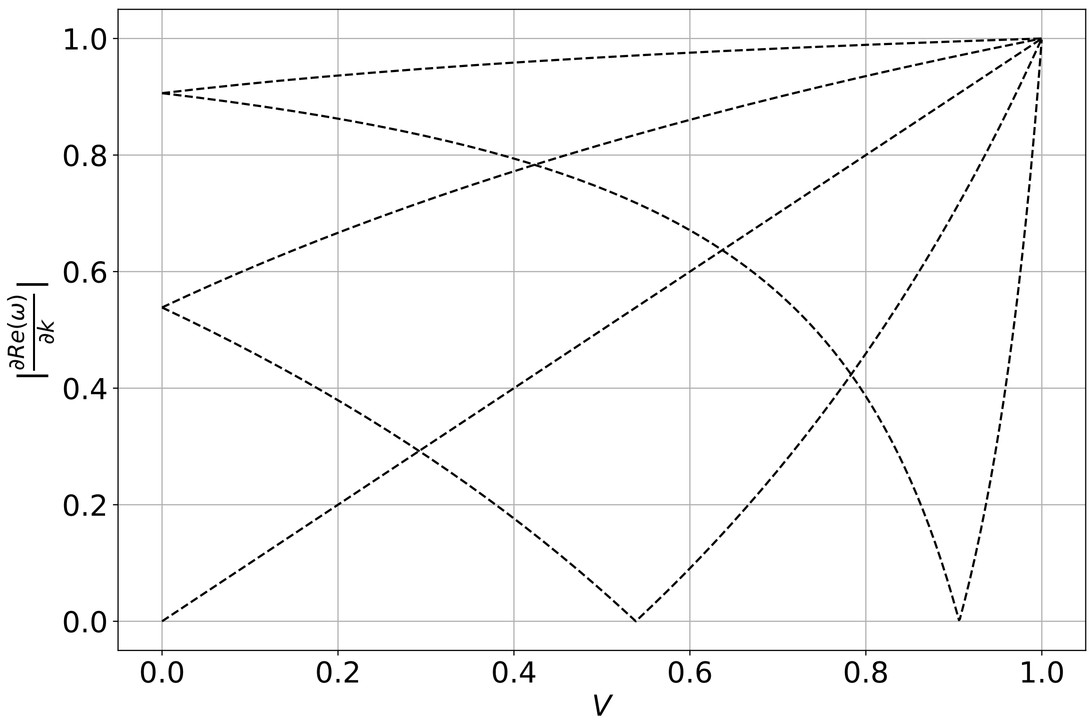

Figure 4.9: Magnitude of the group velocity for the longitudinal modes of the massless third-order R25 hydrodynamics, as a function of the fluid velocity V in the large k limit and with $\tau_R = 5$, in the case of fluid velocity vector being parallel to the wave vector.

Case 2: k is orthogonal to V

As before, we insert Eq. (3.56) into the dispersion relation and solve numerically for the solutions. Fig. (4.10) shows the result. Note that two out of the five solutions have the same imaginary parts, and we can see that all solutions are linearly stable since they all have non-positive imaginary parts for small k. As before, Fig. (4.11) shows the asymptotic behavior of all the modes as k increases, for $V = 0$ and $\tau_R = 5$. This proves that the modes are actually linearly stable for all $k \geq 0$.

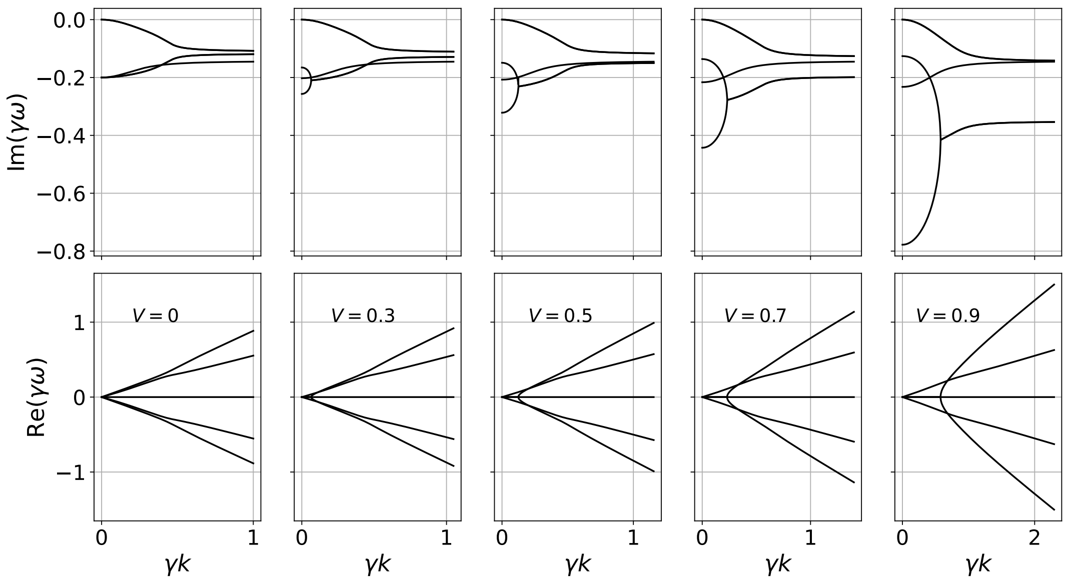

Figure 4.10: Real and Imaginary parts of the longitudinal modes of the massless third-order R25 hydrodynamics, in the case of fluid velocity vector being orthogonal to the wave vector and with $\tau_R = 5$.

To verify the causality of these solutions, we repeat the process from the previous sections. In the large-k limit, the dispersion relation is expanded as

$$-\frac{iV(15-70V^2+63V^4)}{84(1-V^2)^{5/2}}k^5 + \frac{3i\omega^5}{4(1-V^2)^{5/2}} + O(k^4) + O(\omega^4) = 0 \tag{4.37}$$

where all the terms under $O(k^4)$ and $O(\omega^4)$ are included in the actual numerical computations. The corresponding group velocities of the solutions are shown in Fig. (4.12) as a function of the fluid flow velocity. Note that there are three curves in this figure, one of them lies on the x-axis and corresponds to the stationary mode with zero group velocity.

4.4 Discussion

Similar to the second-order case, we would like to compare the third-order R14/R25 theory to other third-order theories and see whether they agree with each other. In [60],

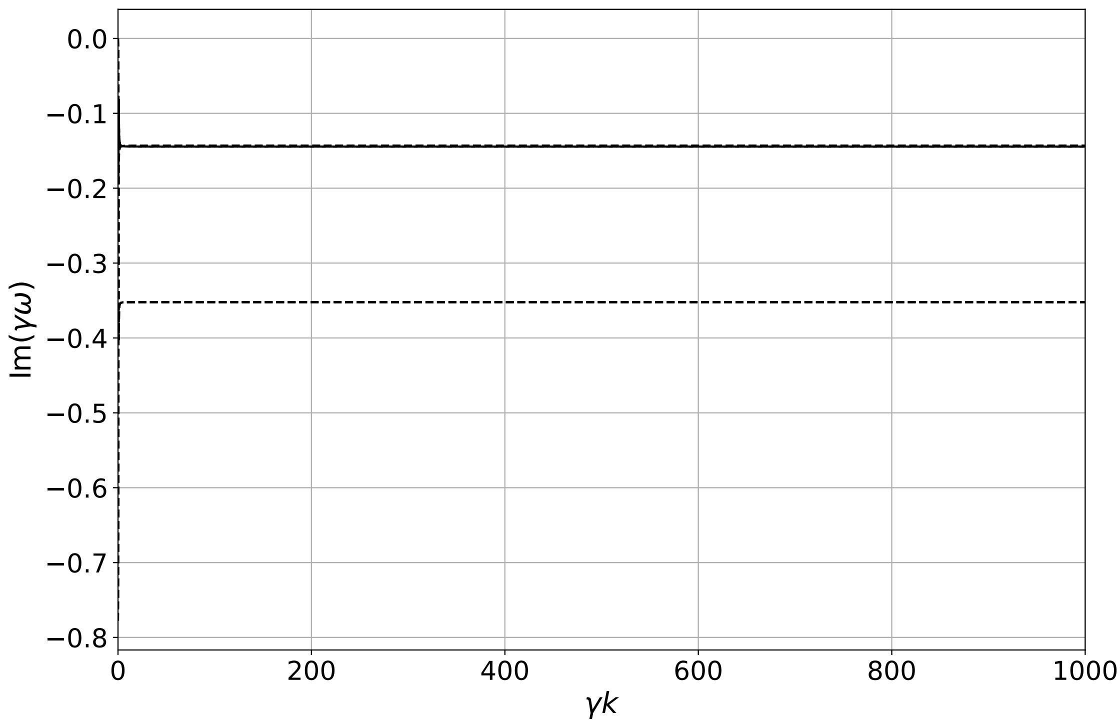

Figure 4.11: The imaginary parts of the longitudinal modes of the massless third-order R25 hydrodynamics plotted for a larger range of k, in the case of fluid velocity vector being orthogonal to the wave vector, for $V = 0.9$ and with relaxation time $\tau_R = 5$.

relativistic third-order viscous hydrodynamics is derived from the Boltzmann equation using Chapman-Enskog expansion. However, similar to the procedure outlined in Section. (4.2), the evolution equation for the shear-stress tensor $\pi^{\mu\nu}$ derived in this work contains second-order gradients of $\pi^{\mu\nu}$ in the expression and is therefore expected to be linearly unstable and acausal. Indeed, the linear stability and causality analysis carried out in [5] shows that this third-order formulation of relativistic viscous hydrodynamics violates linear stability and causality, and this issue cannot be fixed by tuning the transport coefficients.

Consequently, also in [5], Brito and Denicol proposed a modified version of the previous theory. In particular, they promoted the gradient of $\pi^{\mu\nu}$ to a new hydrodynamic

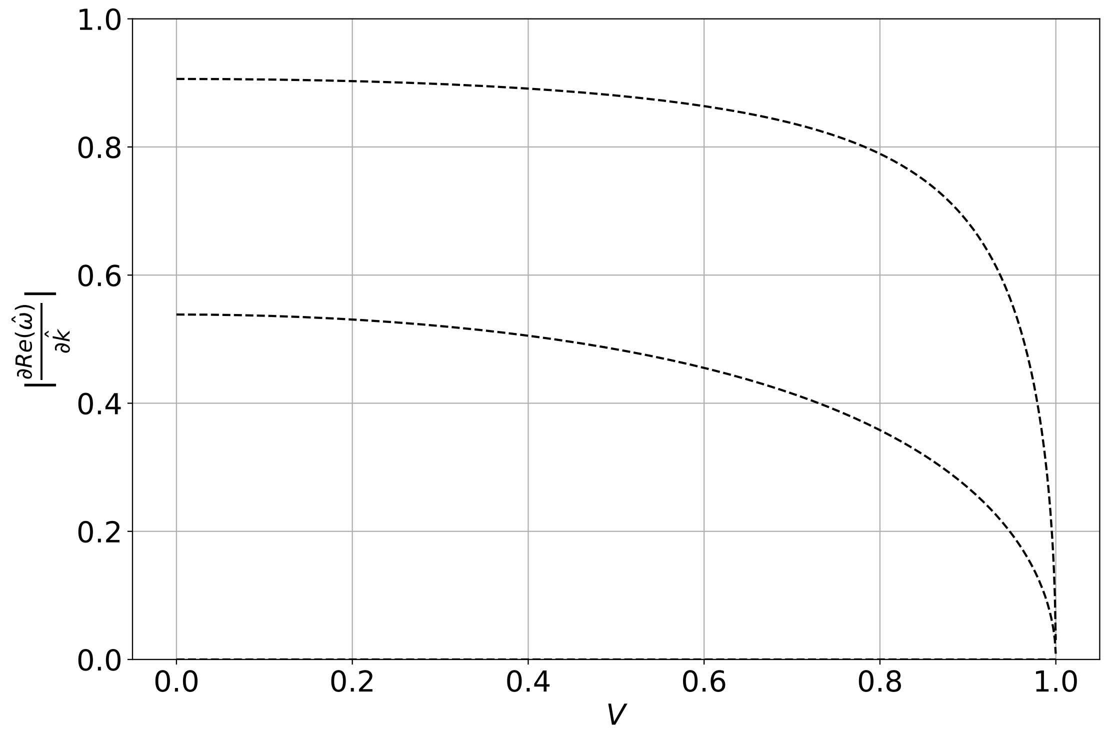

Figure 4.12: Magnitude of the group velocity for the longitudinal modes of the massless third-order R25 hydrodynamics, as a function of the fluid velocity V in the large k limit and with $\tau_R = 5$, in the case of fluid velocity vector being orthogonal to the wave vector. Notice that there is a stationary mode with zero group velocity along the direction of the wave's propagation.

variable

$$\nabla^{\langle\alpha}\pi^{\mu\nu\rangle} \to \rho^{\alpha\mu\nu} \tag{4.38}$$

to eliminate the second-order gradients in the evolution equation of $\pi^{\mu\nu}$. This is analogous to $\xi^{\lambda\mu\nu}$ and $\varsigma^{\alpha\beta\mu\nu}$ that we defined in the third-order R25 theory. Furthermore, this new variable $\rho^{\alpha\mu\nu}$ not only is defined to be proportional to the gradient of $\pi^{\mu\nu}$ but also relaxes to it exponentially, within a time scale associated with the corresponding relaxation time τ_ρ (see Eq. (56) in [5]). This additional requirement serves as the evolution equation for $\rho^{\alpha\mu\nu}$. All these equations, along with the conservation laws, form a closed set of equations. However, just like the second-order Israel-Stewart theory, such modified third-order theory is not always linearly stable and causal, as their transport coefficients must satisfy a set of constraints in order to be so.

The third-order R25 theory, on the other hand, possesses many advantages over the modified third-order theory. For instance, the full hydrodynamic equations are used for $\xi^{\lambda\mu\nu}$ and $\varsigma^{\alpha\beta\mu\nu}$ as the evolution equations, instead of the simplified requirement of exponential relaxation. One of the consequences is that the rank-3 tensor not only is proportional to the gradient of the shear-stress tensor but is also proportional to the product of the acceleration and the shear-stress tensor when $m = 0$ (see Eq. (4.14)). This provides more complete evolution equations.

However, as we have already seen, the third-order R25 theory is extremely analytically-complex. Even extracting the leading-order terms in a series expansion of the modes is not a realistic approach. At this point, properties of the third-order R25 theory can only be examined using numerical approaches. A further investigation of the theory should be carried on in the future to search for a solution to this problem.

Chapter 5

Conclusion

In this dissertation, we introduced the relativistic regularized hydrodynamics initially developed by Struchtrup and Torrilhon in the non-relativistic case [50–53]. In particular, using the regularization method, we derived the second and third-order R14 hydrodynamics and showed that they are linearly stable and causal with the assumption of massless particles without particle number conservation. This result is independent of the choice of transport coefficients. Next, we will briefly summarize the main results in each chapter.

In Chapter 2, we provided some background knowledge of kinetic theory and derived the corresponding equations for energy, momentum, and particle number conservation. We then proceeded to derive the general moment equation so that the relevant moment equations can be derived in the following chapters.

In Chapter 3, using the regularization method, we obtained the second-order R14 hydrodynamics. In particular, the evolution equations for the bulk viscous pressure Π, the diffusion current q^μ, and the shear-stress tensor $\pi^{\mu\nu}$ were derived. This was achieved by directly Chapman-Enskog expanding the moments of δf, small perturbations in the phase density function, instead of expanding the phase density function. A series of linear stability and causality analysis was then performed on the longitudinal and transverse components of the second-order R9 theory by considering two separate cases. In the first one the wave vector is parallel to the background fluid velocity vector, while in the second, they are orthogonal to each other. As a result, the longitudinal and transverse parts of the second-order R9 hydrodynamics are demonstrated to have linearly stable and causal modes in both cases.

In Chapter 4, we derived the third-order R14 hydrodynamics using a similar methodology of regularization as in Chapter 3. With the assumption of massless particles without particle number conservation, we showed that by including the $O(\epsilon^2)$ terms of the moments in the equations for $\pi^{\mu\nu}$, terms with second-order gradients were introduced, and these terms will result in linear instability and acausality in the modes. This problem was then fixed by promoting the $O(\epsilon^2)$ moments $\xi^{\lambda\mu\nu}$ and $\varsigma^{\alpha\beta\mu\nu}$ to hydrodynamic variables, raising the total number of moments from 9 to 25. Analogous to the second-order case, a series of linear stability and causality analysis was performed on the third-order R25 theory. However, the R25 theory is extremely analytically complicated. Therefore, the analysis was carried out using only the numerical approach. As a result, all the modes of the R25 equations are linearly stable and causal, for both the longitudinal and transverse components and for both cases where the wave vector is parallel and orthogonal to the background fluid velocity.

The second and third-order regularized hydrodynamics presented in this dissertation offer a systematically and uniquely derived, stable, and causal framework for modeling the evolution of quark-gluon plasma in the context of heavy-ion collisions. However, since third-order regularized hydrodynamics is analytically inaccessible, the application of such theory in the actual research problems might be restricted. Further investigation into this issue should be conducted in the future in order to make this theory more sophisticated.

Appendix A

Useful Mathematical Identities

The general rank-n projector is

$$\begin{aligned}\Delta^{\mu_1\cdots\mu_n}_{\nu_1\cdots\nu_n} =& \frac{1}{n^2}\left(\sum_{i=1}^{n}\sum_{k=1}^{n}\Delta^{\mu_i}_{\nu_k}\Delta^{\mu_1\cdots\mu_{i-1}\mu_{i+1}\cdots\mu_n}_{\nu_1\cdots\nu_{k-1}\nu_{k+1}\cdots\nu_n}\right)\\ &-\frac{2}{n^2(2n-1)}\left(\sum_{i=1}^{n}\sum_{j=i+1}^{n}\sum_{k=1}^{n}\Delta^{\mu_i\mu_j}\Delta_{\nu_k\alpha}\Delta^{\alpha\mu_1\cdots\mu_{i-1}\mu_{i+1}\cdots\mu_{j-1}\mu_{j+1}\cdots\mu_n}_{\nu_1\cdots\nu_{k-1}\nu_{k+1}\cdots\nu_n}\right)\end{aligned} \tag{A.1}$$

Now consider the following rank-n tensor:

$$A^{\mu_1\cdots\mu_n} = \Delta^{\mu_1\ldots\mu_n}_{\nu_1\ldots\nu_n}Dp^{\langle\nu_1\cdots}p^{\nu_n\rangle} \tag{A.2}$$

Following Eq. C.8 and C.9 in [62], for any symmetric tensor Π we have:

$$\begin{aligned}\Pi_{\langle i_1\ldots i_n\rangle} =& \Pi_{i_1\ldots i_n}\\ &+\alpha_{n1}(\Delta_{i_1i_2}\Pi_{i_3\ldots i_nkk}+permutation)\\ &+\alpha_{n2}(\Delta_{i_1i_2}\Delta_{i_3i_4}\Pi_{i_5\ldots i_nkk}+permutation)\\ &+\ldots\end{aligned} \tag{A.3}$$

where

$$\alpha_{nk} = \frac{(-1)^k}{\Pi_{j=0}^{k-1}(2n-2j-1)} \tag{A.4}$$

Now, if we let

$$\Pi_{i_1 \dots i_n} = p_{\langle \imath_1 \rangle} \dots p_{\langle \imath_n \rangle} \tag{A.5}$$

then all terms in Eq. A.3 except the first one vanish under $\Delta^{i_1 \dots i_n}_{j_1 \dots j_n} D$ due to the present of u_{i_m} and $\Delta_{i_m i_n}$. Consequently, we arrive at the following useful identity:

$$\Delta^{\mu_1 \dots \mu_n}_{\nu_1 \dots \nu_n} D p^{\langle \nu_1 \cdots} p^{\nu_n \rangle} = \Delta^{\mu_1 \dots \mu_n}_{\nu_1 \dots \nu_n} D p^{\langle \nu_1 \rangle} \dots p^{\langle \nu_n \rangle} \tag{A.6}$$

Note that

$$\begin{aligned} Dp^{\langle \mu \rangle} &= D\Delta^{\mu\nu} p_\nu \\ &= D(g^{\mu\nu} + u^\mu u^\nu) p_\nu \\ &= (u^\mu D u^\nu + u^\nu D u^\mu) p_\nu \\ &= u^\mu p_\nu a^\nu - W_p a^\mu \\ &= u^\mu (p^{\langle \nu \rangle} + W_p u^\nu) a_\nu - W_p a^\mu \\ &= u^\mu p^{\langle \nu \rangle} a_\nu - W_p a^\mu \end{aligned} \tag{A.7}$$

where the term with u^μ vanishes when being projected. With some simple algebraic manipulations, we arrive at the following identity:

$$A^{\mu_1 \dots \mu_n} = -n W_p p^{\langle \mu_1 \cdots} p^{\mu_{n-1}} a^{\mu_n \rangle} \tag{A.8}$$

Similarly, one can also argue for the same reasons:

$$\Delta^{\mu_1 \dots \mu_n}_{\nu_1 \dots \nu_n} \nabla_\lambda (p^{\langle \nu_1 \cdots} p^{\nu_n \rangle}) = \Delta^{\mu_1 \dots \mu_n}_{\nu_1 \dots \nu_n} \nabla_\lambda (p^{\langle \nu_1 \rangle} \dots p^{\langle \nu_n \rangle}) \tag{A.9}$$

and

$$\begin{aligned} \nabla_\lambda p^{\langle \nu \rangle} &= \nabla_\lambda (p^\nu - W_p u^\nu) \\ &= -u^\nu \nabla_\lambda W_p - W_p (\nabla_\lambda u^\nu) \end{aligned} \tag{A.10}$$

once again, the first term vanishes when being projected. After some manipulations, we get:

$$\Delta^{\mu_1 \ldots \mu_n}_{\nu_1 \ldots \nu_n} \nabla_\lambda (p^{\langle \nu_1 \cdots} p^{\nu_n \rangle}) = -n W_p p^{\langle \mu_1} \ldots p^{\mu_{n-1}} \nabla_\lambda u^{\nu \rangle} \tag{A.11}$$

Appendix B

Evaluating F integrals

B.1 Conservation laws

To evaluate the F integrals, we first need to know the conservation laws. The stress-energy tensor is

$$T^{\mu\nu} = \int \frac{d^3p}{(2\pi)^3 p^0} f_0 p^\mu p^\nu + \pi^{\mu\nu} + \Pi\Delta^{\mu\nu} \tag{B.1}$$

and the particle number current

$$J^\mu = \int \frac{d^3p}{(2\pi)^3 p^0} f_0 p^\mu + q^\mu \tag{B.2}$$

The energy-momentum conservation law is

$$\begin{aligned} 0 &= \partial_\mu T^{\mu\nu} \\ &= \int \frac{d^3p}{(2\pi)^3 p^0} (\partial_\mu f_0) p^\mu p^\nu + \partial_\mu \pi^{\mu\nu} + (\nabla^\nu \Pi) + \Pi(u^\nu \theta + a^\nu) \end{aligned} \tag{B.3}$$

In the time direction $u_\nu \partial_\mu T^{\mu\nu} = 0$ yields

$$0 = -\pi^{\mu\nu}\sigma_{\mu\nu} - \theta\Pi + I_{3,0} D\beta - I_{2,0} D\alpha - \frac{\beta}{3}\theta I_{3,1} \tag{B.4}$$

where we defined

$$I_{n,m} = \int \frac{d^3p}{(2\pi)^3 p^0} f_0 W_p^{n-2m} (W_p^2 - m^2)^m \tag{B.5}$$

which can be evaluated in the local rest frame. In the spatial direction $\Delta^\rho_\nu \partial_\mu T^{\mu\nu} = 0$ yields

$$0 = \Delta^\rho_\nu \partial_\mu \pi^{\mu\nu} + (\nabla^\rho \Pi) + a^\rho \Pi - I_{3,1} \frac{\nabla^\rho \beta}{3} + \frac{\nabla^\rho \alpha}{3} I_{2,1} + \frac{\beta a^\rho}{3} I_{3,1} \tag{B.6}$$

The particle number conservation $0 = \partial_\mu J^\mu$ yields

$$0 = \partial_\mu q^\mu + \frac{\beta\theta}{3} I_{2,1} - D\beta I_{2,0} + D\alpha I_{1,0} \tag{B.7}$$

Using integration by part, it can be shown that

$$\begin{aligned}
\beta I_{r+2,1} &= \beta \int \frac{d^3p}{(2\pi)^3 p^0} (p^0)^r p^2 e^{-\beta p^0 + \alpha} \\
&= - \int \frac{d^3p}{(2\pi)^3 p^0} (p^0)^{r+1} p \partial_p e^{-\beta p^0 + \alpha} \\
&= \int \frac{d^3p}{(2\pi)^3 p^0} e^{-\beta p^0 + \alpha} \left(3 (p^0)^{r+1} + r (p^0)^{r-1} p^2 \right) \\
&= 3 I_{r+1,0} + r I_{r+1,1}
\end{aligned} \tag{B.8}$$

In particular

$$\begin{aligned}
\beta I_{3,1} &= 3 I_{2,0} + I_{2,1} \\
&= 3(\varepsilon + P)
\end{aligned} \tag{B.9}$$

and

$$\begin{aligned}
\beta I_{2,1} &= 3 I_{1,0} \\
&= 3\nu \\
&= 3\beta P
\end{aligned} \tag{B.10}$$

Solving for the time derivatives $D\beta$, $D\alpha$ and $a^\rho = Du^\rho$, we obtain

$$D\beta = \chi_{\beta|0}\theta + \chi^{q}_{\beta|1}\partial_\mu q^\mu + \chi^{\pi\Pi}_{\beta|1}\left(\pi^{\gamma\rho}\sigma_{\gamma\rho} + \Pi\theta\right) \tag{B.11}$$

where

$$\chi_{\beta|0} = \frac{I_{1,0}(\varepsilon + P) - I_{2,0}I_{1,0}}{I_{3,0}I_{1,0} - I_{2,0}^2} = \frac{I_{1,0}P}{I_{3,0}I_{1,0} - I_{2,0}^2} \tag{B.12}$$

$$\chi^{q}_{\beta|1} = -\frac{I_{2,0}}{I_{3,0}I_{1,0} - I_{2,0}^2} \tag{B.13}$$

$$\chi^{\pi\Pi}_{\beta|1} = \frac{I_{1,0}}{I_{3,0}I_{1,0} - I_{2,0}^2} \tag{B.14}$$

and

$$D\alpha = \chi_{\alpha|0}\theta + \chi^{q}_{\alpha|1}\partial_\mu q^\mu + \chi^{\pi\Pi}_{\alpha|1}\left(\pi^{\gamma\rho}\sigma_{\gamma\rho} + \Pi\theta\right) \tag{B.15}$$

where

$$\chi_{\alpha|0} = \frac{I_{2,0}(\varepsilon + P) - I_{3,0}I_{1,0}}{I_{3,0}I_{1,0} - I_{2,0}^2} \tag{B.16}$$

$$\chi^{q}_{\beta|1} = -\frac{I_{3,0}}{I_{3,0}I_{1,0} - I_{2,0}^2} \tag{B.17}$$

$$\chi^{\pi\Pi}_{\beta|1} = \frac{I_{2,0}}{I_{3,0}I_{1,0} - I_{2,0}^2} \tag{B.18}$$

The acceleration is given by

$$\begin{aligned} a^\rho &= \frac{1}{\varepsilon + P}\left(-\nabla^\rho P - \Pi a^\rho - \nabla^\rho \Pi - \Delta^\rho_\nu \partial_\mu \pi^{\mu\nu}\right) \\ &\approx \frac{1}{\varepsilon + P}\left(-\nabla^\rho P - \nabla^\rho \Pi - \Delta^\rho_\nu \partial_\mu \pi^{\mu\nu}\right) - \frac{1}{(\varepsilon + P)^2}\Pi\left(-\nabla^\rho P\right) \end{aligned} \tag{B.19}$$

where we used

$$\nabla P = -\frac{\nabla\beta}{3}I_{3,1} + \frac{\nabla\alpha}{3}I_{2,1} \tag{B.20}$$

The 0-th order acceleration is

$$a^\rho_{|0} = -\frac{\nabla^\rho P}{\varepsilon + P} \tag{B.21}$$

and the 1st order one is

$$a^{\rho}_{|1} = \frac{1}{\varepsilon + P}\left(-\nabla^{\rho}\Pi - \Delta^{\rho}_{\nu}\partial_{\mu}\pi^{\mu\nu}\right) - \frac{1}{(\varepsilon + P)^2}\Pi\left(-\nabla^{\rho}P\right) \tag{B.22}$$

B.2 F Integrals

The only non-zero F integrals are the spin 0, 1, and 2 integrals. For $n = 0$, we have

$$\begin{aligned} F_r &= \int \frac{d^3p}{(2\pi)^3 p^0} W_p^r p^{\lambda}(\partial_{\lambda} f_0) \\ &= \int \frac{d^3p}{(2\pi)^3 p^0} W_p^r f_0 \left(W_p D\alpha - W_p^2 D\beta + \beta\frac{\theta}{3}(W_p^2 - m^2) \right) \\ &= \phi_{r|0}\theta + \phi^{q}_{r|1}\partial_{\mu}q^{\mu} + \phi^{\pi\Pi}_{r|1}\left(\pi^{\rho\gamma}\sigma_{\rho\gamma} + \theta\Pi\right) \end{aligned} \tag{B.23}$$

upon using Eqs.(B.11) and (B.15) for $D\beta$ and $D\alpha$. The coefficient

$$\phi_{r|0}(\alpha, \beta) = \frac{I_{1,0}I_{r+2,0} - I_{r+1,0}I_{2,0}}{I_{3,0}I_{1,0} - I_{2,0}^2}\frac{\beta}{3}I_{3,1} + \frac{\beta}{3}I_{r+2,1} - \frac{I_{r+1,0}I_{3,0} - I_{r+2,0}I_{2,0}}{I_{3,0}I_{1,0} - I_{2,0}^2}I_{1,0} \tag{B.24}$$

is for the $O(1)$ (or f_0) piece and the coefficients

$$\phi^{q}_{r|1}(\alpha, \beta) = -\frac{I_{r+1,0}I_{3,0} - I_{r+2,0}I_{2,0}}{I_{3,0}I_{1,0} - I_{2,0}^2} \tag{B.25}$$

$$\phi^{\pi\Pi}_{r|1}(\alpha, \beta) = -\frac{I_{r+2,0}I_{1,0} - I_{r+1,0}I_{2,0}}{I_{3,0}I_{1,0} - I_{2,0}^2} \tag{B.26}$$

are for the $O(\epsilon)$ (or δf) pieces. For the Boltzmann statistics, ϕ^{q}_{r} and $\phi^{\pi\Pi}_{r}$ do not depend on α. In the massless limit, we have

$$I_{r,k} = \int \frac{d^3p}{(2\pi)^3} p^{r-1} e^{-p/T} = \frac{T^{r+2}}{2\pi^2}(r+1)! \tag{B.27}$$

For the 14 moments, we need F_{-1} whose coefficients are

$$\phi_{-1|0} = -4\frac{T^2}{2\pi^2} \tag{B.28}$$

$$\phi^{q}_{-1|1} = -\beta \tag{B.29}$$

and

$$\phi^{\pi\Pi}_{-1|1} = -\frac{1}{6}\beta^2 \tag{B.30}$$

The vector integral is

$$\begin{aligned}
F_r^\sigma &= \int \frac{d^3p}{(2\pi)^3 p^0} W_p^r p^\lambda (\partial_\lambda f_0) p^{\langle\sigma\rangle} \\
&= \int \frac{d^3p}{(2\pi)^3 p^0} W_p^r f_0 \left(-W_p p^{\langle\lambda\rangle}\nabla_\lambda\beta + p^{\langle\lambda\rangle}\nabla_\lambda\alpha + W_p\beta p^{\langle\lambda\rangle} a_\lambda\right) p^{\langle\sigma\rangle} \\
&= \psi_{r|0}\nabla^\sigma\alpha + \psi_{r|1}\left(\Delta^\rho_\nu\partial_\mu\pi^{\mu\nu} + \nabla^\sigma\Pi + a^\sigma\Pi\right)
\end{aligned} \tag{B.31}$$

where we used a slight different form of Eq.(B.19)

$$\beta a^\rho - \nabla^\rho\beta = -\frac{3}{I_{3,1}}\left(\Delta^\rho_\nu\partial_\mu\pi^{\mu\nu} + (\nabla^\rho\Pi) + a^\rho\Pi + \frac{\nabla^\rho\alpha}{3}I_{2,1}\right) \tag{B.32}$$

to cleanly separate the $O(1)$ piece and the $O(\epsilon)$ piece. The coefficients are

$$\psi_{r|0} = \frac{I_{r+2,1}I_{3,1} - I_{r+3,1}I_{2,1}}{3I_{3,1}} \tag{B.33}$$

for the $O(1)$ piece and

$$\psi_{r|1} = -\frac{I_{r+3,1}}{I_{3,1}} \tag{B.34}$$

for the $O(\epsilon)$ piece. Here, $I_{3,1} = 3(\varepsilon + P)T$ and $I_{2,1} = 3P$ can be used if needed. With $r = -1$ and $m = 0$,

$$\psi_{-1|0} = \frac{1}{6}\frac{T^3}{2\pi^2} \tag{B.35}$$

$$\psi_{-1|1} = -\frac{1}{4}\beta \tag{B.36}$$

The spin-2 integral is relatively simple since it does not have the $O(\epsilon)$ part

$$
\begin{aligned}
F_r^{\sigma\gamma} &= \int \frac{d^3p}{(2\pi)^3 p^0} W_p^r p^\lambda (\partial_\lambda f_0) p^{\langle\sigma} p^{\gamma\rangle} \\
&= \int \frac{d^3p}{(2\pi)^3 p^0} W_p^r f_0 \left(\beta p^{\langle\lambda} p^{\alpha\rangle} \nabla_\lambda u_\alpha\right) p^{\langle\sigma} p^{\gamma\rangle} \\
&= \varphi_{r|0} \sigma^{\sigma\gamma}
\end{aligned}
\tag{B.37}
$$

where

$$
\varphi_{r|0} = \frac{2}{15} \beta I_{r+4,2} \tag{B.38}
$$

is obtained with the help of the normalization condition (Eq.(16) in [63]). With $r = -1$ and $m = 0$,

$$
\varphi_{-1|0} = \frac{16}{5} \frac{T^4}{2\pi^2} \tag{B.39}
$$

Bibliography

[1] "The big bang and expansion of the universe," Aug 2012. [Online]. Available: https://www.jpl.nasa.gov/infographics/the-big-bang-and-expansion-of-the-universe

[2] "Start-up of 22*nd* run at the relativistic heavy ion collider (RHIC)," Dec 2021. [Online]. Available: https://www.bnl.gov/newsroom/news.php?a=119262

[3] "Time for lead collisions in the LHC," Nov 2018. [Online]. Available: https://home.cern/news/news/accelerators/time-lead-collisions-lhc

[4] A. Schmitt, "Phases of QCD at large baryon densities and applications to neutron stars," Jun 2022. [Online]. Available: https://indico.in2p3.fr/event/26074/contributions/112558/attachments/71858/102485/schmitt1.pdf

[5] C. Brito and G. Denicol, "Linear causality and stability of third-order relativistic dissipative fluid dynamics," *Physical Review D*, vol. 105, no. 096026, 2022. [Online]. Available: https://doi.org/10.1103/PhysRevD.105.096026

[6] G. S. Denicol, H. Niemi, E. Molnár, and D. H. Rischke, "Derivation of transient relativistic fluid dynamics from the boltzmann equation," *Physical Review D*, vol. 85, no. 114047, 2012. [Online]. Available: https://doi.org/10.1103/PhysRevD.85.114047

[7] D. Griffiths, *Introduction to Elementary Particles*, 2nd ed. WILEY-VCH, 2008.

[8] G. Hooft, "The birth of asymptotic freedom," *Nuclear Physics B*, vol. 254, pp. 11–18, 1985. [Online]. Available: https://doi.org/10.1016/0550-3213(85)90206-8

[9] H. D. Politzer, "Reliable perturbative results for strong interactions?" *Physical Review Letters*, vol. 30, no. 1346, 1973. [Online]. Available: https://doi.org/10.1103/PhysRevLett.30.1346

[10] D. J. Gross and F. Wilczek, "Ultraviolet behavior of non-abelian gauge theories."

[11] P. Arnold, "Quark-gluon plasma and thermalization," *International Journal of Modern Physics E*, vol. 16, no. 09, pp. 2555–2594, 2007. [Online]. Available: https://doi.org/10.1142/S021830130700832X

[12] E. W. Kolb and M. S. Turner, *The Early Universe*, 1st ed. CRC Press, 1990.

[13] U. W. Heinz, "Concepts of heavy-ion physics," 2004. [Online]. Available: https://doi.org/10.48550/arXiv.hep-ph/0407360

[14] B. V. Jacak and B. Müller, "The exploration of hot nuclear matter," *Science*, vol. 337, pp. 310–314, 2012. [Online]. Available: https://doi.org/10.1126/science.1215901

[15] "The STAR detector." [Online]. Available: https://www.bnl.gov/rhic/star.php

[16] "The sPHENIX detector." [Online]. Available: https://www.bnl.gov/rhic/sphenix.php

[17] "The PHENIX detector." [Online]. Available: https://www.bnl.gov/rhic/phenix.php

[18] "PHOBOS and BRAHMS detectors." [Online]. Available: https://www.bnl.gov/rhic/phobos-brahms.php

[19] "The physics of RHIC." [Online]. Available: https://www.bnl.gov//rhic/physics.php

[20] "Relativistic heavy ion collider (RHIC)." [Online]. Available: https://science.osti.gov/np/Facilities/User-Facilities/RHIC

[21] "ALICE: Overview." [Online]. Available: https://alice.cern/overview

[22] B. W. Carroll and D. A. Ostlie, *An Introduction to Modern Astrophysics*, 2nd ed. Cambridge University Press, 2017.

[23] G. Raaijmakers *et al.*, "A nicer view of psr j0030+0451: Implications for the dense matter equation of state," *The Astrophysical Journal Letters*, vol. 887, no. 1, 2019. [Online]. Available: https://doi.org/10.3847/2041-8213/ab451a

[24] D. Viganò *et al.*, "Unifying the observational diversity of isolated neutron stars via magneto-thermal evolution models," *Monthly Notices of the Royal Astronomical Society*, vol. 434, pp. 123–141, 2013. [Online]. Available: https://doi.org/10.1093/mnras/stt1008

[25] G. Nijs, "Holography in quark-gluon plasma and neutron stars," 2020. [Online]. Available: https://doi.org/10.48550/arXiv.2009.01138

[26] G. Baym, T. Hatsuda, T. Kojo, P. D. Powell, Y. Song, and T. Takatsuka, "From hadrons to quarks in neutron stars: a review," *Reports on Progress in Physics*, vol. 81, no. 5, 2018. [Online]. Available: https://doi.org/10.1088/1361-6633/aaae14

[27] C. Gale, S. Jeon, and B. Schenke, "Hydrodynamic modeling of heavy-ion collisions," *International Journal of Modern Physics A*, vol. 28, no. 11, 2013. [Online]. Available: https://doi.org/10.1142/S0217751X13400113

[28] K. H. Ackermann *et al.*, "Elliptic flow in $Au + Au$ collisions at $\sqrt{s_{NN}} = 130$ *GeV*," *Physical Review Letters*, vol. 86, no. 402, 2001. [Online]. Available: https://doi.org/10.1103/PhysRevLett.86.402

[29] P. F. Kolb and U. Heinz, "Hydrodynamic description of ultra relativistic heavy-ion collisions," *Quark–Gluon Plasma 3*, pp. 634–714, 2004. [Online]. Available: https://doi.org/10.1142/9789812795533_0010

[30] U. Heinz, ""rhic serves the perfect fluid" – hydrodynamic flow of the qgp," 2005. [Online]. Available: https://arxiv.org/abs/nucl-th/0512051v1

[31] P. Huovinen, "Hydrodynamical description of collective flow," *Quark–Gluon Plasma 3*, pp. 600–633, 2004. [Online]. Available: https://doi.org/10.1142/9789812795533_0009

[32] S. Jeon and U. Heinz, "Introduction to hydrodynamics," 2015. [Online]. Available: https://doi.org/10.48550/arXiv.1503.03931

[33] P. K. Kovtun, D. T. Son, and A. O. Starinets, "Viscosity in strongly interacting quantum field theories from black hole physics," *Physical Review Letters*, vol. 94, no. 111601, 2005. [Online]. Available: https://doi.org/10.1103/PhysRevLett.94.111601

[34] P. Romatschke and U. Romatschke, "Viscosity information from relativistic nuclear collisions: How perfect is the fluid observed at rhic?" *Physical Review Letters*, vol. 99, no. 172301, 2007. [Online]. Available: https://doi.org/10.1103/PhysRevLett.99.172301

[35] C. Eckart, "The thermodynamics of irreversible processes. iii. relativistic theory of the simple fluid," *Physical Review Journals Archive*, vol. 58, no. 919, 1940. [Online]. Available: https://doi.org/10.1103/PhysRev.58.919

[36] L. D. Landau and E. M. Lifshitz, *Fluid Mechanics - Course of Theoretical Physics: Volume 6*, 2nd ed. Butterworth-Heinemann, 1987.

[37] S. Chapman and T. G. Cowling, *The Mathematical Theory of Non-uniform Gases*, 3rd ed. Cambridge University Press, 1991.

[38] W. A. Hiscock and L. Lindblom, "Generic instabilities in first-order dissipative relativistic fluid theories," *Physical Review D*, vol. 31, no. 725, 1985. [Online]. Available: https://doi.org/10.1103/PhysRevD.31.725

[39] ——, “Linear plane waves in dissipative relativistic fluids,” *Physical Review D*, vol. 35, no. 3723, 1987. [Online]. Available: https://doi.org/10.1103/PhysRevD.35.3723

[40] ——, “Nonlinear pathologies in relativistic heat-conducting fluid theories,” *Physics Letters A*, vol. 131, pp. 509–513, 1988. [Online]. Available: https://doi.org/10.1016/0375-9601(88)90679-2

[41] G. S. Denicol, T. Kodama, T. Koide, and P. Mota, “Stability and causality in relativistic dissipative hydrodynamics,” *Journal of Physics G: Nuclear and Particle Physics*, vol. 35, no. 11, 2008. [Online]. Available: https://doi.org/10.1088/0954-3899/35/11/115102

[42] W. A. Hiscock and L. Lindblom, “Stability and causality in dissipative relativistic fluids,” *Annals of Physics*, vol. 151, pp. 466–496, 1983. [Online]. Available: https://doi.org/10.1016/0003-4916(83)90288-9

[43] S. Pu, T. Koide, and D. H. Rischke, “Does stability of relativistic dissipative fluid dynamics imply causality?” *Physical Review D*, vol. 81, no. 114039, 2010. [Online]. Available: https://doi.org/10.1103/PhysRevD.81.114039

[44] W. Israel and J. M. Stewart, “Thermodynamics of nonstationary and transient effects in a relativistic gas,” *Physics Letters A*, vol. 58, pp. 213–215, 1976. [Online]. Available: https://doi.org/10.1016/0375-9601(76)90075-X

[45] W. Israel, “Nonstationary irreversible thermodynamics: A causal relativistic theory,” *Annals of Physics*, vol. 100, pp. 310–331, 1976. [Online]. Available: https://doi.org/10.1016/0003-4916(76)90064-6

[46] W. Israel and J. M. Stewart, “Transient relativistic thermodynamics and kinetic theory,” *Annals of Physics*, vol. 118, pp. 341–372, 1979. [Online]. Available: https://doi.org/10.1016/0003-4916(79)90130-1

[47] H. Grad, "On the kinetic theory of rarefied gases," *Communications on Pure and Applied Mathematics*, vol. 2, pp. 331–407, 1949. [Online]. Available: https://doi.org/10.1002/cpa.3160020403

[48] T. S. Olson, "Stability and causality in the israel-stewart energy frame theory," *Annals of Physics*, vol. 199, pp. 18–36, 1990. [Online]. Available: https://doi.org/10.1016/0003-4916(90)90366-V

[49] C. Brito and G. Denicol, "Linear stability of israel-stewart theory in the presence of net-charge diffusion," *Physical Review D*, vol. 102, no. 116009, 2020. [Online]. Available: https://doi.org/10.1103/PhysRevD.102.116009

[50] H. Struchtrup and M. Torrilhon, "Regularization of grad's 13 moment equations: Derivation and linear analysis," *Physics of Fluids*, vol. 15, no. 2668, 2003. [Online]. Available: https://doi.org/10.1063/1.1597472

[51] H. Struchtrup, "Stable transport equations for rarefied gases at high orders in the knudsen number," *Physics of Fluids*, vol. 16, no. 3921, 2004. [Online]. Available: https://doi.org/10.1063/1.1782751

[52] H. Struchtrup and M. Torrilhon, "Regularized 13-moment equations: shock structure calculations and comparison to burnett models," *Journal of Fluid Mechanics*, vol. 513, pp. 171–198, 2004. [Online]. Available: https://doi.org/10.1017/S0022112004009917

[53] ——, "*H* theorem, regularization, and boundary conditions for linearized 13 moment equations," *Physical Review Letters*, vol. 99, no. 014502, 2007. [Online]. Available: https://doi.org/10.1103/PhysRevLett.99.014502

[54] J. D. Bjorken, "Highly relativistic nucleus-nucleus collisions: The central rapidity region," *Physical Review D*, vol. 27, no. 140, 1983. [Online]. Available: https://doi.org/10.1103/PhysRevD.27.140

[55] A. Muronga, “Causal theories of dissipative relativistic fluid dynamics for nuclear collisions,” *Physical Review C*, vol. 69, no. 034903, 2004. [Online]. Available: https://doi.org/10.1103/PhysRevC.69.034903

[56] M. Martinez and M. Strickland, “Constraining relativistic viscous hydrodynamical evolution,” *Physical Review C*, vol. 79, no. 044903, 2009. [Online]. Available: https://doi.org/10.1103/PhysRevC.79.044903

[57] A. Jaiswal, “Relativistic dissipative hydrodynamics from kinetic theory with relaxation-time approximation,” *Physical Review C*, vol. 87, no. 051901(R), 2013. [Online]. Available: https://doi.org/10.1103/PhysRevC.87.051901

[58] A. El, Z. Xu, and C. Greiner, “Extension of relativistic dissipative hydrodynamics to third order,” *Physical Review C*, vol. 81, no. 041901(R), 2010. [Online]. Available: https://doi.org/10.1103/PhysRevC.81.041901

[59] C. Chattopadhyay, A. Jaiswal, S. Pal, and R. Ryblewski, “Relativistic third-order viscous corrections to the entropy four-current from kinetic theory,” *Physical Review C*, vol. 91, no. 024917, 2015. [Online]. Available: https://doi.org/10.1103/PhysRevC.91.024917

[60] A. Jaiswal, “Relativistic third-order dissipative fluid dynamics from kinetic theory,” *Physical Review C*, vol. 88, no. 021903(R), 2013. [Online]. Available: https://doi.org/10.1103/PhysRevC.88.021903

[61] S. R. de Groot, W. A. van Leeuwen, and C. G. van Weert, *Relativistic Kinetic Theory: Principles and Applications*. North-Holland Publishing Company, 1980.

[62] H. Struchtrup, “Zur irreversiblen thermodynamikder strahlung,” Ph.D. dissertation, Technical University of Berlin, 1996.

[63] G. S. Denicol, E. Molnár, H. Niemi, and D. H. Rischke, “Derivation of fluid dynamics from kinetic theory with the 14-moment approximation,” *The*

European Physical Journal A, vol. 48, no. 170(2012), 2012. [Online]. Available: https://doi.org/10.1140/epja/i2012-12170-x

[64] C. Brito and G. Denicol, "Linear stability of israel-stewart theory in the presence of net-charge diffusion," *Physical Review D*, vol. 102, no. 116009, 2020. [Online]. Available: https://doi.org/10.1103/PhysRevD.102.116009

[65] J. D. Jackson, *Classical Electrodynamics*, 3rd ed. Wiley, 1999.

[66] C. V. Brito, "On the linear stability and causality of transient fluid dynamics," 2021.